

AD-A021 872

A DESIGN OF A MODAL CONTROLLER FOR THE B-52 CONTROL
CONFIGURED VEHICLE (CCV)

Ronald M. Adams

Air Force Institute of Technology
Wright-Patterson Air Force Base, Ohio

December 1975

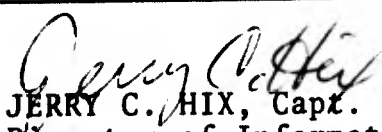
DISTRIBUTED BY:

NTIS

National Technical Information Service
U. S. DEPARTMENT OF COMMERCE

UNCLASSIFIED

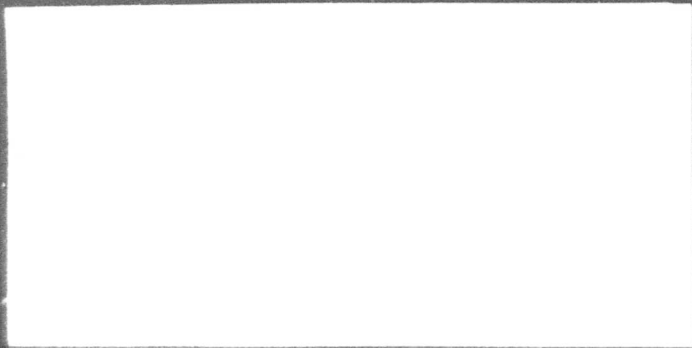
SECURITY CLASSIFICATION OF THIS PAGE (When Data Entered)

REPORT DOCUMENTATION PAGE		READ INSTRUCTIONS BEFORE COMPLETING FORM
1. REPORT NUMBER GE/EE/75D-9	2. GOVT ACCESSION NO.	3. RECIPIENT'S CATALOG NUMBER
4. TITLE (and Subtitle) A Design of a Modal Controller for the B-52 Control Configured Vehicle (CCV)		5. TYPE OF REPORT & PERIOD COVERED MS Thesis
		6. PERFORMING ORG. REPORT NUMBER
7. AUTHOR(s) Ronald M. Adams Captain, USAF		8. CONTRACT OR GRANT NUMBER(s)
9. PERFORMING ORGANIZATION NAME AND ADDRESS		10. PROGRAM ELEMENT, PROJECT, TASK AREA & WORK UNIT NUMBERS
11. CONTROLLING OFFICE NAME AND ADDRESS Air Force Flight Dynamics Laboratory Wright-Patterson AFB, Ohio 45433		12. REPORT DATE December 1975
		13. NUMBER OF PAGES 177 170
14. MONITORING AGENCY NAME & ADDRESS (if different from Controlling Office)		15. SECURITY CLASS. (of this report) Unclassified
		15a. DECLASSIFICATION/DOWNGRADING SCHEDULE
16. DISTRIBUTION STATEMENT (of this Report) Approved for public release; distribution unlimited.		
17. DISTRIBUTION STATEMENT (of the abstract entered in Block 20, if different from Report)		
18. SUPPLEMENTARY NOTES Approved for public release; IAW AFR 190-17 <div style="text-align: right;">  JERRY C. HIX, Capt. USAF Director of Information </div>		
19. KEY WORDS (Continue on reverse side if necessary and identify by block number) Multivariable control Modal control Modern control theory Control applications		
20. ABSTRACT (Continue on reverse side if necessary and identify by block number) A large-order multi-input multi-output state-variable model and design specification was recently developed for the B-52 Control Configured Vehicle (CCV) longitudinal axis. This model gives the opportunity to use modern control techniques to design the CCV concepts of interest. Previously the B-52 CCV control task was designed in increments using conventional control techniques. When the entire control problem is formulated and drawn up in one		

specification however, the designer's job becomes significantly more difficult. Modern control techniques are available which permit the large multi-input multi-output control problem to be addressed.

For this thesis, modal control theory is applied to the B-52 CCV state-variable model. The pertinent theory is presented and then a multi-stage design procedure is applied. Three of five available inputs are used to shift 14 of the eigenvalues associated with 39 modes. The theory and equations of three system testing techniques are also discussed and are applied to the modal control design. The performance of the modal controller is then compared with that of the open-loop system and a recently-designed optimal controller. The extensive computer program used for the modal controller design and comparison is appended to the report along with the specification.

ADA021872



REPRODUCED BY
NATIONAL TECHNICAL
INFORMATION SERVICE
U. S. DEPARTMENT OF COMMERCE
SPRINGFIELD, VA. 22161

Preface

The purpose of this thesis project was to apply modal control theory to the B-52 CCV state-variable model and to compare the results with those obtained for an optimal controller. The model was developed by the Air Force Flight Dynamics Laboratory and was used by their Control Configured Vehicle Advanced Development Program Office to design the optimal controller. Initially this thesis was to include a design for both the longitudinal and lateral axes of the B-52 CCV model but due to time-constraints, the lateral axis was dropped. Throughout the thesis, several other items of interest in the design were investigated as the project progressed and as a successful design was sought. In its entirety, the project required the use of nearly all the conventional and modern control theory to which I have been exposed in my Air Force career and in my studies at AFIT. This aspect of the thesis has been very satisfying.

On the other hand, the achievement of only an initial design instead of a final one is somewhat disappointing but not without its rewards. Hopefully this project leaves future students of control theory with a computer program which permits them to achieve the successful design I originally sought. If they receive from their advisors the encouragement which I did, they should have no problem.

Throughout this thesis, I have become indebted to several people for their assistance, their interest, and mostly their patience and encouragement. First, I wish to extend a

thanks to my sponsor, Mr. Robert D. Poyneer, of the AFFDL CCV ADPO. Mr. Poyneer developed the B-52 CCV state-variable model and designed the optimal controller. Discussions with him of his design problems were very beneficial. A special thank you is also due Professors Constantine H. Houppis, Thomas E. Moriarty and Richard M. Potter of the Electrical Engineering Department at AFIT. Their encouragement and interest as readers caused several mountains to be moved, scribbles on blackboards and Saturday afternoon cups of coffee notwithstanding. Another to whom a thank you is given is Professor Brian Porter of the University of Salford, England. Twice during this thesis, Prof. Porter visited the Air Force Institute of Technology. During the first, he helped formulate the project, and during the second he offered numerous suggestions of design alternatives and improvements. Of course, without the text by Prof. Porter and his colleague, Dr. Crossley, I would have gone nowhere.

Perhaps the most appreciative thank you should be to Professor John J. D'Azzo of the AFIT Electrical Engineering Department. Prof. D'Azzo performed the role of thesis advisor and based on my vote of one, was the greatest. His quiet manner of encouragement at weekly meetings and his very strong interest in my personal gains in knowledge was far more influential in progress being made than an equal number of half-time locker-room coaching sessions.

With all deference to Prof. D'Azzo however, none of this project would have been completed without the help, en-

couragement, and understanding of my wife, Beverly. Her unselfishness for the past year-and-a-half has permitted me the opportunity to achieve a personal goal I have wanted for some time. She is certainly deserving of that high degree of PhT: Putting husband Through.

Finally, I am very grateful to Mrs. Charlette Kjesbo for her patience as a typist. Her willingness to type at most any hour is appreciated.

Ronald M. Adams

Contents

	Page
Preface	ii
List of Figures	vii
List of Tables	viii
Abstract	ix
I. Introduction	1
Summary of the B-52 CCV Program	1
Optimal Control Design	5
Statement of the Problem	7
The B-52 CCV Model	8
Scope	14
Assumptions	14
Sequence of Presentation	15
II. Modal Control Theory	16
Pertinent Modal Control Theory	16
Selection of the Closed-loop Eigenvalues	24
The Multi-stage Modal Controller	27
Testing the Design	31
Covariance Analysis	33
Transfer Function Analysis	37
Frequency Response Analysis	42
III. A Modal Controller for the B-52 CCV	47
The System Specification	47
Modal Analysis of the B-52 CCV State- variable Model	48
Eigenanalysis of the Plant Matrix	49
Mode-controllability Characteristics	55
Mode-observability Characteristics	57
Determination of the Closed-loop Eigenvalues	57
Design of a Multi-stage Modal Controller	61
Computer Routines Used for Multi-stage Design	71
IV. Results and Comparisons	74
Results of the Multi-stage Modal Controller Design	74
The Modal Controller Versus the Specification	76
Comparison of Open-loop and Closed-loop Systems	76

Performance in Wind-induced Turbulence	77
Performance with Pilot-induced Elevator Oscillations	80
Performance for Step-elevator Input . .	81
Control Loop Stability	85
Control Surface Displacements and Rates	86
Eigenvalue Restriction Locations . . .	87
Comparison of Modal Controller Performance with Other B-52 CCV Controllers	87
Summary of Results and Comparisons	89
V. Conclusions and Recommendations	91
Conclusions	91
Recommendations	92
Bibliography	97
Appendix A: Computer Routines	99
Appendix B: Specification	162
Vita	165

List of Figures

Figure	Page
1 B-52 CCV Control Surface, Sensor, and Bending Moment Station Locations	9
2 Open-loop System	18
3 Multi-stage Modal Controller	32
4 Block Diagrams for Frequency Response	43
5 Distribution of Non-zero Elements of Matrices \underline{A} , \underline{B} , \underline{H} , and \underline{C} as Given by Eqs (1) and (2) . . .	50
6 Wind Model for B-52 CCV	54
7 Restrictions of Eigenvalue Shifts as Given by Specification Paragraph 1.4, Appendix B	62
8 Locations of Shifted Open-loop and Closed- loop Eigenvalues in Third Quadrant of Complex Plane	63
9 B-52 CCV Pitch Rate Response Based on Sensor Output at BS815	83

List of Tables

Table		Page
I	States, Inputs, Disturbances and Outputs for B-52 Longitudinal-axis State-variable Model	10
II	Eigenvalue Data for Open-loop Plant	52
III	The Mode-controllability Matrix for the Open-loop System	56
IV	Open-loop and Closed-loop Structural Mode and Short-Period Mode Eigenvalue Locations with Natural Frequencies and Damping Ratios	64
V	Matrix of Magnitudes of Terms for $P_{\sim 1}$ - $\text{mag}P_{\sim 1}$	65
VI	Matrix of Magnitudes of Terms for $P_{\sim 2}$ - $\text{mag}P_{\sim 2}$	67
VII	Matrix of Magnitudes of Terms for $P_{\sim 3}$ - $\text{mag}P_{\sim 3}$	68
VIII	The Modal Controller Feedback Matrix	69
IX	Eigenvalue Data for Closed-loop Plant with Modal Controller	70
X	Summary of Specification Requirements met By Multi-stage Modal Controller	77
XI	Comparison of Measured RMS Values of Specified Accelerations and Stresses for Open-loop, Modal Controller and Optimal Controller Systems When Forced by Wind- induced Turbulence	79
XII	Percent Reductions for Normal Accelerations and Normal Stresses Due to Wind-induced Turbulence	80
XIII	Eigenvalue Data for Closed-loop Plant with Optimal Controller	84
XIV	Covariance Analysis Data from Routine NOISE for Surface Displacements and Rates for Wind-induced Turbulence and for Pilot- induced Elevator Oscillations	88

Abstract

A large-order multi-input multi-output state-variable model and design specification was recently developed for the B-52 Control Configured Vehicle (CCV) longitudinal axis. This model gives the opportunity to use modern control techniques to design the CCV concepts of interest. Previously the B-52 CCV control task was designed in increments using conventional control techniques. When the entire control problem is formulated and drawn up in one specification however, the designer's job becomes significantly more difficult. Modern control techniques are available which permit the large multi-input multi-output control problem to be addressed.

For this thesis, modal control theory is applied to the B-52 CCV state-variable model. The pertinent theory is presented and then a multi-stage design procedure is applied. Three of five available inputs are used to shift 14 of the eigenvalues associated with 39 modes. The theory and equations of three system testing techniques are also discussed and are applied to the modal control design. The performance of the modal controller is then compared with that of the open-loop system and a recently-designed optimal controller. The extensive computer program used for the modal controller design and comparison is appended to the report along with the specification.

I. Introduction

This thesis presents the results of a study to design an active control system for the B-52 Control Configured Vehicle (CCV) using modal control theory. Previous design work and flight-testing of a modified B-52 has been accomplished by the Air Force Flight Dynamics Laboratory (AFFDL) as part of their development of CCV concepts for future aircraft designs. This thesis represents a part of the continuing effort by the AFFDL to extend their CCV work, particularly in the area of using multivariable control system design techniques to design for several CCV concepts at one time.

To establish a frame of reference, this chapter provides a summary of the past CCV development work, including a short discussion of an in-house AFFDL design study which used optimal control theory. In turn, the specific problem to be addressed by this thesis is outlined, along with a discussion of the model, the scope of the project, and pertinent assumptions. The chapter concludes with an overview of the remainder of this report.

Summary of the B-52 CCV Program

The B-52 CCV program began in 1966 under the sponsorship of the AFFDL, and has evolved through several phases of design, development, and flight-testing. The project has also included an in-house AFFDL design study to encompass all of the CCV concepts in one design effort using optimal con-

trol theory.

The first portion of the B-52 CCV program started as the LAMS (Load Alleviation and Mode Stabilization) program. Its purpose was "to demonstrate the capability of an advanced flight control system (FCS) to alleviate gust loads and to control structural modes on a large flexible aircraft using existing aerodynamic control surfaces as force producers" [Ref 1:iii]. The actual LAMS-FCS was primarily designed using conventional frequency-domain control theory, but some design work was accomplished using optimal control theory. The LAMS-FCS was flight tested on a specially modified NB-52E aircraft which used existing control surfaces (rudder, ailerons, elevator, and spoilers) driven by various actuating systems, including a fly-by-wire system for LAMS-FCS evaluation purposes. The work completed under this first phase forms the basis for today's CCV concept of Fatigue Reduction (FR) and was reported in 1969 [Ref 2:2-7].

The second step in the AFFDL CCV program was started in July 1971 and included the CCV concepts of Ride Control, Maneuver Load Control, Augmented Stability, and Flutter Mode Control. The Ride Control System (RCS) included the addition of active horizontal and vertical canard surfaces near the nose of the NB-52E test aircraft. The purpose of the RCS was "to reduce the root mean square (rms) acceleration level at the pilot station by at least 30% without increasing the aircraft accelerations at other fuselage stations by more than 5%;" [Ref 2:1]. This system was successfully

flight-tested and was documented in 1973 [Ref 2;3].

The Maneuver Load Control (MLC) system performed the role of reducing wing root vertical bending moments by moving the mean aerodynamic center (MAC) of the wing inboard. The NB-52E test aircraft was modified with special three-segment flaperon control surfaces used to generate additional lift inboard. At the same time, special outboard aileron surfaces were used to reduce the lift on the outboard sections of the wing [Ref 4:3,67].

The purpose of the Augmented Stability (AS) concept in the CCV program was to provide the almost standard control function of Dutch roll damping and at the same time was to provide short-period damping when longitudinal static margins were relaxed [Ref 4:88]. This latter stability augmentation function would permit aircraft operation at aft c.g. conditions where drag-due-to-lift (also known as induced drag or trim drag) is at a minimum [Ref 4:170-182]. This relaxed static stability would then permit increased aircraft range and/or reduced power settings to maintain the same cruising speed. The rudder and the elevator were used to provide augmented stability.

The last CCV concept that was included in the B-52 CCV program was the Flutter Mode Control (FMC) system. This control system was designed to permit aircraft operation at speeds up to 30% above flutter placard speed [Ref 4:3,48]. The system was installed onboard the NB-52E test aircraft along with outboard fuel tanks which had 2000 lbs weights

installed in their nose sections. The modified tanks were used to induce a predicted flutter condition within the flight envelope at an altitude of 21,000 feet and 285 KCAS. The outboard aileron and outboard flaperon control surfaces were used to control the flutter mode and the aircraft was successfully flown at speeds of 10 to 12 knots above the artificially induced flutter speed at the test altitude [Ref 4:7].

The CCV concepts of Maneuver Load Control, Augmented Stability, and Flutter Mode Control were reported in 1975 [Ref 4]. Like the LAMS system, these systems and the RCS were designed using conventional control theory. Each was designed individually and in each case the LAMS-FCS was modified to be compatible with that particular concept. All of these concepts, except the longitudinal Augmented Stability system, have been flight-tested and shown to be successful and compatible concepts.*

In conclusion, from an advanced control system standpoint, all of these concepts proved to be realizable, but were designed individually and then implemented together. The question thus became: if all of these CCV concepts were to be designed at one time, could a successful design be realized? To answer this question, the CCV Advanced Development Program Office (ADPO) within the AFFDL undertook the task of designing a multivariable control system

* The AS system has been exercised but the benefits in terms of range improvements were not known due to flight test program termination before all tests were made [Ref 4:321].

for the B-52 CCV using optimal control theory.

Optimal Control Design

The task of designing a multiple-input, multiple-output control system can be formidable using conventional control theory and design techniques, even for low-order systems with less than ten degrees-of-freedom. In the case of the B-52 CCV, the problem is compounded by the fact that there are as many as 20 degrees-of-freedom involved in the MLC, RCS, FMC, and AS systems when considered individually and over 70 when taken together. Furthermore, the interactive effects of as many as nine sets of control surfaces makes the conventional control design even more difficult. In short, the design effort required for this type of problem dictates the use of some form of modern control theory which will handle the large-order multivariable problem.

To tackle this problem, optimal control theory was used. An optimal control computer program which was previously written by the System and Research Center of Honeywell, Inc. for the Flight Dynamics Laboratory was used [Ref 5,6]. The results of the study are presented in Reference 7. This Multi-Surface System (MSS) design problem required the reduction of the B-52 CCV equations of motion from their standard second-order differential equation form to first-order equations in matrix form relating inputs, state variables and outputs. As the same time, a quadratic cost function was chosen as a performance index and a design specification was drawn up.

Using weighting matrices that were suggested by Honeywell engineers as being good starting points, the AFFDL engineer was able to use the Honeywell computer program to successfully design a control system which met 36 of 41 longitudinal axis design goals, and met 35 of 37 lateral-directional axis design goals [Ref 7:30]. The final results represent a practical design which uses 7 sensors, 19 feedback gains, and 4 control surfaces for the longitudinal axis, and 5 sensors, 10 feedback gains, and 4 control surfaces for the lateral-directional axis [Ref 7:7].

In contrast to the achievement of a satisfactory design however, the AFFDL engineer did note certain drawbacks to the method used. In his technical memorandum, Mr. Poyneer cites four specific problems as summarized below [Ref 7:30]:

- 1) The computer programs used were too expensive due to their being general purpose routines.

- 2) The computer programs were only design tools, requiring considerable experience on the part of the engineer in using the programs and simplifying the design along the way.

- 3) The equations used in three of the programs were coupled. Thus, altering one weighting factor caused the modification of more than one system characteristic, when only one characteristic was to be changed.

- 4) The optimization performance index is based on the time domain. Therefore, the stability margins of the feedback gains were not guaranteed since stability margins are based on the frequency response and are not a part of the

optimization.

Recognizing that some of these difficulties might be overcome by a different design procedure than that of optimal control, the CCV ADPO became interested in a thesis project to achieve a realistic design using modal control theory.

Statement of the Problem

The problem posed for this thesis was to apply modal control theory to the B-52 CCV in order to achieve a design which would satisfactorily control the aircraft longitudinal axis. A comparison was to be made with the results of the previous CCV work to the largest extent possible. To provide this design and comparison, the B-52 CCV model and design specification used by Mr. Poyneer for his optimal control design was used. This was in keeping with the desire to develop an alternative to the optimal design. Further, this modal control design was restricted to the longitudinal axis because of thesis time constraints. Due to the nature of the model, the comparison of the modal design versus those developed and flight-tested for the B-52 CCV was also restricted. In this instance, the restriction was due to the flight condition used for the modal control design; not all of the previous CCV designs were based on the same condition. In the end, the thesis project was to demonstrate the practical use of modal control theory and to provide a technical comparison between the application of optimal control theory and modal control theory when applied to the CCV problem.

The B-52 CCV Model

The model of the B-52 CCV that was used for this project is the same as that used by the AFFDL for their optimal control design. The data for the model is presented in AFFDL-TM-74-138-FGB [Ref 7] and is in matrix state equation format.* The data represents linearized second-order longitudinal-axis equations of motion for a single flight condition when reduced to state equation form. A complete discussion of the procedure used to generate the model is contained in AFFDL-TM-74-138FGB and is not repeated here [Ref 7:1,3-5, 14].

The model contains coefficients for the short-period motion, the largest of 27 symmetric body-bending modes plus the steady-state residuals of the 21 smaller body-bending modes, vertical gust inputs, and symmetric operation of the elevator, flaperons, inboard and outboard ailerons, and horizontal canards. In addition, lift-growth-effects coefficients were developed from Kussner, Wagner, and R. T. Jones functions. In all, the model is represented by 39 states with 5 inputs (control surfaces), 10 outputs (sensors), and 2 disturbances [Ref 7:14-15]. An illustration of the aircraft is given in Fig. 1, and a listing of the states, inputs, outputs and disturbances is given in Table I. The flight condition represented by the model is: 260,731 lbs gross weight, 29.26% MAC center-of-gravity location, .517 Mach, 330 KCAS, and 2000 ft MSL altitude [Ref 7:13]. It is

* The data for the model is not reproduced in this report due to test and evaluation data distribution restrictions.

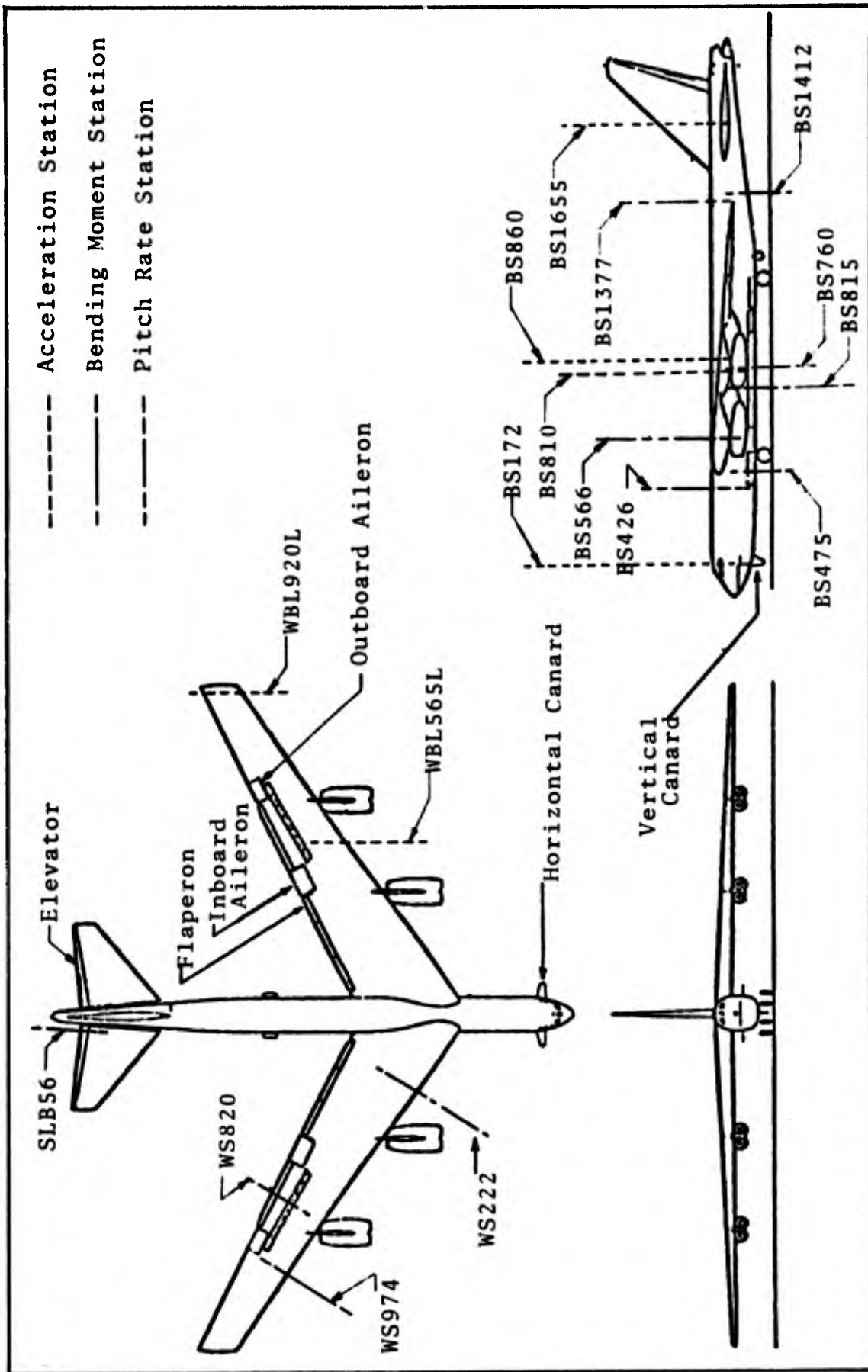


Fig. 1. B-52 CCV Control Surface, Sensor, and Bending Moment Station Locations [Adapted from Ref 2:8; 7:6]

Table I
States, Inputs, Disturbances, and Outputs for
B-52 CCV Longitudinal-axis State-variable Model

(a) System States

<u>State</u>	<u>Symbol</u>	<u>Description</u>
1	w	Vertical Velocity
2	q	Pitch Rate
3	\dot{n}_1	1st Flexible Mode Rate
4	\dot{n}_2	2nd Flexible Mode Rate
5	\dot{n}_5	5th Flexible Mode Rate
6	\dot{n}_7	7th Flexible Mode Rate
7	\dot{n}_8	8th Flexible Mode Rate
8	\dot{n}_{12}	12th Flexible Mode Rate
9	n_1	1st Flexible Mode Displacement
10	n_2	2nd Flexible Mode Displacement
11	n_5	5th Flexible Mode Displacement
12	n_7	7th Flexible Mode Displacement
13	n_8	8th Flexible Mode Displacement
14	n_{12}	12th Flexible Mode Displacement
15	\bar{n}_1	1st Flexible Wagner Mode
16	\bar{n}_2	2nd Flexible Wagner Mode
17	\bar{n}_5	5th Flexible Wagner Mode
18	\bar{n}_7	7th Flexible Wagner Mode
19	\bar{n}_8	8th Flexible Wagner Mode
20	\bar{n}_{12}	12th Flexible Wagner Mode
21	δ_e	Elevator Deflection
22	δ_f	Flaperon Deflection

[Adapted from Ref 7:32,33]

Table I - cont'd

(a) System States - cont'd

<u>State</u>	<u>Symbol</u>	<u>Description</u>
23	δ_{a_i}	Inboard Aileron Deflection
24	δ_{a_o}	Outboard Aileron Deflection
25	δ_c	Horizontal Canard Deflection
26	w_m	Vertical-velocity model
27	q_m	Pitch-rate model
28	$\frac{s}{s+2}\delta_e$	Washed-out Elevator Deflection
29	$\frac{s}{s+2}\delta_f$	Washed-out Flaperon Deflection
30	$\frac{s}{s+2}\delta_{a_i}$	Washed-out Inboard Aileron Deflection
31	$\frac{s}{s+2}\delta_{a_o}$	Washed-out Outboard Aileron Deflection
32	$\frac{s}{s+2}\delta_c$	Washed-out Horizontal Canard Deflection
33	$w_1^{(0)}$	Wind Model Output for BS600
34	$w_2^{(0)}$	Wind Model Output for BS1020
35	$w_3^{(0)}$	Wind Model Output for BS1690
36	W_g	Dryden Wind Filter Output
37	P_1	1st Kussner Lag Output
38	P_2	2nd Kussner Lag Output
39	$\hat{\delta}_{e_c}$	Pilot-input Elevator Command Model

[Adapted from Ref 7:32,33]

Table I - cont'd

(b) System Inputs

<u>Inputs</u>	<u>Symbol</u>	<u>Description</u>
1	δ_{ec}	Elevator Input
2	δ_{fc}	Flaperon Input
3	δ_{aic}	Inboard Aileron Input
4	δ_{aoc}	Outboard Aileron Input
5	δ_{cc}	Horizontal Canard Input

(c) System Disturbances

<u>Disturbance</u>	<u>Symbol</u>	<u>Description</u>
1	η_g	Wind Gust Disturbance
2	η_{δ_e}	Pilot-Induced Elevator Disturbance

(d) System Outputs

<u>Output</u>	<u>Symbol</u>	<u>Description</u>
1	N_{z172}	Normal Acceleration at BS172
2	N_{z860}	Normal Acceleration at BS860
3	N_{z1655}	Normal Acceleration at BS1655
4	$\dot{\theta}_{426}$	Pitch Rate at BS426

[Adapted from Ref 7:33,36]

Table I - cont'd

(d) System Outputs - cont'd

<u>Outputs</u>	<u>Symbol</u>	<u>Description</u>
5	N_{z810}	Normal Acceleration at BS810
6	N_{z920L}	Normal Acceleration at WBL920L
7	N_{z565L}	Normal Acceleration at WBL565L
8	$\dot{\theta}_{566}$	Pitch Rate at BS566
9	$\dot{\theta}_{815}$	Pitch Rate at BS815
10	$\dot{\theta}_{1377}$	Pitch Rate at BS1377

[Adapted from Ref 7:36]

noted that this flight condition is the same as that used for the design of the RCS [Ref 2:21].

Scope

The scope of this project was that of designing a longitudinal control system for the B-52 CCV using modal control theory. The design was accomplished for a single flight condition. The results were to be compared with those of previous designs which were based on the same flight condition. The project included researching previous work in modal control theory, developing a set of computer programs to be used as design tools, developing a concise design specification, achieving the design, proving that the design met the specification, and finally comparing the results.

Assumptions

The assumptions used for this project were the same as those used for the AFFDL optimal control design. There, the longitudinal and lateral-directional equations were assumed to be uncoupled and random turbulence inputs were simulated in each axis by the one-dimensional Dryden wind filter [Ref 7:5]. Based on these assumptions the system was modelled by the AFFDL as a linear, time-invariant, multi-input, multi-output system for a single operating point. The equations for the model as given in AFFDL-TM-74-138-FGB were used for this project and were not validated. Further, throughout this project, complete state availability was assumed, al-

though from a practical standpoint not all of the states are accessible for control purposes.

Sequence of Presentation

The following sequence is used for the remainder of this report. Chapter 2 is devoted to presenting the theory and equations which are pertinent to this project. The theory and equations presented also include items related to the testing of the design in order to show that a design meets the specification. Chapter 3 presents the design sequence as applied to the B-52 CCV. It starts with an analysis of the open-loop system and continues through the selection of an initial modal control design. Chapter 4 covers the results and comparative aspects of the project. This includes the comparison of the initial modal control design with the optimal control design, and with the designs which were based primarily on the convention control theory and were flight-tested during the B-52 CCV program. The last chapter, Chapter 5, presents recommendations and conclusions. The recommendations are primarily oriented toward possible future work in modal control design for the B-52 CCV.

II. Modal Control Theory

This chapter presents the theory and equations of modal control theory that were pertinent to this design project. At the outset, it is noted that the theory presented is only a small aspect of that available. However, there are several excellent sources in the literature which provide broader or more in-depth discussions of the theory and which are readily available. These include the work by Simon and Mitter [Ref 8], and Porter and Crossley [Ref 9]. The latter text served as a primary reference for this project.

This chapter is divided into five sections. The first summarizes the general equations of modal control theory, namely those that provide modal decomposition of the state equation and allow the designer to determine the mode-controllability and mode-observability characteristics of the system. The second section discusses the selection of a set of closed-loop eigenvalues, while the third section discusses the design procedure which was used for this thesis project: the multi-stage design procedure. The fourth section presents the theory which can be used to determine system responses to white noise disturbances, system transfer functions, and system frequency responses. The chapter concludes with a summary of the theory and introduces the material to be presented in Chapter III.

Pertinent Modal Control Theory

To provide a working definition of modal control theory,

the following is quoted from Porter and Crossley:

The central concept of modal control is very simple; it is merely that of generating the input vector of a system by linear feedback of the state vector in such a way that prescribed eigenvalues are associated with the dynamical modes of the resulting closed-loop system. [Ref 9:2]

In other words, given an open-loop system whose dynamical characteristics can be determined, the task of designing a controller becomes that of feeding back the states of the system in such a way as to alter the input vector of the system to yield a desired set of dynamical characteristics for the closed-loop system. When the controller specifically acts on the open-loop modes to yield the desired closed-loop modes, then the controller is called a modal controller.

Consider the linear time-invariant open-loop system represented by the state equation

$$\dot{\underline{x}}(t) = \underline{A}\underline{x}(t) + \underline{B}\underline{z}(t) + \underline{H}\underline{\eta}(t) \quad (1)$$

and the output equation

$$\underline{y}(t) = \underline{C}\underline{x}(t) \quad (2)$$

and illustrated in Fig. 2. Here, $\underline{x}(t)$ is the $n \times 1$ state vector, $\underline{z}(t)$ is the $r \times 1$ input vector, $\underline{\eta}(t)$ is the $m \times 1$ disturbance input vector, and $\underline{y}(t)$ is the $p \times 1$ output vector. The matrices \underline{A} , \underline{B} , \underline{H} , and \underline{C} are all real matrices, where \underline{A} is the $n \times n$ plant matrix, \underline{B} is the $n \times r$ control matrix, \underline{H} is the $n \times m$ disturbance matrix, and \underline{C} is the $p \times n$ output matrix. In this format (and throughout this report), vectors are taken to mean column vectors and row vec-

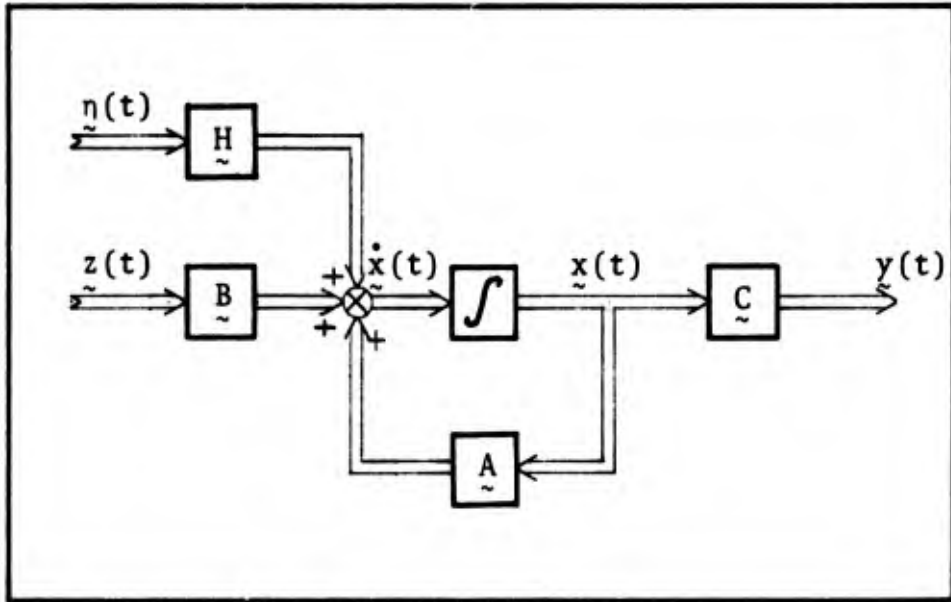


Figure 2. Open-loop System

tors are written as the transpose of a column vector; i.e., the row vector is written as \tilde{d}^T .

The dynamical modes of the open-loop system are determined from the eigenproperties of the autonomous system represented by

$$\dot{\tilde{x}}(t) = \tilde{A}\tilde{x}(t) \quad (3)$$

The eigenvalues of \tilde{A} , namely λ_i ; ($i = 1, 2, \dots, k$ where $k \leq n$), are found from the characteristic equation

$$\det[\lambda\tilde{I} - \tilde{A}] = 0 \quad (4)$$

The $n \times 1$ eigenvectors of \tilde{A} , namely \tilde{u}_i ($i = 1, 2, \dots, k$ where $k \leq n$), are found from the relationship

$$\tilde{A}\tilde{u}_i = \lambda_i\tilde{u}_i \quad (5)$$

If none of the eigenvalues are repeated, they are all con-

sidered to be "distinct" and in such a case, $k = n$. If some of the eigenvalues are repeated, then $k < n$. The first case is called a distinct eigenvalue problem, whereas the second is called a repeated eigenvalue problem. In either case, the eigenvalues may be real or complex or both.

The eigenvectors found from Eq (5) will be linearly independent; however, there may be less than n found in this manner. If n eigenvectors are found, then they constitute a basis for the state space of the system represented by Eq (3). If $k < n$, then m eigenvectors may be found, where $k \leq m < n$. In this case, a procedure to find the $n - m$ additional "eigenvectors" must be used. These vectors are called generalized eigenvectors and texts such as those by Chen, Nering, or Kwakernaak and Sivan present methods for finding them [Ref 10:39-40, 11:118-127, 12:20]. In either case, a basis formed by the eigenvectors or generalized eigenvectors must be found in order to design a modal controller. For the problem reported in this thesis, some of the eigenvalues of the open-loop system are repeated, but there are n linearly independent eigenvectors associated with those eigenvalues and no generalized eigenvectors were required to form a basis. The remainder of this section deals only with this type of problem.

Once the eigenvalues and eigenvectors of the system represented by Eq (3) are known, the mode composition of the autonomous system can be found. Consider the linear transformation

$$\underline{\underline{x}}(t) = \underline{\underline{U}}\underline{\underline{q}}(t) \quad (6)$$

When Eq (6) and its derivative are substituted into Eq (3), then the system can be represented by

$$\underline{\underline{U}}\dot{\underline{\underline{q}}}(t) = \underline{\underline{A}}\underline{\underline{U}}\underline{\underline{q}}(t) \quad (7)$$

Since $\underline{\underline{U}}$ is made up of n linearly independent vectors, it has an inverse, and Eq (7) becomes

$$\dot{\underline{\underline{q}}}(t) = \underline{\underline{U}}^{-1}\underline{\underline{A}}\underline{\underline{U}}\underline{\underline{q}}(t) \quad (8)$$

or
$$\dot{\underline{\underline{q}}}(t) = \underline{\underline{J}}\underline{\underline{q}}(t) \quad (9)$$

where
$$\underline{\underline{J}} = \underline{\underline{U}}^{-1}\underline{\underline{A}}\underline{\underline{U}} \quad (10)$$

and is of the form (for this problem)

$$\underline{\underline{J}} = \text{diag}[\lambda_1, \lambda_2, \dots, \lambda_h, \lambda_h, \dots, \lambda_k] \quad (11)$$

Eq (9) is the Jordan normal form of Eq (3) and some of the elements on the diagonal of $\underline{\underline{J}}$ are understood to be repeated as in Eq (11). In Eq (11), $\underline{\underline{J}}$ is $n \times n$, so there are n elements on the diagonal. However, some of the eigenvalues such as λ_h are repeated according to their individual multiplicities.

The individual homogeneous first-order differential equations of Eq (9) are of the form

$$\dot{q}_i(t) = \lambda_i q_i(t) \quad (12)$$

and have solutions of the form

$$q_i(t) = q_i(t_0)\exp(\lambda_i t) \quad (13)$$

where $q_i(t_0)$ is the value of the i -th element of the initial condition vector $\underline{q}(t_0)$ [Ref 9:8]. In turn, the homogeneous solution, or free response, of the system represented by Eq (3) can be found as

$$\underline{x}(t) = \sum_{i=1}^n [\exp(\lambda_i t)] \underline{u}_i \underline{v}_i^T \underline{x}(0) \quad (14)$$

where the \underline{v}_i^T row vector is the i -th row of the inverse of \underline{U} [Ref 9:8]. In Eq (14) is found the dynamical mode description which is required. The modes themselves are given by the expression $[\exp(\lambda_i t)] \underline{u}_i$. As Porter and Crossley point out: "..., the 'shape' of a mode is described by its associated eigenvector, \underline{u}_i , and its time-domain characteristics by its associated eigenvalue, λ_i :..." [Ref 9:8].

With the equations required to find the eigenproperties and modal composition of the autonomous system presented above, the mode-controllability and mode-observability characteristics are now explored. For this discussion, the open-loop system given by Eq (1), less the disturbance term, is used:

$$\dot{\underline{x}}(t) = \underline{A}\underline{x}(t) + \underline{B}\underline{z}(t) \quad (15)$$

Substituting in the transformation equation given by Eq (6), Eq (15) becomes

$$\dot{\underline{q}}(t) = \underline{J}\underline{q}(t) + \underline{P}\underline{z}(t) \quad (16)$$

where
$$\underline{P} = \underline{U}^{-1}\underline{B} \quad (17)$$

and \underline{P} is called the mode-controllability matrix.

Like the matrix \underline{B} , the matrix \underline{P} is $n \times r$, but it has complex elements if any of the eigenvalues of \underline{A} are complex. By inspecting the rows of \underline{P} , the controllable modes of the open-loop system may be determined by the following rules:

- 1) If the mode is associated with a non-repeated eigenvalue, then that j -th mode is controllable by the k -th input, $z_k(t)$, if the k -th element of the j -th row of \underline{P} is non-zero; i.e., $p_{jk} \neq 0$.
- 2) If the mode is associated with a Jordan block in \underline{J} , and the repeated eigenvalue λ_j appears only in this block*, then that block is controllable by the k -th input if the k -th element of the row of \underline{P} associated with the last row of the Jordan block is non-zero. Furthermore, that block is partially controllable if the k -th element in the last row is zero but at least one of the remaining elements in the k -th column of the block of rows of \underline{P} associated with the Jordan block is non-zero. The block is uncontrollable by the k -th input if all of the elements of that k -th column are zero [Ref 9:47].
- 3) If the mode is associated with a Jordan block in \underline{J} , and there are other Jordan blocks associated with that eigenvalue, λ_j , then all of these blocks are considered collectively and they are "...controllable by the input vector $\underline{z}(t)$ if and only if all the rows of the mode-controllability matrix which correspond to the last rows

* Porter and Crossley label these blocks as "distinct Jordan blocks" [Ref 9:47].

of its constituent Jordan blocks are linearly independent:..."[Ref 9:49]. As a consequence, the minimum number of inputs required to control all of the Jordan blocks associated with a particular λ_j is the same as the number of blocks [Ref 8:322].

An excellent illustration of these rules is provided by Chen [Ref 10: 192-194]. These three rules permit the designer to determine the controllability of the modes of a system. This knowledge of controllability is required if the modes of the system are to be modified by a modal controller; that is, if a mode is to be modified by feedback, then it must be controllable. It is noted that in the problem used for this thesis, the controllability of all of the modes can be determined by rules (1) and (3).

Attention is now turned to the mode-observability of a system. Here, the transformation given by Eq (6) is substituted into the output equation, Eq (2), to yield

$$\underline{y}(t) = \underline{R}\underline{q}(t) \quad (18)$$

where
$$\underline{R} = \underline{C}\underline{U} \quad (19)$$

and \underline{R} is called the mode-observability matrix.

Parallel to the discussion of the mode-controllability matrix, it is noted that the mode-observability matrix contains complex elements if any of the eigenvalues of \underline{A} are complex. Also, \underline{R} is $p \times n$, as is \underline{C} . Furthermore, there are three rules for determining the observability of the modes, but here the columns of \underline{R} are considered instead of the rows

of \underline{P} , and the k -th output is of importance rather than the k -th input. Because the rules for determining mode-observability are the dual of the rules for determining mode-controllability, the rules are not given here except rule 1) as an example: If the mode is associated with a non-repeated eigenvalue, then that j -th mode is observable in the k -th output, $y_k(t)$, if the k -th element of the j -th column of \underline{R} is non-zero; i.e., $r_{kj} \neq 0$.

For the problem of modal control using linear feedback of the states, knowledge of mode-observability is of less importance than that of mode-controllability. Assuming all states are available, then in general, the ability to observe the modes in the output is required only to the extent necessary to insure that overall output specifications have been met. This is the case for the problem at hand, and thus information on mode-observability is required.

Selection of the Closed-loop Eigenvalues

With the basic equations given above, the criteria that might be considered in the selection of a set of closed-loop eigenvalues are now discussed. Having found the eigenvalues and eigenvectors of the open-loop system, and having determined the mode-controllability and mode-observability characteristics of the system, the eigenvalues which are to be modified can be assigned their closed-loop values. The selection criteria for the desired closed-loop eigenvalues may be based on stability requirements, on closed-loop damping requirements, on changing natural or damped frequencies, on

a requirement to cancel an open-loop zero of a transfer function, or other reasons associated with a particular system. The open-loop eigenvalues associated with the observable and controllable modes are the poles of the open-loop transfer functions of the system, and relocation of these poles may be to the designer's advantage. Whatever the specific criteria may be, however, the underlying requirement is that of shifting the eigenvalues to their new, closed-loop locations in the complex plane "...in such a way that those prescribed eigenvalues are associated with the dynamical modes of the resulting closed-loop system" [Ref 9:2].

There are two basic problems in selecting the closed-loop eigenvalues. The first problem deals with the question of how they are to be selected, and the second deals with the limitations that must be realized in making the selections. The method of first establishing design requirements or specifications and then translating them into a list of desired closed-loop eigenvalues is not, in general, discussed in the technical literature for large scale multi-output systems. After a review of the literature, only two sources were found which dealt with the subject of how the closed-loop eigenvalues might be selected [Ref 13:89-92; 14:Chapter 12]. The design of a modal controller requires the selection of a set of desired closed-loop eigenvalues, and the designer must use his own judgment in applying the limited guidelines available in making the selection. The method used for this thesis problem is discussed in Chapter III.

The second problem in selecting a set of eigenvalues has to do with the limitation of influencing only the eigenvalue part of the closed-loop modal response of the system. Recall Eq (14)

$$\underline{x}(t) = \sum_{i=1}^n [\exp(\lambda_i t)] \underline{u}_i \underline{v}_i^T \underline{x}(0) \quad (14)$$

where the modes of the system are given by the expression $[\exp(\lambda_i t)] \underline{u}_i$. For the closed-loop system, these λ_i 's are the closed-loop eigenvalues. In effect, the designer is limited to directly influencing only the eigenvalues in his desire to achieve a satisfactory closed-loop system. The designer does not have direct control over the mode shapes (the eigenvectors, \underline{u}_i) which influence the overall time response. This is not to say that the mode shapes cannot be changed, but it does say that a series of designs by trial-and-error may be necessary.

With the modal analysis equations previously stated and a list of selected closed-loop eigenvalues in hand, a modal controller design procedure must be found. The purpose of the procedure is to systematically determine the appropriate controller which shifts the eigenvalues and causes the closed-loop system to meet the design specification. Numerous design procedures are available in the technical literature, and several are presented in the text by Porter and Crossley [Ref 9:Chapter 6]. For this project, all but two of the available procedures were quickly eliminated for one reason or another. Of these two, one was the "dyadic modal control-

ler" design procedure given by Porter and Crossley. It was initially selected as an appropriate procedure due to its ease of implementation and because it did provide some insight into the behavior of the open-loop system. However, it was ultimately rejected due to its reliance on a lack of inherent coupling between system inputs (control surfaces in this case). That is to say, the dyadic modal controller design procedure determines a feedback matrix which has the effect of changing the open-loop multiple-input system to a closed-loop single-input system with fixed "gearing" or ratios between input signals. For this procedure to work effectively, there can be no existing inherent coupling or gearing between inputs. Unfortunately, the B-52 CCV model does reflect input coupling, both structurally and aerodynamically. Thus, the dyadic modal controller procedure was rejected. The other procedure which was initially considered is the one which was used for this project. Porter and Crossley call this procedure the "multi-stage design procedure" and the theory of its use is presented next.

The Multi-stage Modal Controller

This section presents the theory behind the multi-stage design procedure and is based on material given by Porter and Crossley [Ref 9:92-93]. The procedure essentially treats the open-loop system as a series of single-input systems and is readily coded for computer-aided design work.

For the multi-stage or sequentially-designed modal controller, the system equation Eq (15), is rewritten in summa-

tion form:

$$\dot{\underline{x}}(t) = \underline{A}\underline{x}(t) + \sum_{i=1}^r \underline{b}_i z_i(t) \quad (20)$$

where the \underline{b}_i vectors are the columns of the open-loop control matrix. The sequential design procedure starts with the selection of a control law

$$z_j(t) = \underline{k}_j^T \underline{x}(t) \quad (21)$$

based on using just one of the available inputs $z_j(t)$ to shift certain of the open-loop eigenvalues to new locations. This control law is then used to close a minor loop, so to speak, and a new system equation is formed

$$\underline{\dot{x}}(t) = \hat{\underline{A}}\underline{x}(t) + \sum_{\substack{i=1 \\ i \neq j}}^r \underline{b}_i z_i(t) \quad (22)$$

where

$$\hat{\underline{A}} = \underline{A} + \underline{b}_j \underline{k}_j^T \quad (23)$$

The procedure is repeated sequentially until all of the eigenvalues are shifted. When the sequence is completed, the resulting closed-loop plant is

$$\hat{\underline{A}} = \underline{A} + \sum_{i=1}^{\ell} \underline{b}_{j_i} \underline{k}_i^T \quad (24)$$

where ℓ is the number of inputs used and \underline{b}_{j_i} is the control vector used for the i -th stage of design. This closed-loop plant has the desired eigenvectors.

To use this multi-stage design technique, the problem becomes one of prescribing the closed-loop eigenvalues, of determining with inputs should be used to shift which eigen-

values, and of finding the k_i vectors. The order of the use of the inputs is also a variable and should be considered. Porter and Crossley present an example of using the inputs in their numerical order in the input vector $z(t)$ [Ref 9: 92-93]. This may serve as a starting point and then other orderings can be tried if not satisfactory.

Assuming the closed-loop eigenvalues have been selected, Porter and Crossley suggest inspection of the mode-controlability matrix to determine which inputs to use for which eigenvalue shifts. Their inspection technique is to determine the magnitudes of the elements in the \tilde{P} matrix which correspond to the eigenvalues to be shifted. If input #1 is to be used first, use it to shift those modes where the largest of the elements in a row of the array of magnitudes appears in the first column (the rows being considered are the same as the rows corresponding to the eigenvalues to be shifted) [Ref 9:92-93]. With these decisions made, the control law for the first input can be found.

To determine the control law, a single-input feedback vector is required and is given by

$$k_i^T = \sum_{j=1}^m \frac{\prod_{k=1}^m (\rho_k - \lambda_j) v_j^{(i)T}}{p_i \prod_{\substack{k=1 \\ k \neq j}}^m (\lambda_k - \lambda_j)} \quad (25)$$

where (1) i is the number of the stage being designed, (2) m is the total number of eigenvalues to be shifted, (3) ρ_k is the value of the k -th desired closed-loop eigenvalue at

this point in the design, (4) λ_j is the value of the j -th current open-loop eigenvalue, (5) $\underline{v}_j^{(i)T}$ is the j -th row of the \underline{U}^{-1} matrix associated with the i -th stage of the design, and (6) p_i is the scalar product of $\underline{v}_j^{(i)T}$ and \underline{b}_i :

$$p_i = \underline{v}_j^{(i)T} \underline{b}_i \quad (26)$$

For the first iteration of the design then, the eigenvalues of the open-loop plant and the eigenvalues of the plant given by Eq (23) for $j = 1$ are the same except for the eigenvalues to be shifted by the first input. Also, the $\underline{v}_j^{(1)}$ vectors are based on the original open-loop plant and its associated \underline{U}^{-1} matrix. Furthermore, the value of p_i will depend on $\underline{v}_j^{(i)}$ and on the column of \underline{B} associated with the input being used, and is determined from Eq (26). All of these parameters are updated at each stage of the design. For example, for the second stage, the "open-loop" eigenvalues (the λ_j 's) will be the same as the eigenvalues just found for $\hat{\underline{A}}$ of Eq (23), and the eigenvalues for the plant given by Eq (24) for $\ell = 2$ (the ρ_k 's) will be the same as the eigenvalues of $\hat{\underline{A}}$ except for the eigenvalues to be shifted by the second input. Similarly, the $\underline{v}_j^{(2)}$ vectors are also based on the inverse of the modal matrix associated with the plant represented by Eq (23).

The mode-controllability matrix is also updated at each stage. For the second stage, the revised inverse of the modal matrix is used, but only the remaining $r-1$ columns of \underline{B} are considered. At the same time, only those rows of \underline{P} cor-

responding to the yet-to-be-changed eigenvalues are inspected for relative magnitudes. From these magnitudes, the second input to be used is selected, and the entire design procedure is repeated until all of the eigenvalues are shifted. An excellent example of this procedure is provided by Pai, et. al. [Ref 13].

When the designer completes the final iteration of his design, it is ready to be tested to see if it meets the design specification. If it does not, then the design may require reiterating with a different set of prescribed closed-loop eigenvalues, or with a different ordering of the sequence in which the inputs are used. As with most all of the various modal controller design techniques, the multi-stage modal controller provides an infinity of design choices. For the multi-stage modal controller, the choices to be made are between the lists of eigenvalues and the lists of input sequences. Figure 3 illustrates the multi-stage design in block diagram form.

Testing the Design

When the design of the modal controller has been selected, with a feedback matrix or set of feedback vectors having been found, the closed-loop system is tested to show that it does or does not comply with the design specification. In general this means that system responses to prescribed input signals are to be found and compared with similar responses for the open-loop system. For this thesis project the inputs were in the form of random gust disturbances, random pilot-

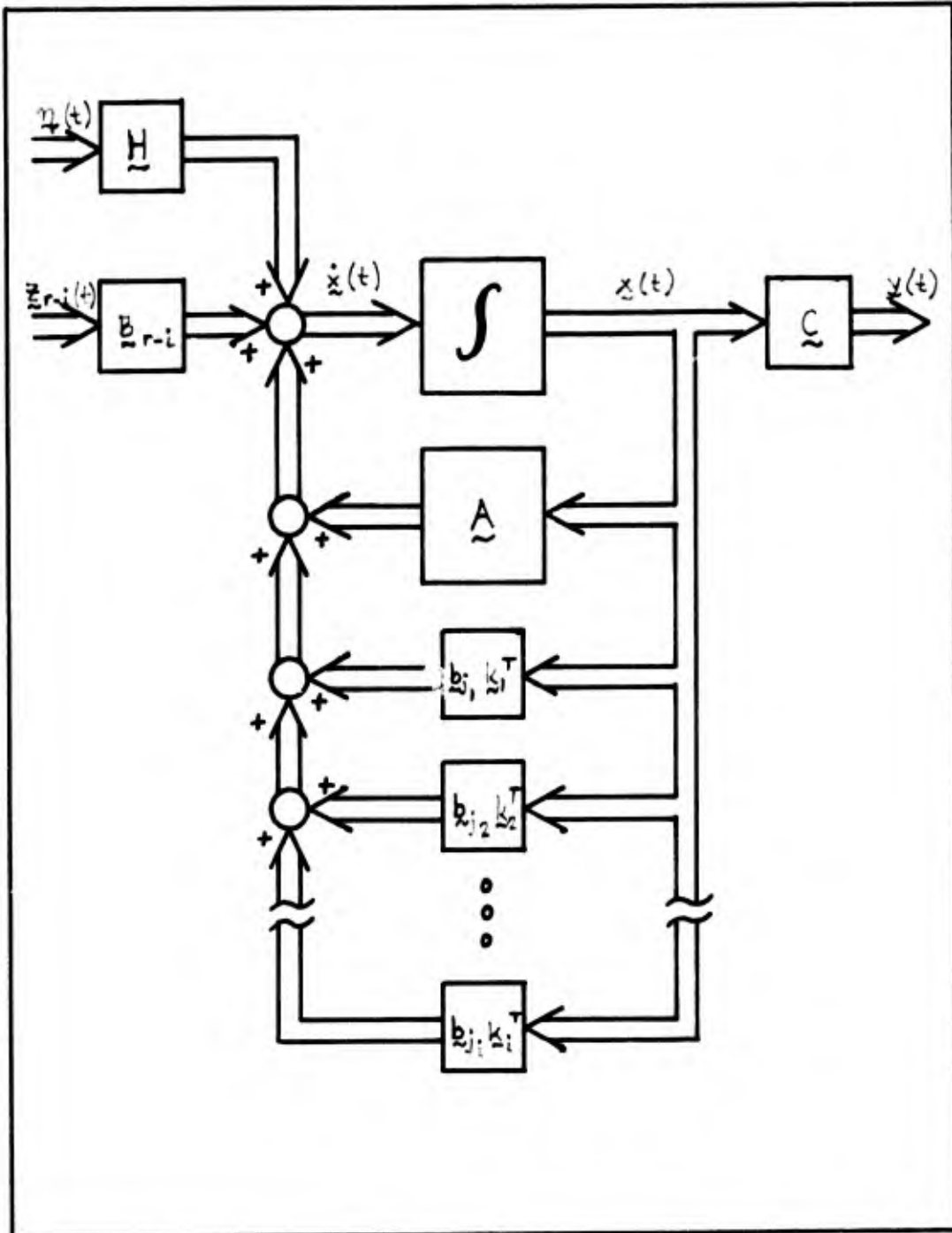


Fig. 3. Multi-stage Modal Controller

induced elevator disturbances, or step elevator disturbances. The outputs were the sensed accelerations, sensed pitch rates, calculated stresses induced by the disturbances, or control surface deflections and deflection rates. In addition, the closed-loop system must exhibit minimum levels of phase margin and gain margin as stability considerations. The question then becomes: How is the system to be tested? This section provides answers to that question.

To be more specific, this section presents the three different methods that were used in this project to test the closed-loop system. First, for the responses to random gust or pilot-induced disturbances, a covariance analysis was used. Second, to check the system response to a step elevator response, transfer function analysis was used. Third, to check the stability of the control loops, a frequency response analysis was made. The theory and methodology behind each of these methods is now presented.

Covariance Analysis. To determine the response of the closed-loop system at various body and wing stations to random inputs, a covariance analysis is used. For a zero-mean, Gaussian, white noise input, which is the type of random input considered here, a covariance analysis can determine the rms values of the states of the system. In turn, linear combinations of the states are formed as transformations of the states into sensor outputs, stresses, or control surface deflections and deflection rates. The following discussion provides more detail for such a covariance analysis.

First, the state equation, Eq (1) is recalled:

$$\dot{\underline{x}}(t) = \underline{A}\underline{x}(t) + \underline{B}\underline{z}(t) + \underline{H}\underline{\eta}(t) \quad (1)$$

For this thesis, $\underline{\eta}(t)$ consists of two different disturbances, either $\eta_1(t)$ or $\eta_2(t)$, where $\eta_1(t)$ is defined as an 8 fps rms random gust, and $\eta_2(t)$ is defined as a 0.1 rad rms random pilot-induced elevator deflection. Also, these disturbances are considered individually; that is, one disturbance is present at a time. Therefore, $E\{\underline{\eta}(t)\underline{\eta}(t+\tau)\} = E\{\eta_1(t)\eta_1(t+\tau)\} = Q_1d(\tau)$ with $Q_1 = (8)^2$, or $E\{\underline{\eta}(t)\underline{\eta}(t+\tau)\} = E\{\eta_2(t)\eta_2(t+\tau)\} = Q_2d(\tau)$ with $Q_2 = (0.1)^2$. Finally, the input vector $\underline{z}(t)$ is assumed to be zero for the analysis. Eq (1) then reduces to the single-input linear differential equation given by

$$\dot{\underline{x}}(t) = \underline{A}\underline{x}(t) + \underline{h}\eta(t) \quad (27)$$

where \underline{h} is the appropriate column of \underline{H} for $\eta(t) = \eta_1(t)$ or $\eta(t) = \eta_2(t)$.

A proper solution to Eq (27) can be obtained by considering it a notational variation of the stochastic linear differential equation:

$$d\underline{x}(t) = \underline{A}\underline{x}(t)dt + \underline{h}d\beta(t) \quad (28)$$

In Eq (28), $d\beta(t)$ is the differential of a scalar Brownian motion process, and $\beta(t)$, the Brownian motion, is said to have diffusion strength $Q(t)$, corresponding to the white noise strength described previously. The solution of Eq (28) is known and can be shown to have the form

$$\underline{x}(t) = \underline{\phi}(t, t_0) \underline{x}(t_0) + \int_{t_0}^t \underline{\phi}(t, \tau) \underline{h} d\beta(\tau) \quad (29)$$

where $\underline{\phi}(t, t_0)$ is the state transition matrix.

At this point, two basic approaches to using Eq (29) to determine $\underline{x}(t)$ can be used: A Monte Carlo approach which develops individual process samples that can be averaged to obtain statistical characteristics, or a covariance analysis which yields the rms values of the states for a rms disturbance; the latter approach is used. From Eq (29), the "expected" or "mean" value of the states for the system becomes

$$E\{\underline{x}(t)\} = \underline{\phi}(t, t_0) E\{\underline{x}(t_0)\} + E\left\{\int_{t_0}^t \underline{\phi}(t, \tau) \underline{h} d\beta(\tau)\right\} \quad (30)$$

and the mean square is written as

$$\begin{aligned} E\{\underline{x}(t)\underline{x}^T(t)\} &= \underline{\phi}(t, t_0) E\{\underline{x}(t_0)\underline{x}^T(t_0)\} \underline{\phi}^T(t, t_0) \\ &+ \int_{t_0}^t \underline{\phi}(t, \tau) \underline{h} Q(\tau) \underline{h}^T \underline{\phi}^T(t, \tau) d\tau \end{aligned} \quad (31)$$

The integral on the right hand side of Eq (31) is now an ordinary integral.

Under the premise of zero-mean noise and zero mean $\underline{x}(t_0)$, the covariance matrix is written as

$$\underline{P}_X(t) = E\{\underline{x}(t)\underline{x}^T(t)\} \quad (32)$$

For $t = t_0$, Eq (32) becomes

$$\underline{P}_X(t_0) = E\{\underline{x}(t_0)\underline{x}^T(t_0)\} \quad (33)$$

Using Eqs (32) and (33), Eq (31) becomes

$$\begin{aligned} \underline{P}_X(t) &= \underline{\phi}(t, t_0) \underline{P}_X(t_0) \underline{\phi}^T(t, t_0) \\ &+ \int_{t_0}^t \underline{\phi}(t, \tau) \underline{h} Q(\tau) \underline{h}^T \underline{\phi}^T(t, \tau) d\tau \end{aligned} \quad (34)$$

At this point, it is noted that if $\underline{x}(t_0)$ is known exactly, or is a Gaussian random variable, then the solution to Eq (28) is a Gaussian process where the mean and covariance completely determine the density function of $\underline{x}(t)$. That is, the rms values of the states as a function of time can be determined as the square roots of the diagonal elements of $\underline{P}_X(t)$.

To obtain the covariance matrix, the system is observed at fixed intervals of time, ΔT . Then $\underline{\phi}(t_i + \Delta T, t_i)$ is a fixed matrix, which is evaluated once to give

$$\underline{\phi}(t_i + \Delta T, t_i) = \underline{\phi} = \exp [\underline{A}(\Delta T)] \quad (35)$$

Furthermore, the integral on the right of Eq (34) is also evaluated once to give

$$\underline{W} = \int_{t_i}^{t_i + \Delta T} \underline{\phi}(t, \tau) \underline{h}Q(\tau) \underline{h}^T \underline{\phi}^T(t, \tau) d\tau \quad (36)$$

where $Q(\tau)$ is fixed for the specific disturbance considered here. Finally, the covariance matrix, $\underline{P}_X(t_0)$ is zero since $\underline{x}(t_0)$ is zero and Eq (33) holds. Substituting Eqs (35) and (36) into Eq (34) yields

$$\underline{P}_X(t_1) = \underline{W} \quad (37)$$

and

$$\underline{P}_X(t_{i+1}) = \underline{\phi} \underline{P}_X(t_i) \underline{\phi}^T + \underline{W} \quad (38)$$

where Eq (38) is a linear difference equation. On an iterative basis then, $\underline{P}_X(t_{i+1})$ can be calculated. In turn, the rms values of the states are found by determining the square

roots of the diagonal elements of $P_x(t_{i+1})$:

$$x_{j \text{ RMS}}(t_{i+1}) = [P_{x_{jj}}(t_{i+1})]^{1/2} \quad (39)$$

For this thesis project, certain of the specification parameters are stated in terms of the rms values of specific states. When this is true, those states can be evaluated directly from Eq (29). Certain other specifications are stated in terms of the rms values of the system outputs, $y_{\text{RMS}}(t)$. When this is the case, Eqs (37) and (38) must be extended. The mean square of the output vector is $E\{y(t)y^T(t)\}$. Using the relationship of Eq (2) yields

$$E\{y(t)y^T(t)\} = E\{[Cx(t)][Cx(t)]^T\} \quad (40)$$

or

$$E\{y(t)y^T(t)\} = C E\{x(t)x^T(t)\}C^T \quad (41)$$

Substituting Eq (32) into Eq (41) and taking the square root gives the desired result:

$$y_{j \text{ RMS}}(t_{i+1}) = \{\text{diag}[C P_x(t_{i+1})C^T]\}^{1/2} \quad (42)$$

Eq (42) can be generalized to cover other measurements in addition to sensors. These measurements could be internal structural stresses or most any other "output" which from a deterministic standpoint can be represented in the form of Eq (2). The specific manner in which this covariance analysis was used for this project is discussed in Chapter III.

Transfer Function Analysis. The previous subsection presented a development of covariance analysis for use in determining the response of a system to stochastic (random)

disturbances of a special type. This subsection and the next present developments of two types of analysis for use in determining the response of a system to deterministic (analytic) disturbances. This subsection gives the equations necessary to obtain the system transfer matrix, $\underline{G}(s)$ in partial-fraction expansion form, and in turn to obtain the system output equations as functions of time for unit step-input disturbances.

Consider the state equation which represents a system with only analytic disturbance inputs:

$$\dot{\underline{x}}(t) = \underline{A}\underline{x}(t) + \underline{H}\eta(t) \quad (43)$$

The output equation remains $y(t) = \underline{C}\underline{x}(t)$. The Laplace operator notation is adopted and Eq (43), when transformed, becomes

$$s\underline{X}(s) = \underline{A}\underline{X}(s) + \underline{H}\eta(s) \quad (44)$$

where zero initial conditions are assumed. Further manipulation yields

$$\underline{X}(s) = [s\underline{I} - \underline{A}]^{-1}\underline{H}\eta(s) \quad (45)$$

where the matrix $[s\underline{I} - \underline{A}]$ is assumed to be non-singular.

The Laplace transform of the output equation is

$$\underline{Y}(s) = \underline{C}\underline{X}(s) \quad (46)$$

Combining Eqs (45) and (46) gives the usual transfer matrix representation of the system:

$$\underline{\tilde{G}}(s) = \frac{\underline{\tilde{Y}}(s)}{\underline{\tilde{\eta}}(s)} = \underline{\tilde{C}} [s\underline{\tilde{I}} - \underline{\tilde{A}}]^{-1} \underline{\tilde{H}} \quad (47)$$

Unfortunately, this form of the system transfer matrix is difficult to handle on the computer, therefore a similarity transformation is performed.

Consider the term $[s\underline{\tilde{I}} - \underline{\tilde{A}}]^{-1}$ which is commonly called the resolvent matrix and appears on the right side of Eq (47). Using the identity

$$\underline{\tilde{U}} \underline{\tilde{U}}^{-1} = \underline{\tilde{I}} \quad (48)$$

Eq (10) is rewritten as

$$\underline{\tilde{A}} = \underline{\tilde{U}} \underline{\tilde{J}} \underline{\tilde{U}}^{-1} \quad (49)$$

Substituting Eqs (48) and (49) into the resolvent matrix and rearranging terms gives

$$[s\underline{\tilde{I}} - \underline{\tilde{A}}]^{-1} = [\underline{\tilde{U}}(s\underline{\tilde{I}} - \underline{\tilde{J}})\underline{\tilde{U}}^{-1}]^{-1} \quad (50)$$

Using the identity $(FG)^{-1} = G^{-1} F^{-1}$, Eq (50) becomes

$$[s\underline{\tilde{I}} - \underline{\tilde{A}}]^{-1} = \underline{\tilde{U}} [s\underline{\tilde{I}} - \underline{\tilde{J}}]^{-1} \underline{\tilde{U}}^{-1} \quad (51)$$

Substitution of Eq (51) into Eq (47) yields a more useful form of the transfer matrix:

$$\underline{\tilde{G}}(s) = \underline{\tilde{C}} \underline{\tilde{U}} [s\underline{\tilde{I}} - \underline{\tilde{J}}]^{-1} \underline{\tilde{U}}^{-1} \underline{\tilde{H}} \quad (52)$$

Using Eq (19) and the definition $\underline{\tilde{T}} = \underline{\tilde{U}}^{-1} \underline{\tilde{H}}$, Eq (52) can be modified to a form which is easily coded for computer-aided transfer function analysis, especially when $\underline{\tilde{J}}$ is a diagonal

matrix. Then Eq (52) becomes

$$\tilde{G}(s) = \tilde{R} [s\tilde{I} - \tilde{J}]^{-1} \tilde{T} \quad (53)$$

where $[s\tilde{I} - \tilde{J}]^{-1}$ is of the form

$$[s\tilde{I} - \tilde{J}]^{-1} = \begin{bmatrix} \frac{1}{s - \lambda_1} & & & & & \\ & \frac{1}{s - \lambda_2} & & & & \\ & & \ddots & & & \\ & & & \frac{1}{s - \lambda_h} & & \\ & & & & \frac{1}{s - \lambda_h} & \\ & & & & & \ddots \\ & & & & & & \frac{1}{s - \lambda_k} \end{bmatrix} \quad (54)$$

and where for the problem in this thesis, there are no ones on the super-diagonal of Eq (54), but some of the diagonal elements are repeated [Ref 15:259-260].

Consider that the elements of \tilde{R} are r_{ij} and the elements of \tilde{T} are t_{ij} . Multiplying-out the right hand side of Eq (53) yields a $p \times m$ transfer matrix of partial-fraction expansions whose elements are of the form

$$\frac{Y_i(s)}{\eta_j(s)} = G_{ji}(s) = \frac{r_{1j} t_{i1}}{s - \lambda_1} + \frac{r_{2j} t_{i2}}{s - \lambda_2} + \dots + \frac{r_{nj} t_{in}}{s - \lambda_k} \quad (55)$$

An inspection of Eq (55) reveals that the right hand side is the sum of n first-order terms, with some of the terms hav-

ing identical denominator factors where there are repeated eigenvalues. It is also seen that the numerators of the individual terms are scalar products of the appropriate elements of the R and T matrices, and these scalars are in fact the residues of the poles of the transfer functions; they are also commonly known as the coefficients of the partial-fraction expansion terms. The terms with identical denominators can be combined to complete the partial-fraction expansion process and Eq (52) becomes

$$G_{ji}(s) = \sum_{\ell=1}^k \frac{A_{\ell}}{s - \lambda_{\ell}} \quad (56)$$

where $A_{\ell} = r_{j\ell} t_{\ell i}$ if λ_{ℓ} is not repeated, or $A_{\ell} = r_{jh} t_{hi} + r_{j(h+1)} t_{(h+1)i} + \dots + r_{j(h+g-1)} t_{(h+g-1)i}$ if $\lambda_{\ell} = \lambda_h$ and λ_h is a repeated value of multiplicity g .

To complete the time response calculations, Eq (56) may be multiplied by the Laplace transform of the unit-step input to yield the output equation in Laplace form for $\lambda_{\ell} \neq 0$:

$$Y_j(s) = \frac{B}{s} + \sum_{\ell=1}^k \frac{B_{\ell}}{s - \lambda_{\ell}} \quad (57)$$

where, in general, the A_{ℓ} 's of Eq (56) are not the B_{ℓ} 's of Eq (57). The inverse-Laplace transform of Eq (57) gives the desired output as a function of time.

$$y_j(t) = B + \sum_{\ell=1}^k B_{\ell} \exp(\lambda_{\ell} t) \quad (58)$$

The solution of Eq (58) for the range of values of t that are of interest gives the output at that time. Eq (58) also shows that the steady-state value of $y_i(t)$ is B if all the

λ_{ℓ} 's have negative real parts. This concludes the development of the equations which may be used to obtain the time response of the system to an analytic input using transfer functions and the inverse Laplace transform.

Frequency Response Analysis. The previous two subsections present the theory used in this thesis for covariance analysis and transfer function analysis. This subsection concludes the material on testing the design by presenting the theory for obtaining frequency response information about the closed-loop multi-stage modal controller system.

The open-loop system equation is recalled:

$$\dot{\tilde{x}}(t) = \tilde{A}\tilde{x}(t) + \tilde{B}z(t) \quad (15)$$

For the multi-stage modal controller problem, Eq (15) was rewritten as Eq (20):

$$\dot{\tilde{x}}(t) = \tilde{A}\tilde{x}(t) + \sum_{i=1}^r \tilde{b}_i z_i(t) \quad (20)$$

For the closed-loop system, the plant was found as Eq (24):

$$\hat{A} = \tilde{A} + \sum_{i=1}^{\ell} \tilde{b}_j \tilde{k}_i^T \quad (24)$$

The closed-loop system is illustrated in Fig. 4a.

For the frequency response of one control loop, that loop is broken and the "signal" from the particular gain vector, \tilde{k}_h^T , is routed to an external point for measurement. Simultaneously, the path for that input which goes through the corresponding control vector, \tilde{b}_g , is used as an input path for the incoming sinusoidal signal. This concept is

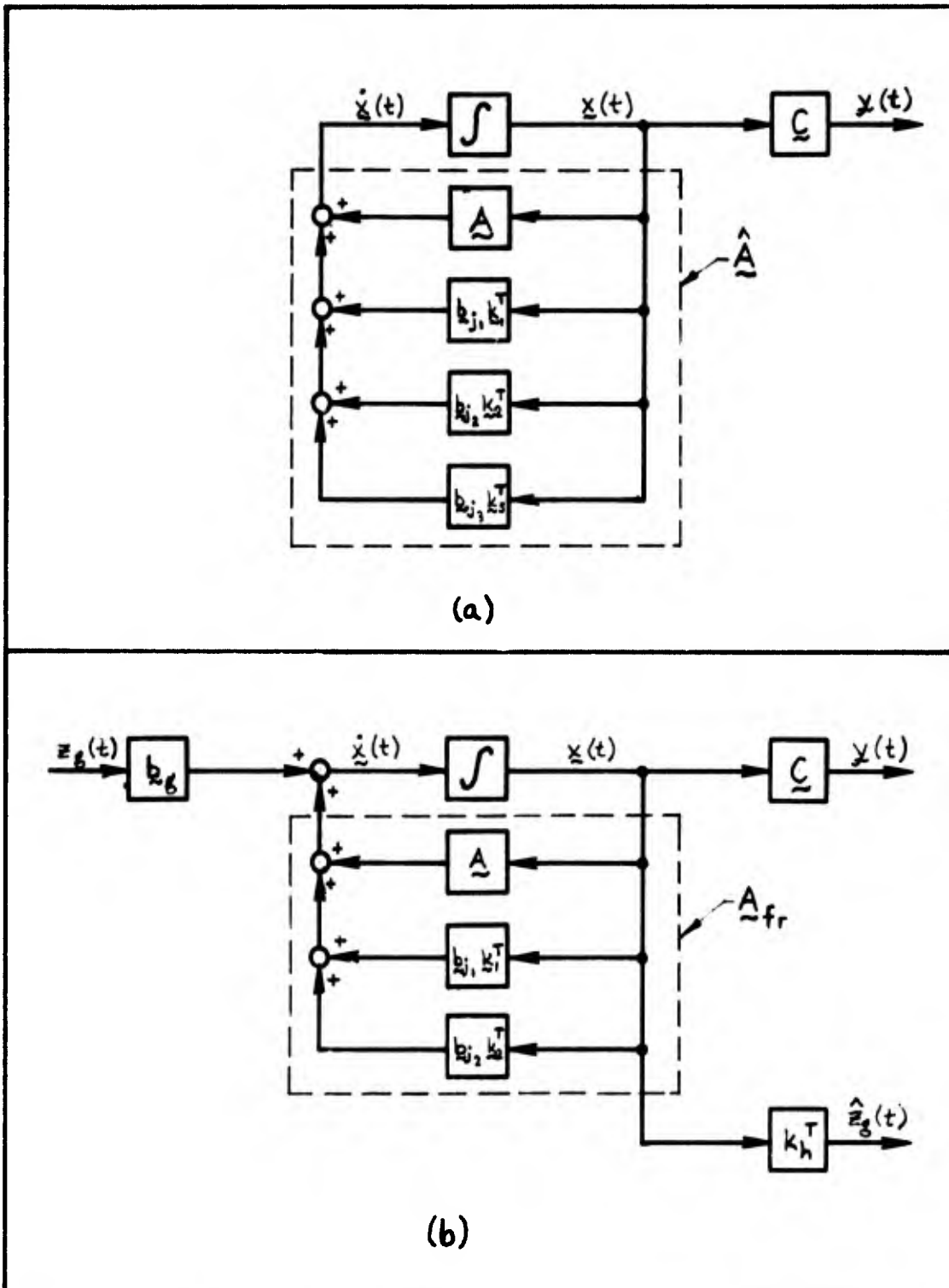


Fig. 4. Block Diagrams for Frequency Response

illustrated in Fig. 4b.

With the control loop of interest broken as in Fig. 4b, Eq (24) can be reformulated as

$$\hat{\underline{A}} = \underline{A}_{fr} + \underline{b}_g \underline{k}_h^T \quad (59)$$

where \underline{A}_{fr} is the plant matrix of the system shown in Fig. 4b, and \underline{b}_g is the control vector and \underline{k}_h^T is the gain vector of interest. Rearranging Eq (59) and substituting it into Eq (20) gives the desired form of the state equation for a frequency response evaluation:

$$\dot{\underline{x}}(t) = \underline{A}_{fr} \underline{x}(t) + \underline{b}_g z_g(t) \quad (60)$$

The output equation is written as

$$\hat{z}_g(t) = \underline{k}_h^T \underline{x}(t) \quad (61)$$

Next, a modal analysis of \underline{A}_{fr} is performed and the eigenvalues, the modal matrix, and the inverse of the modal matrix are found. Using the Laplace operator and the form of Eq (49), the transfer function for the ratio of the output $\hat{z}_g(s)$ to the input $z_g(s)$ becomes

$$G(s) = \underline{k}_h^T \underline{U}_{fr} [s\underline{I} - \underline{J}_{fr}]^{-1} \underline{U}_{fr}^{-1} \underline{b}_g \quad (62)$$

where \underline{J}_{fr} is the Jordan normal form of \underline{A}_{fr} and is diagonal. The transfer function, $G(s)$, appears in partial-fraction expansion form and has as many terms as there are distinct eigenvalues with non-zero residues. Hence Eq (62) can be written in the form

$$G(s) = \frac{R_1}{s - \lambda_1} + \frac{R_2}{s - \lambda_2} + \dots + \frac{R_k}{s - \lambda_k} \quad (63)$$

where some of the residues, R_j , may be zero. In addition, the residues will be complex if the corresponding eigenvalue, λ_j , is complex. Substituting $j\omega = s$ into Eq (63) gives

$$\bar{G}(j\omega) = \frac{R_1}{-\lambda_1 + j\omega} + \frac{R_2}{-\lambda_2 + j\omega} + \dots + \frac{R_k}{-\lambda_k + j\omega} \quad (64)$$

Using values of ω of interest, Eq (64) can be solved to yield magnitude and phase data. From this data, log-magnitude and phase information is obtained to determine gain margins and phase margins for the control loop so evaluated. Selection of other control loops with their associated control and gain vectors permits a frequency response analysis to be performed for any of the control loops of the multi-stage modal controller.

It should be explained that the above technique does not yield useful information about the open-loop system which does not have any feedback paths. Furthermore, useful information about other types of controllers, modal or otherwise, is not obtainable by this method unless those controllers have specific gain vectors fed back to each individual controller. The above method is limited to those systems which can be expressed in the form of Eq (20) and subsequently in the form of Eqs (61) and (62). The use of this frequency response analysis is presented in Chapter III.

This second chapter has presented the theory of modal control as applicable to this thesis project. Specifically,

the subjects of modal analysis, closed-loop eigenvalue selection, multi-stage modal controllers design, and system testing have been addressed. The next chapter presents the use of this material when applied to the B-52 CCV.

III. A Modal Controller for the B-52 CCV

The purpose of this chapter is to present the details of a modal controller design for control of the B-52 CCV. The state-variable model for this aircraft is mentioned in Chapter I, and now the results of evaluating that model via the theory presented in Chapter II are presented. This chapter essentially proceeds in the same order as Chapter II following a discussion of the system specification in the first section. In the second section, the results of the modal analysis are given, and in the third, a set of desired closed-loop eigenvalues is determined. The fourth section presents the design decisions relative to finding a multi-stage modal controller, and the fourth section presents specific details on the testing of the system. Since this design project relied heavily on digital computer calculations, each of these four sections refers to the computer program codes given in Appendix A as the use of the programs arise in the discussion. Once the basic design for the controller is completed, the responses of this system are compared in Chapter IV with those of the aforementioned optimal design.

The System Specification

The modal controller that was designed for this thesis project was intended to meet the same specified requirements as the longitudinal-axis optimal controller designed by the AFFDL CCV ADPO. Since this project included only the longitudinal-axis, the lateral requirements were deleted from the

optimal controller specification. The resulting longitudinal axis controller specification is presented in Appendix B to this thesis report.

To summarize, the specification requires the achievement of reduced vertical accelerations at the crew station and tail and reduced vertical stresses at six body and wing stations for rms gust inputs. In addition, rigid-body pitch rate responses for a step elevator input are to be within certain bounds, and the stability of the control loops is to meet 6 db gain margins and 60° phase margins. Also, for rms gust and elevator inputs, the surface displacements and rates are to stay within prescribed bounds. Finally, the controller is not to change the natural frequencies of the structural modes by more than 10%, nor to degrade the damping ratios of the structural modes by more than 10%. The reader is referred to Appendix B for specific details on the system specification.

Modal Analysis of the B-52 CCV State-variable Model

The state-variable model used for this thesis was the same as that used by the CCV ADPO for their optimal controller design study. As the first step in determining a modal controller design following the completion of the system specification, a modal analysis of the model was performed. As pointed out in Chapter II, the purpose of the modal analysis is to determine the eigenproperties of the system along with its mode-controllability and mode-observability characteristics.

The model for the state-variable representation of the system is in the format given by Eqs (1) and (2). There are 39 states as listed in Table I and the plant matrix \underline{A} is 39×39 . Although specific data for the plant is not provided herein (see footnote, p. 8), an illustration of the distribution of the non-zero elements is given in Fig. 5. From this figure, it is seen that the plant matrix is sparse and that certain of the eigenvalues of the matrix could be determined by inspection, or by partitioning and subsequent analysis of the smaller blocks: this feature can serve as a check in some of the calculations. As for the system inputs, there are five as listed in Table I, and hence the control matrix, \underline{B} , is 39×5 . All of the elements of this matrix except ten are zero; the locations of these ten are shown in Fig. 5. The number of disturbance inputs as given by Table I is two, and the disturbance matrix, \underline{H} , is 39×2 . There are just two non-zero elements in \underline{H} , and their locations are also shown in Fig. 5. Finally, there are ten outputs as listed in Table I, and the output matrix, \underline{C} , is 10×39 . The distribution of non-zero elements in \underline{C} is also illustrated in Fig. 5. With this orientation, the following modal analysis was performed.

Eigenanalysis of the Plant Matrix. Proceeding as in Chapter II, the eigenproperties of the plant matrix, \underline{A} , are determined. The set of computer-coded eigenanalysis programs under the library name EISPACK was used via the EISPACK driver RGEIG. The EISPACK programs are a set of routines deve-

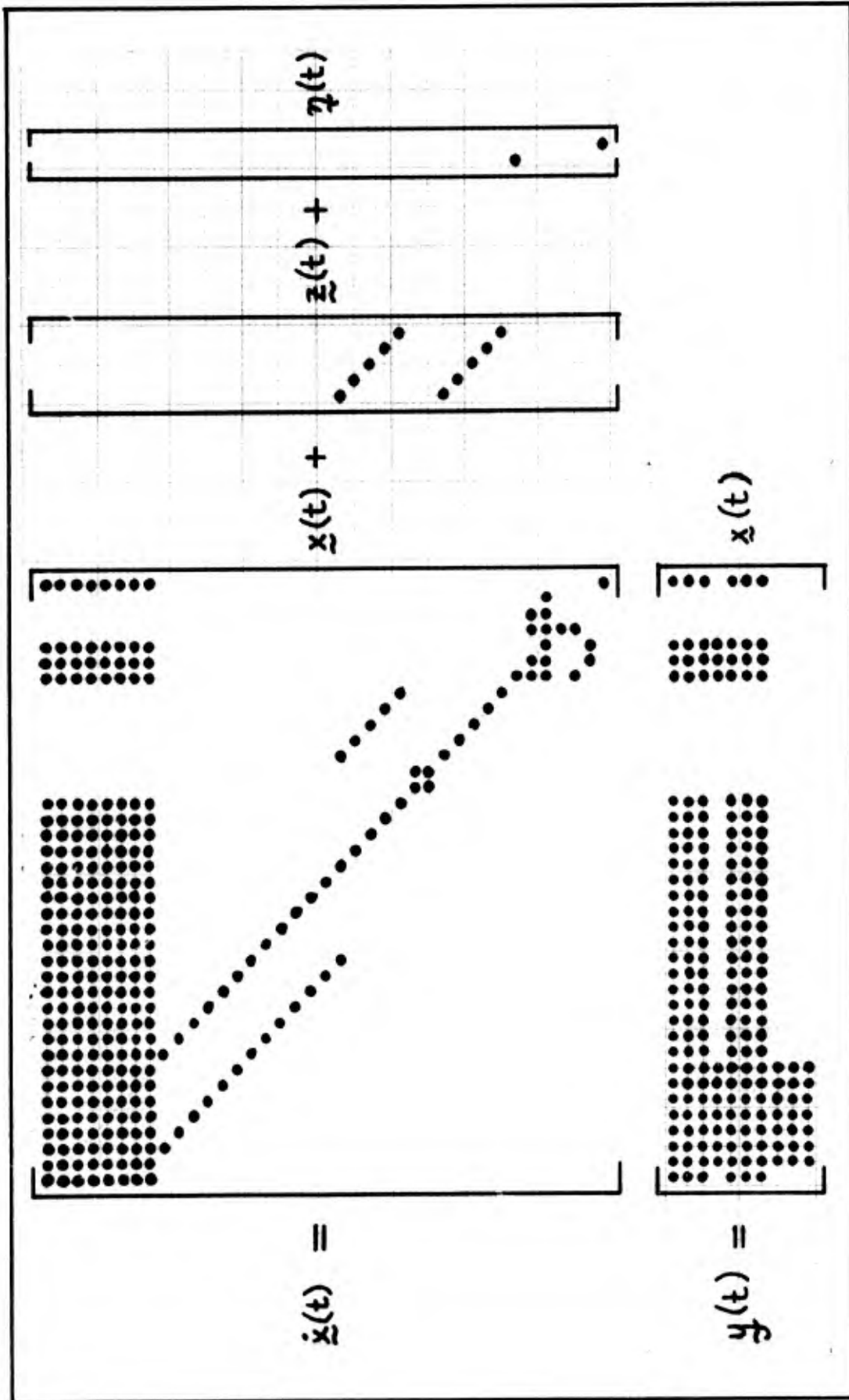


Fig. 5. Distribution of Non-Zero Elements of Matrices \tilde{A} , \tilde{B} , \tilde{H} , and \tilde{C} as given by Eqs (1) and (2)

developed by the Argonne National Laboratory, and consist of 34 separate subroutines for use in eigenanalysis [Ref 16]. A call to the driver RGEIG causes certain of the routines to automatically be attached for use in the eigenanalysis of real general matrices. In this one call, the complete list of eigenvalues are calculated, as is the modal matrix \underline{U} which is made up of the eigenvectors of \underline{A} . Further details on the use of EISPACK in general and RGEIG in particular are given in Appendix A1.

At this point in the analysis, the open-loop eigenvalues are known and are listed in Table II. From Table II it is noted that all of the eigenvalues have negative real parts. Whether it is controllable or not, the system is seen to be stable in the open-loop case. Next it is seen that there are 26 distinct, non-repeated eigenvalues. There are also three repeated eigenvalues, two with geometric multiplicity 2 and one with geometric multiplicity 5 [Ref 11:107].

In ascending order, all 39 eigenvalues can be attributed to specific modal sources. The first 12 eigenvalues are seen to be 6 complex pairs and these are associated with the 6 structural modes included in the model. In order of appearance, these are the 12th, 7th, 8th, 5th, 2nd, and 1st symmetric bending modes. The next complex pair of eigenvalues is associated with the short period mode. Eigenvalues 15 through 20 are the eigenvalues associated with the six real flexible Wagner modes, one mode for each structural mode. The five eigenvalues 21 through 25 are associated

Table II - Eigenvalue Data For Open-loop Plant

NO	REAL PART		IMAG PART		DAMPING	PATIO	NAT FREQ(RPS)		NAT FREQ(HZ)
1	-1.15160426	38.01922200	0.0327827	38.03666151	0.3027827	38.03666151	6.05372269	6.05372269	
2	-1.15160426	-38.01922200	0.0327827	38.03666151	0.3027827	38.03666151	6.05372269	6.05372269	
3	-0.92703383	19.23854692	0.04813043	19.26086913	0.04813043	19.26086913	3.06546253	3.06546253	
4	-0.92703383	-19.23854692	0.04813043	19.26086913	0.04813043	19.26086913	3.06546253	3.06546253	
5	-0.25690334	19.56891151	0.01312701	19.57059777	0.01312701	19.57059777	3.11475737	3.11475737	
6	-0.25690334	-19.56891151	0.01312701	19.57059777	0.01312701	19.57059777	3.11475737	3.11475737	
7	-0.45961359	15.04757733	0.03052979	15.05459492	0.03052979	15.05459492	2.39601320	2.39601320	
8	-0.45961359	-15.04757733	0.03052979	15.05459492	0.03052979	15.05459492	2.39601320	2.39601320	
9	-1.49170545	12.56618351	0.11799026	12.65441240	0.11799026	12.65441240	2.01401228	2.01401228	
10	-1.49170545	-12.56618351	0.11799026	12.65441240	0.11799026	12.65441240	2.01401228	2.01401228	
11	-0.88095870	6.10387256	0.14284771	6.16711833	0.14284771	6.16711833	0.98152737	0.98152737	
12	-0.88095870	-6.10387256	0.14284771	6.16711833	0.14284771	6.16711833	0.98152737	0.98152737	
13	-1.62111715	1.90542499	0.64799781	2.50173244	0.64799781	2.50173244	0.39816308	0.39816308	
14	-1.62111715	-1.90542499	0.64799781	2.50173244	0.64799781	2.50173244	0.39816308	0.39816308	
15	-7.32986527	0.00000000	1.00000000	7.32986527	1.00000000	7.32986527	1.16658429	1.16658429	
16	-6.84946107	0.00000000	1.00000000	6.84946107	1.00000000	6.84946107	1.09012559	1.09012559	
17	-6.84946107	0.00000000	1.00000000	6.84946107	1.00000000	6.84946107	1.09552559	1.09552559	
18	-6.84946107	0.00000000	1.00000000	6.84946107	1.00000000	6.84946107	1.09384801	1.09384801	
19	-6.87848928	0.00000000	1.00000000	6.87848928	1.00000000	6.87848928	1.09474557	1.09474557	
20	-6.87848928	0.00000000	1.00000000	6.87848928	1.00000000	6.87848928	1.09432102	1.09432102	
21	-52.89335550	0.00000000	1.00000000	52.89335550	1.00000000	52.89335550	8.41823500	8.41823500	
22	-10.57864440	0.00000000	1.00000000	10.57864440	1.00000000	10.57864440	1.69364355	1.69364355	
23	-34.38200000	0.00000000	1.00000000	34.38200000	1.00000000	34.38200000	5.47206525	5.47206525	
24	-34.38200000	0.00000000	1.00000000	34.38200000	1.00000000	34.38200000	6.31827083	6.31827083	
25	-34.38200000	0.00000000	1.00000000	34.38200000	1.00000000	34.38200000	6.31827083	6.31827083	
26	-1.92500000	2.32874795	0.63712766	3.02137254	0.63712766	3.02137254	0.48086637	0.48086637	
27	-1.92500000	-2.32874795	0.63712766	3.02137254	0.63712766	3.02137254	0.48086637	0.48086637	
28	-45.00000000	0.00000000	1.00000000	45.00000000	1.00000000	45.00000000	7.16197244	7.16197244	
29	-45.00000000	0.00000000	1.00000000	45.00000000	1.00000000	45.00000000	7.16197244	7.16197244	
30	-50.00000000	0.00000000	1.00000000	50.00000000	1.00000000	50.00000000	7.95774715	7.95774715	
31	-50.00000000	0.00000000	1.00000000	50.00000000	1.00000000	50.00000000	7.95774715	7.95774715	
32	-50.40000000	0.00000000	1.00000000	50.40000000	1.00000000	50.40000000	8.02149913	8.02149913	
33	-2.00000000	0.00000000	1.00000000	2.00000000	1.00000000	2.00000000	0.31830989	0.31830989	
34	-2.00000000	0.00000000	1.00000000	2.00000000	1.00000000	2.00000000	0.31830989	0.31830989	
35	-2.00000000	0.00000000	1.00000000	2.00000000	1.00000000	2.00000000	0.31830989	0.31830989	
36	-2.00000000	0.00000000	1.00000000	2.00000000	1.00000000	2.00000000	0.31830989	0.31830989	
37	-2.00000000	0.00000000	1.00000000	2.00000000	1.00000000	2.00000000	0.31830989	0.31830989	
38	-0.65950000	0.00000000	1.00000000	0.65950000	1.00000000	0.65950000	0.13679367	0.13679367	
39	-1.00000000	0.00000000	1.00000000	1.00000000	1.00000000	1.00000000	0.15915494	0.15915494	

with five of the six modes of the wind model. The sixth eigenvalue of the wind model is listed as No. 38 and a block diagram of the wind model is given in Fig. 6. This model provides a distribution of gust inputs to three longitudinal body stations, with each input delayed in time from nose to tail. Eigenvalues 26 and 27 are a complex pair and they are associated with the modes of the vertical-velocity model, state x_{26} , and the patch-rate model, state x_{27} . Eigenvalues 28 and 29 are the first set of repeated eigenvalues, and they are associated with the elevator and flaperon actuator modes. Eigenvalues 30 and 31 are the second set of repeated eigenvalues and are associated with the inboard and outboard aileron actuator modes. Eigenvalue 32 is associated with the horizontal canard actuator mode. Eigenvalues 33 through 37 are the third set of repeated eigenvalues and are associated with the modes of five washout filters of the form $\frac{s}{s+2}$; there is one filter for each actuator. Finally, the 39th eigenvalue is associated with the mode of the model for pilot elevator commands.

As a final comment on the eigenvalue list, the damping of the six structural modes is seen to be quite low. All have ζ 's of less than 0.15 and four of them (modes 5, 7, 8, and 12) have ζ 's of less than 0.05.

Since part of the B-52 CCV control problem is one of controlling structural displacements in turbulence, it may be necessary to control these modes, as is shown shortly. However, first the system's mode-controllability character-

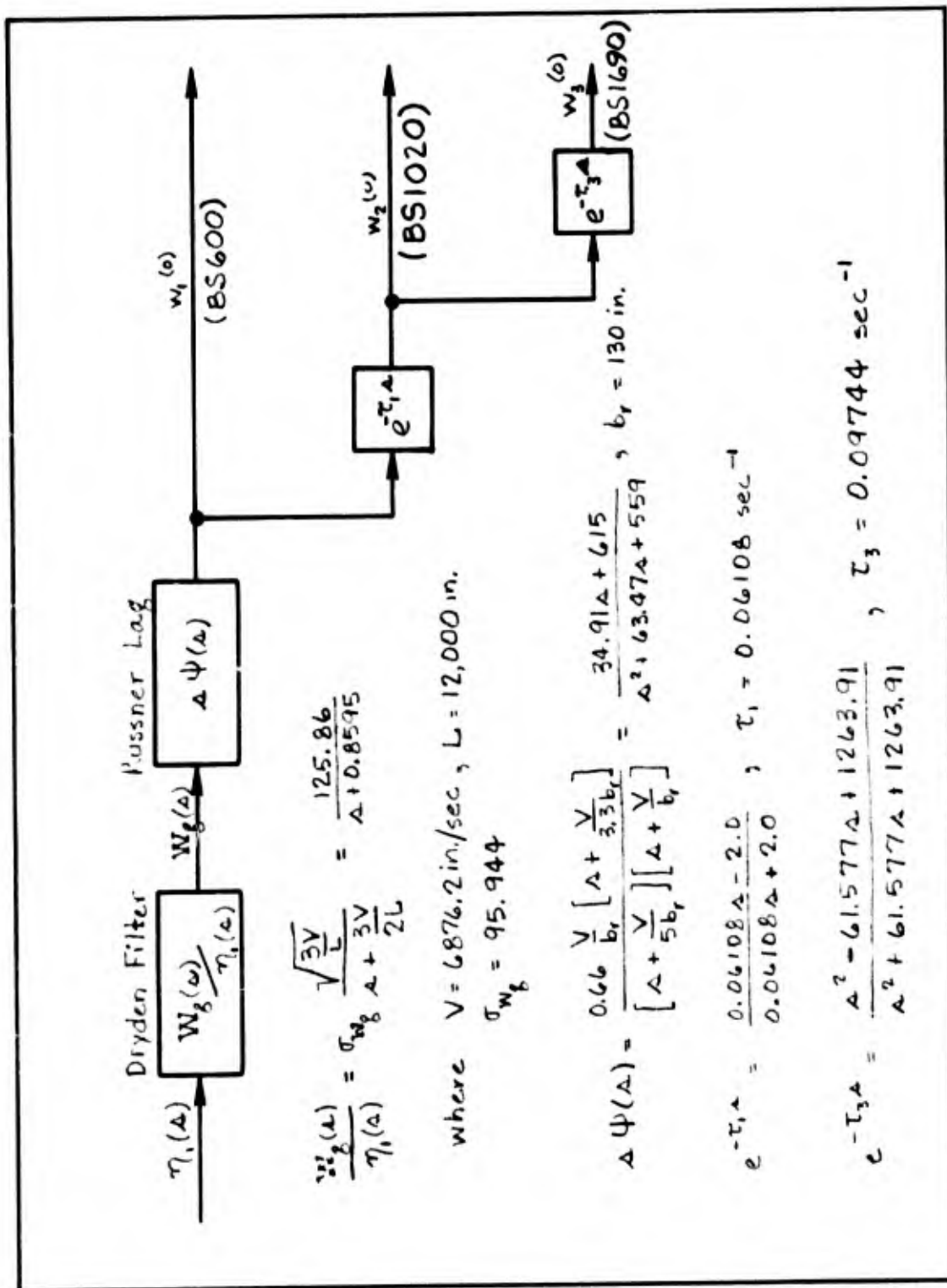


Fig. 6. Wind Model for B-52 CCV

istics must be determined.

Mode-controllability Characteristics. To determine the mode-controllability characteristics of the system, the mode-controllability matrix \underline{P} must be found. For this, the system representation given by Eq (15) is used. The inverse of the modal matrix, namely \underline{U}^{-1} , is required and must be calculated. This inverse can be found by any of a number of readily available complex matrix inversion routines. The routine used for this thesis project is called MINVC and is available in the AFITSUBPROGRAM library of routines. Further details of MINVC are given in Appendix A2. Using the routine MCRM as given in Appendix A3, the product $\underline{P} = \underline{U}^{-1}\underline{B}$ is determined and the mode-controllability characteristics can be discussed.

A computer print-out of the matrix \underline{P} is provided as Table III. Using the rules given on pp 22 of Chapter II, a quick study of Table III reveals that all of the first 20 modes are controllable by any of the inputs. Next, modes 21 through 27, are seen to be uncontrollable. This might be expected since these modes are a function of the wind, vertical-velocity, and pitch-rate models and not of the aircraft model itself. These seven modes arise from attempts to model physical realities in the B-52 CCV flight environment at 2,000 ft. and 330 KCAS. Modes 28 through 37 are controllable but only by single, specific inputs; this is expected since these modes are attributed to the washout filters and time-constants of specific actuators. Finally, modes 38 and 39 are seen to be uncontrollable. This also is expected

Table III

THE MODE-CONTROLLABILITY MATRIX FOR THE OPEN-LOOP SYSTEM

ROW	ELEVATOR	FLAPERON	INRD AIL	OUTB AIL	CANARD
1	-.1014E+02	.7174E+01	-.172E+01	.1520E+01	-.4651E+01
2	-.1314E+02	-.7174E+01	-.172E+01	.1520E+01	-.4551E+01
3	.379E+01	.6127E+02	-.6A20F+00	-.2649E+01	-.4271E+01
4	.3095E+01	-.5127E+02	-.6A20F+00	-.2649E+01	-.4271E+01
5	.1039E+02	.2807E+01	-.130E+01	.1860E+00	.1066E+02
6	-.1039E+02	-.2807E+01	-.130E+01	.1860E+00	.1066E+02
7	.2945E+02	.2403E+02	-.1190E+02	-.1232E+01	-.1022E+02
8	.7114E+01	-.3913E+01	-.1190E+02	-.1232E+01	-.1022E+02
9	.7114E+01	.3913E+01	-.1190E+02	-.1232E+01	-.1022E+02
10	-.2122E+01	.7322E+00	-.2213E+02	-.4266E+02	.5313E+01
11	-.2122E+01	-.7322E+00	-.2213E+02	-.4266E+02	.5313E+01
12	-.6455E+04	-.3448E+04	-.9137E+03	-.4491E+03	-.1730E+04
13	-.6455E+04	.3448E+04	-.9137E+03	-.4491E+03	-.1730E+04
14	-.1914E+03	-.7411E+02	-.1127E+02	-.4970E+02	.4792E+02
15	-.1135E+02	.4980E+02	.1530E+02	.3465E+01	.7223E+01
16	-.3247E+01	.4063E+01	.1935E+01	.3015E+01	-.2761E+01
17	-.5124E+00	-.1737E+01	-.4933E+00	.1094E+00	-.5291E+00
18	-.8107E-01	-.1737E+01	-.4933E+00	.1094E+00	-.5291E+00
19	-.8296E-01	-.1737E+01	-.4933E+00	.1094E+00	-.5291E+00
20	0.	0.	-.0560E-01	.0029E-02	.1043E+00
21	0.	0.	0.	0.	0.
22	0.	0.	0.	0.	0.
23	0.	0.	0.	0.	0.
24	0.	0.	0.	0.	0.
25	0.	0.	0.	0.	0.
26	0.	0.	0.	0.	0.
27	0.	0.	0.	0.	0.
28	0.	0.	0.	0.	0.
29	-.9854E+02	0.	0.	0.	0.
30	0.	0.	0.	0.	0.
31	0.	0.	0.	0.	0.
32	0.	0.	0.	0.	0.
33	-.8786E+04	0.	0.	0.	0.
34	0.	0.	0.	0.	0.
35	0.	0.	0.	0.	0.
36	0.	0.	0.	0.	0.
37	0.	0.	0.	0.	0.
38	0.	0.	0.	0.	0.
39	0.	0.	0.	0.	0.

since these modes arise from the uncontrollable disturbances of wind-induced turbulence or pilot-induced elevator oscillations. In conclusion, the 14 modes which may have to be controlled are indeed controllable and are controllable by any of the inputs.

Mode-Observability Characteristics. Now that the mode-controllability characteristics are known, the mode-observability characteristics are discussed. First, the mode-observability matrix, \tilde{R} , as given by Eq (19) is calculated from the product $\tilde{C} \tilde{U}$ using the routine MRCM (see Appendix A3). Due to its size in printed form as a 10×39 complex matrix, \tilde{R} is not reproduced herein. In passing however, it is noted that all but modes 26 and 27 are observable when \tilde{R} is evaluated in accordance with the dual of the rules given on pp22 of Chapter II. The reason for this is that these two modes are excited only by elevator disturbances which are not considered as inputs when calculating the mode-observability matrix. The fact that these two modes are not observable is of no consequence however, since these two modes - or states - have no influence over any other modes as seen in \tilde{A} in Fig. 5, rows 26 and 27, and columns 26 and 27.

Determination of the Closed-loop Eigenvalues

For this thesis project, the locations of the closed-loop eigenvalues was determined in the following manner. First, the list of eigenvalues to be shifted was determined, and then the specific closed-loop values were found.

The determination of the list of eigenvalues to be shif-

ted was based on (1) the results of the modal analysis and an inspection of the system outputs relative to the controllable and observable modes, and (2) the performance specification. From the modal analysis it was seen that all of the first 20 modes are controllable by any of the inputs and that all of modes 28 through 37 are controllable, but each by only a specific input. Furthermore, all of these modes are observable in any of the ten sensor outputs. Hence, a shift of any of the eigenvalues of these modes should be reflected in the outputs, since these modes are controllable and observable.

The specific nature of the outputs is also of interest. All of these outputs are sensed outputs, such as body and wing station accelerations or pitch rates. In particular, the reduction of accelerometer readings by 30% at BS172 and BS1655 without more than a 5% increase in the accelerometer reading at BS860 is required. These readings are primarily influenced by the excitation of structural modes. Consider also the requirement to reduce the vertical stresses at six wing, body, and horizontal-tail station locations: BS475, BS760, BS1412, WS222, WS974, and HT56. These stresses are basically linear combinations of the states for structural-mode rates and displacements, flexible Wagner modes, control surface positions, and wind model inputs [Ref 7:5,32-34, 53-54,65-68]. These stresses are also influenced by the excitation of structural modes. Finally, the requirement to have the pitch rate response to a step elevator disturbance

fall within the "bounds" of Fig. B1 of Appendix B is considered. Achievement of this specification may require shifts in the short period eigenvalues. In summary, the list of eigenvalues to be shifted consists of the 12 eigenvalues associated with the structural modes, and the two eigenvalues associated with the short period mode.

The question now is: By how much should the first 14 eigenvalues be shifted: Or equivalently: Where should the closed-loop eigenvalues be located? The answers to these questions lie in part in the restriction of para 1.4 of the specification, and also may be determined from an intuitive review of simple slender beam theory.

First, paragraph 1.4 of the system specification restricts the relocation of the structural mode eigenvalues to less than a 10% change in natural frequency and limits the degradation of structural mode damping to 10%. Although from a positive viewpoint this means that damping can be increased by any amount, the more the damping is increased, the larger the feedback gains must be. Too large an increase may require too much control authority and prohibit the system from meeting the requirements of specification paragraph 1.3.

On the other hand, simple slender beam theory says that in order to reduce the displacements of a mode of a vibrating slender beam, either Young's modulus should be increased or the moment of inertia should be increased, or both [Ref 17: 172-184]. The B-52 CCV fuselage and wing can intuitively be

thought of as slender beams. Thus, increasing Young's modulus or the moment of inertia or both is essentially the same as artificially increasing the damping or the natural frequency, or both, of a structural mode. This is the basis upon which the eigenvalues of the structural modes are re-located.

Attention is now given to the short period mode and the shifts of its two associated eigenvalues. Table II shows that the short period mode has a damping ratio of 0.648 and a natural frequency of 2.502 rad/sec. Although these values are quite satisfactory for most aircraft such as the B-52, it is also noted from Table II that the short period eigenvalues are among the roots closest to the origin. Thus, it is assumed that their location plays a dominant role in the aircraft response after most of the higher frequency transients have died out. In particular, an increase in the damping will reduce overshoots in the aircraft pitch rate response to a step elevator disturbance. At the same time, the natural frequency will affect the mode by reducing the settling time if the frequency is increased, and will increase the settling time if the frequency is reduced. In light of this situation and that posed by Fig. B1 of Appendix B, a preliminary analysis of the $\dot{\theta}_{815}(s)/\delta_{ec}(s)$ transfer function was performed for: (1) no change in the short period roots, (2) increased damping and increased natural frequency of the roots, and (3) increased damping and reduced natural frequency of the roots. The second combination, with

$\zeta_{sp} = 0.80$ and $\omega_{n_{sp}} = 3.34$ rad/sec was found to provide a satisfactory level of dominance of the short period mode in the pitch rate response. The corresponding eigenvalues for the closed-loop short period mode are selected for inclusion in the prescribed list.

To summarize this discussion of how the list of closed-loop eigenvalues were selected, Fig. 7 illustrates the restrictions of paragraph 1.4 of the specification when applied to the complex plane, and Fig. 8 shows the open-loop and the prescribed closed-loop eigenvalue locations. The specific values for each of these sets is given in Table IV.

Design of a Multi-stage Modal Controller

Having performed the required modal analysis, and having found a set of desired closed-loop eigenvalues, the multi-stage design procedure is used to determine the gains for a modal controller. According to the procedure given in Chapter II, the first step is to inspect the magnitudes of the terms of the mode-controllability matrix (labelled as $\text{mag}\tilde{P}_1$) to determine which input should be used to shift which set of eigenvalues. The $\text{mag}\tilde{P}_1$ matrix is displayed in Table V.

In Table V, the largest term in each of the first 14 rows is boxed to show which is the dominant input to control that mode. If the elevator is chosen as the first input to be used, then the eigenvalues of modes 1, 2, 3, 4, 7, 8, 13, and 14 are shifted first. Assuming satisfactory results can be achieved by first using the elevator, the feedback vector, \tilde{k}_1 is found from Eq (25).

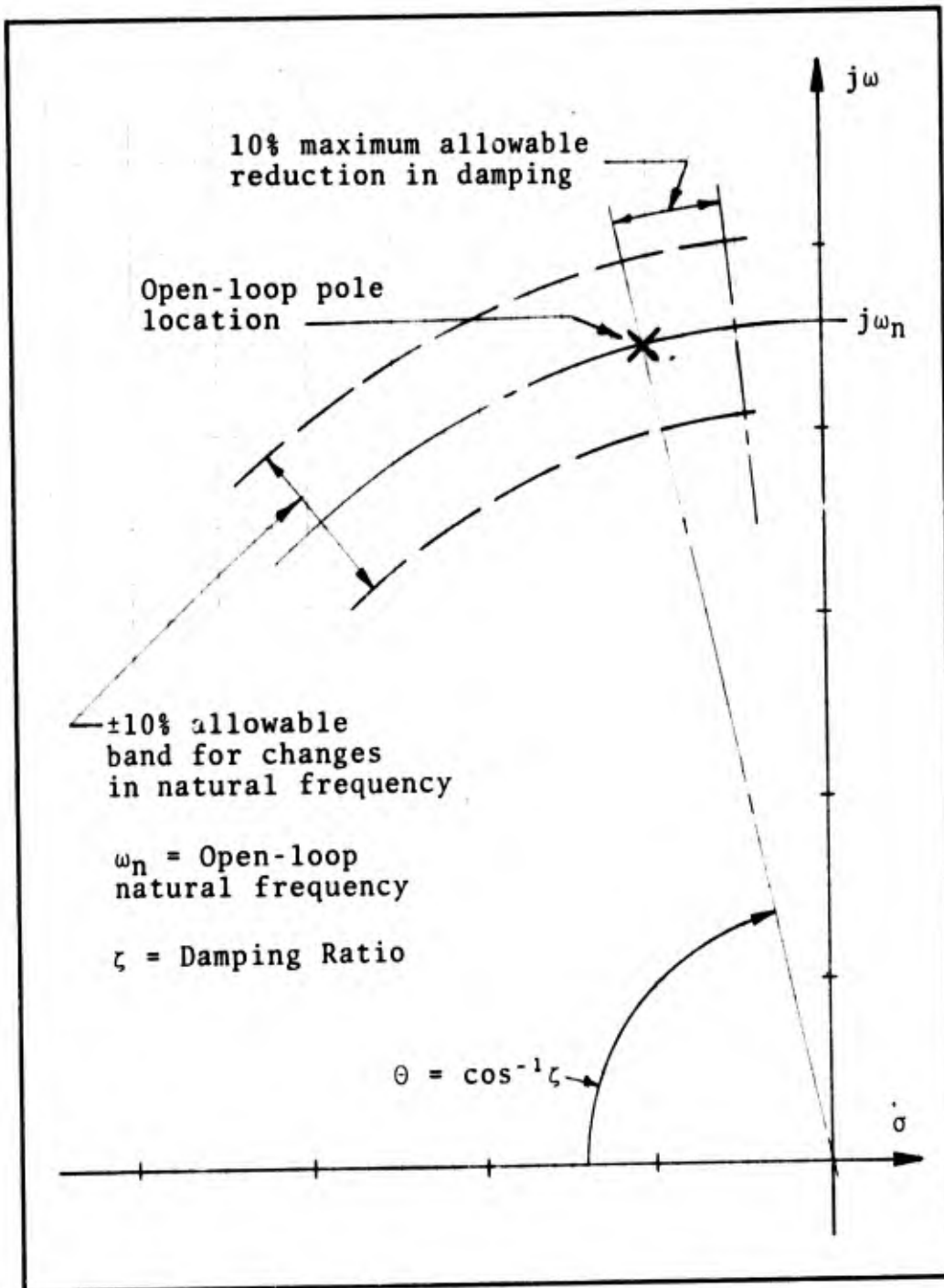


Fig. 7. Restrictions of Eigenvalues Shifts as Given by Specification Paragraph 1.4, Appendix B

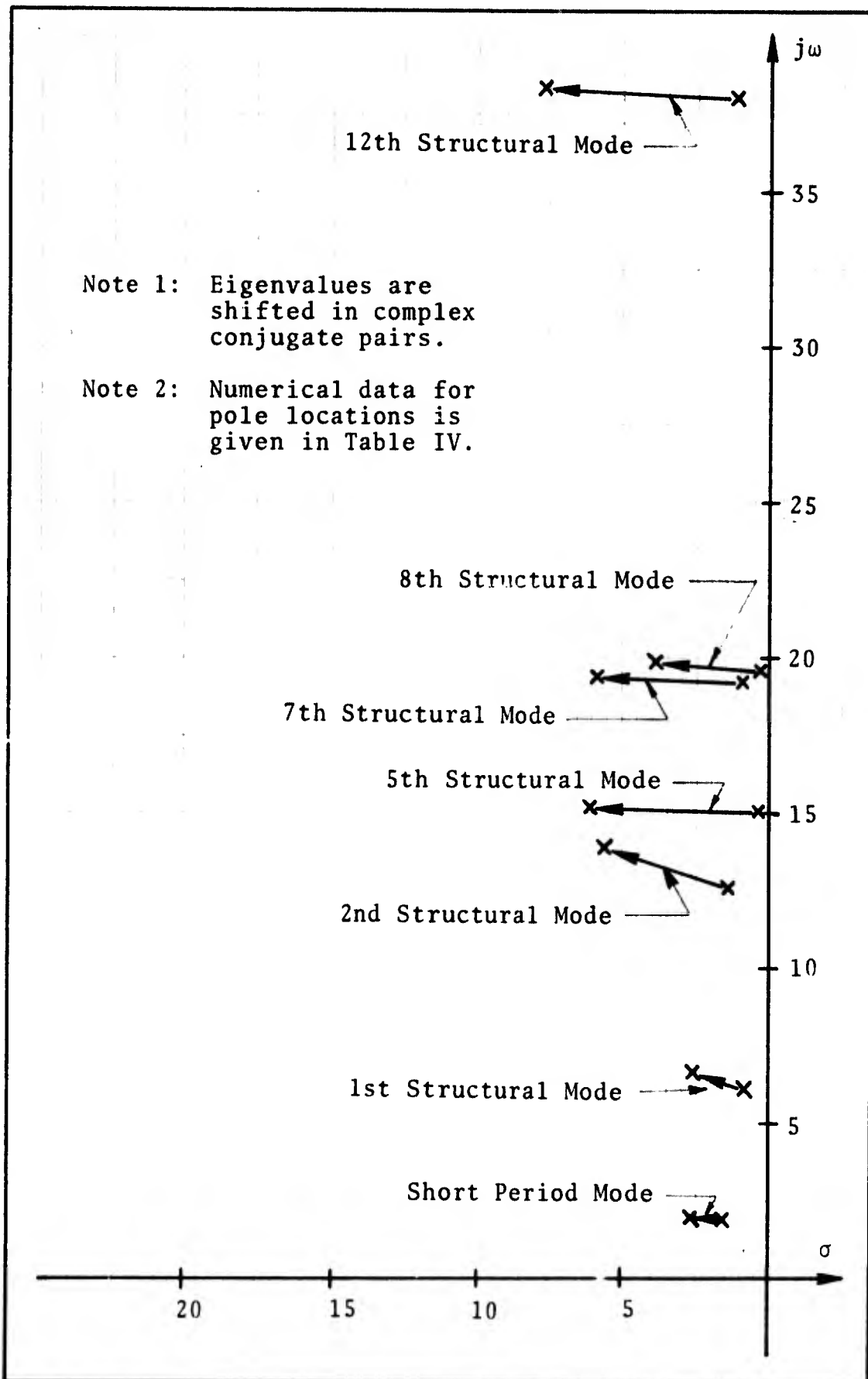


Fig. 8. Locations of shifted Open-loop and Closed-loop Eigenvalues in Third Quadrant of Complex Plane.

Table IV
 Open-loop and Closed-loop Structural
 Mode and Short Period Mode Eigenvalue
 Locations with Natural Frequencies and Damping Ratios

(a) Open-loop Data			
Mode	Eigenvalues	Nat Freq (RPS)	Damping Ratio
1st Structural	-0.88±j 6.10	6.167	0.143
2nd Structural	-1.49±j12.57	12.654	0.118
5th Structural	-0.45±j15.05	15.055	0.031
7th Structural	-0.92±j19.24	19.261	0.048
8th Structural	-0.26±j19.57	19.571	0.013
12th Structural	-1.15±j38.02	38.037	0.030
Short Period	-1.62±j1.905	2.501	0.648
(b) Selected Closed-loop Data			
1st Structural	-2.68±j 6.7	7.216	0.371
2nd Structural	-5.56±j13.9	14.971	0.371
5th Structural	-6.06±j15.2	16.363	0.370
7th Structural	-5.82±j19.4	20.254	0.287
8th Structural	-3.94±j19.7	20.090	0.196
12th Structural	-7.68±j38.4	39.160	0.196
Short Period	-2.67±j2.00	3.336	0.80

Table V - Matrix of magnitudes of terms for $P_1 - \text{mag } P_1$

ROW 1	.12425E+02	.29827E+01	.19778E+01	.18812E+01	.55449E+01
2	.12425E+02	.29827E+01	.19730E+01	.18812E+01	.55449E+01
3	.41390E+02	.40116E+02	.39575E+01	.80610E+01	.15271E+02
4	.41390E+02	.40116E+02	.39575E+01	.80610E+01	.15271E+02
5	.10478E+02	.45901E+01	.18658E+01	.20003E+00	.11821E+02
6	.10478E+02	.45901E+01	.18658E+01	.20003E+00	.11821E+02
7	.39015E+02	.36907E+02	.15444E+02	.17635E+01	.23106E+02
8	.39015E+02	.36907E+02	.15444E+02	.17635E+01	.23106E+02
9	.90752E+01	.39943E+02	.22537E+02	.43058E+02	.53509E+01
10	.90752E+01	.39943E+02	.22537E+02	.43058E+02	.53509E+01
11	.22444E+01	.11059E+02	.55520E+01	.10459E+02	.14384E+02
12	.22444E+01	.11059E+02	.55520E+01	.10459E+02	.14384E+02
13	.56334E+04	.18805E+04	.10773E+04	.59093E+03	.23533E+04
14	.56334E+04	.18805E+04	.10773E+04	.59093E+03	.23533E+04
15	.19137E+03	.78106E+02	.11272E+02	.49703E+02	.47824E+02
16	.11347E+02	.49797E+02	.15303E+02	.34650E+01	.72229E+01
17	.32470E+01	.60629E+01	.19346E+01	.30152E+01	.27615E+01
18	.51238E+00	.17371E+01	.49929E+00	.10941E+00	.52905E+00
19	.81066E-01	.17731E+00	.10430E+00	.83548E-01	.12646E+00
20	.82857E-01	.97821E-01	.85797E-01	.88250E-02	.18431E+00
21	0.	0.	0.	0.	0.
22	0.	0.	0.	0.	0.
23	0.	0.	0.	0.	0.
24	0.	0.	0.	0.	0.
25	0.	0.	0.	0.	0.
26	0.	0.	0.	0.	0.
27	0.	0.	0.	0.	0.
28	.99542E+02	0.	0.	0.	0.
29	0.	.81910E+03	0.	0.	0.
30	0.	0.	.27768E+03	.98887E+02	0.
31	0.	0.	0.	0.	.27450E+03
32	0.	0.	0.	0.	0.
33	.87860E+04	0.	0.	0.	0.
34	0.	.30502E+04	0.	0.	0.
35	0.	0.	.16289E+04	0.	0.
36	0.	0.	0.	.94912E+03	0.
37	0.	0.	0.	0.	.37282E+04
38	0.	0.	0.	0.	0.
39	0.	0.	0.	0.	0.

Using the feedback vector, \tilde{k}_1 , the first loop is closed and a new, interim state equation is found from Eq (23). The new mode-controllability matrix, \tilde{P}_2 , is found from a modal analysis of the new interim system, and the magnitude of its terms are inspected. The new $\text{mag}\tilde{P}_2$ matrix is given in Table VI.

At this point, the boxed terms of Table VI show that only the outboard ailerons and the horizontal canards are required to shift the remaining six eigenvalues. In the order of presentation, the outboard aileron is chosen as the second input to be used in the multi-stage design.

As before, Eq (25) is used to find the next feedback vector, \tilde{k}_2 . In turn, another interim state equation is formed, a modal analysis is performed, and the mode-controllability matrix \tilde{P}_3 , is determined. The $\text{mag}\tilde{P}_3$ matrix is given in Table VII. The final feedback vector, \tilde{k}_3 , is then found and the closed-loop plant matrix is obtained from Eq (24). A modal analysis of this plant can be performed and the location of the closed-loop eigenvalues can be confirmed. Fig. 3 shows the closed-loop system with the feedback paths obtained in the multi-stage design procedure.

To complete the data presented here, a list of the three feedback vectors is given in Table VIII and a list of the closed-loop eigenvalues is given in Table IX. The closed-loop system can now be tested for compliance with the specification and for comparison with the open-loop system and the AFFDL optimal design. First however; the com-

Table VI - Matrix of Magnitudes of Terms for $P_2 - \text{mag}P_2$

1	.1459AE+03	.42260F+02	.29559E+02	.94703E+01	.38476E+02
2	.97774E+02	.83137E+02	.32752F+02	.19737E+02	.63062E+02
3	.07774E+02	.3137E+02	.32752E+02	.19737E+02	.63062E+02
4	.41367E+03	.57129E+03	.26719E+03	.12759E+03	.31850E+03
5	.41367E+03	.57129E+03	.26719E+03	.12759E+03	.31850E+03
6	.75591E+00	.62487E+01	.33164F+01	.20015E+01	.76475E+01
7	.75591E+00	.62487E+01	.33164E+01	.20015E+01	.76475E+01
8	.62205E+03	.80779E+03	.49113E+03	.10703E+03	.58459E+03
9	.62205E+03	.80779E+03	.49113E+03	.10703E+03	.58459E+03
10	.30933E+01	.30501E+02	.18424E+02	.43619F+02	.11801E+02
11	.37932E+01	.30501E+02	.18424E+02	.43619E+02	.11801E+02
12	.14640F+01	.10774E+02	.53894E+01	.10371E+02	.14256E+02
13	.14640E+01	.10774E+02	.53894E+01	.10371E+02	.14256E+02
14	.59240E+04	.7274E+04	.69519E+03	.59705F+03	.18011E+04
15	.59240F+04	.7274F+04	.69519E+03	.59705F+03	.18011E+04
16	.62797E+04	.16288E+04	.27500E+04	.36806F+03	.85461E+02
17	.34632E+03	.21451E+03	.10746E+03	.33705E+02	.34224E+02
18	.20310E+02	.57345E+02	.20727E+02	.25494E+01	.11626E+02
19	.58159E+01	.82339E+01	.34926E+01	.27526E+01	.14920E+01
20	.91753E+00	.13950E+01	.25373E+00	.68009E-01	.32920E+00
21	.14510E+00	.12315E+00	.14317E+00	.76994E-01	.94799E-01
22	.14830E+00	.42484E-01	.46075E-01	.21274E-02	.21665E+00
23	0.	0.	0.	0.	0.
24	0.	0.	0.	0.	0.
25	0.	0.	0.	0.	0.
26	0.	0.	0.	0.	0.
27	0.	0.	0.	0.	0.
28	0.	0.	0.	0.	0.
29	0.	0.	0.	0.	0.
30	0.	.81566E+03	0.	0.	0.
31	0.	0.	.27768E+03	0.	0.
32	0.	0.	0.	.98087E+02	.27450E+03
33	0.	0.	0.	0.	0.
34	0.	.49529E+02	0.	0.	0.
35	0.	0.	.29791E+04	0.	0.
36	0.	0.	0.	.28587E+03	.19917E+04
37	0.	0.	0.	0.	0.
38	0.	0.	0.	0.	0.
39	0.	0.	0.	0.	0.

12th
7th
8th
5th
2nd
1st
s.p.

ROW	13612F+01	.95114E+01	.20774E+02	.11760E+03	.50042E+01	
1	.19612E+03	.84991E+02	.26976E+02	.11107E+02	.39009E+02	
2	.97477E+02	.83885E+02	.32341E+02	.20912E+02	.63253E+02	12th
3	.97477E+02	.83885E+02	.32341E+02	.20912E+02	.63253E+02	
4	.75487E+00	.70376E+01	.37520E+01	.17399E+01	.79733E+01	7th
5	.76487E+00	.70376E+01	.37520E+01	.17399E+01	.79733E+01	
6	.41150E+03	.53032E+03	.22391E+03	.16157E+03	.34266E+03	8th
7	.41150E+03	.53032E+03	.22391E+03	.16157E+03	.34266E+03	
8	.63425E+03	.59353E+03	.36968E+03	.39178E+03	.67961E+03	5th
9	.63425E+03	.59353E+03	.36968E+03	.39178E+03	.67961E+03	
10	.15513E+02	.11906E+02	.71397E+02	.17731E+02	.52149E+02	2nd
11	.15513E+02	.11906E+02	.71397E+02	.17731E+02	.52149E+02	
12	.15930E+01	.13743E+02	.34180E+01	.67324E+01	.15009E+02	1st
13	.15930E+01	.13743E+02	.34180E+01	.67324E+01	.15009E+02	
14	.15930E+01	.13743E+02	.34180E+01	.67324E+01	.15009E+02	
15	.59400E+04	.24196E+04	.69743E+03	.46873E+03	.18178E+04	s.p.
16	.58400E+04	.24196E+04	.69743E+03	.46873E+03	.18178E+04	
17	.74497E+03	.21203E+03	.10574E+03	.32959E+02	.32917E+02	
18	.62712E+04	.17934E+04	.27692E+04	.27606E+03	.75418E+02	
19	.24683E+02	.83643E+02	.83623E+02	.22632E+03	.82219E+02	
20	.20210E+02	.57123E+02	.20576E+02	.24414E+01	.11541E+02	
21	.91487E+00	.14009E+01	.25774E+00	.65186E-01	.33147E+00	
22	.14217E+00	.12981E+00	.13864E+00	.73826E-01	.97376E-01	
23	.14830E+00	.42669E-01	.46200E-01	.20396E-02	.21657E+00	
24	.57081E+01	.79961E+01	.33307E+01	.26399E+01	.15843E+01	
25	0.	0.	0.	0.	0.	
26	0.	0.	0.	0.	0.	
27	0.	0.	0.	0.	0.	
28	0.	0.	0.	0.	0.	
29	0.	0.	0.	0.	0.	
30	0.	0.	0.	0.	0.	
31	0.	0.	0.	0.	0.	
32	0.	.81193E+03	0.	0.	0.	
33	0.	0.	.30403E+03	0.	0.	
34	0.	0.	0.	0.	.27450E+03	
35	0.	.94699E+02	0.	0.	0.	
36	0.	0.	.28498E+04	0.	0.	
37	0.	0.	0.	0.	.21007E+04	
38	0.	0.	0.	0.	0.	
39	0.	0.	0.	0.	0.	

Table VIII

THE MODAL CONTROLLER FEEDBACK MATRIX

ELEVATOR	FLAPERON	INBD. AIL.	ORD. AIL.	CANARD
.56693E-03	0.	0.	.65948E-03	.10498E-02
-.51561	0.	0.	-.99619	-1.8373
.40877E-02	0.	0.	.86633E-01	.43913
.33265	0.	0.	1.0894	-.62198
1.7129	0.	0.	.69592	.45352E-01
.43102	0.	0.	-.22541	.32971
-.42549	0.	0.	-.45035E-01	-2.2935
.52280	0.	0.	.23737E-02	-.93539E-02
-.45328E-01	0.	0.	-.80807E-01	1.8822
-1.0252	0.	0.	8.6917	-.76980
-23.137	0.	0.	-1.3673	.91914
26.611	0.	0.	4.1423	2.2080
.99625	0.	0.	-1.1938	-3.0245
7.2132	0.	0.	.45012	.19116
.44892	0.	0.	-.10272E-01	-.12142
-.45578	0.	0.	-.28739	-.45033
.21342	0.	0.	.13950	.23191
.65967	0.	0.	.81100E-01	.10269E-02
-.17905	0.	0.	-.17915	-.31417
-.46171	0.	0.	-.46873E-01	.13861E-01
-.73814	0.	0.	-.14339E-01	.78635E-02
.48386	0.	0.	-.10158	.16109
.13313	0.	0.	-.54613E-01	.41372E-01
-.35402E-01	0.	0.	-.14690	-.40810E-01
.16390	0.	0.	.44899E-01	-.19867
0.	0.	0.	0.	0.
0.	0.	0.	0.	0.
1.4624	0.	0.	-.62215E-01	.21916
-.64607	0.	0.	.34788	-.60996
.33545	0.	0.	.19750	.95338E-02
.15078	0.	0.	.39579	.26557
.49626	0.	0.	-.75483E-01	.47561
-.32571E-03	0.	0.	-.78980E-03	-.54096E-03
-.17506E-03	0.	0.	-.43924E-03	-.35908E-03
-.89767E-04	0.	0.	-.22840E-05	-.23188E-05
.13539E-02	0.	0.	.15498E-02	.18339E-02
.24496E-04	0.	0.	.12815E-04	.17600E-05
-.52635E-05	0.	0.	0.	0.
.97663	0.	0.	-.74707E-01	.26246

Table IX - Eigenvalue Data for Closed-loop Plant with Modal Controller

NO	REAL PART	IMAG PART	DAMPING	PAYIO	NAT FREQ(RPS)	NAT FREQ(HZ)
1	-50.40000000	0.00000000	1.00000000	1.00000000	50.40000000	8.02140913
2	-50.00000000	0.00000000	1.00000000	1.00000000	50.00000000	7.95774715
3	-45.00000000	0.00000000	1.00000000	1.00000000	45.00000000	7.16197244
4	-7.68000000	38.40000000	.19611614	.19611614	39.16046986	6.23258235
5	-7.68000000	-38.40000000	.19611614	.19611614	39.16046986	6.23258235
6	-3.94000000	19.70000000	.19511614	.19511614	20.09013688	3.19744459
7	-3.94000000	-19.70000000	.19511614	.19511614	20.09013688	3.19744459
8	-5.82000000	19.40000000	.28734789	.28734789	20.25419463	3.22355519
9	-5.82000000	-19.40000000	.28734789	.28734789	20.25419463	3.22355519
10	-6.05000000	15.20000000	.37031679	.37031679	16.36348374	2.60432932
11	-6.05000000	-15.20000000	.37031679	.37031679	16.36348374	2.60432932
12	-5.56000000	13.90000000	.37139068	.37139068	14.97075816	2.38267016
13	-5.56000000	-13.90000000	.37139068	.37139068	14.97075816	2.38267016
14	-2.68000000	6.70000000	.80035957	.80035957	7.21612084	1.14948130
15	-2.68000000	-6.70000000	.80035957	.80035957	7.21612084	1.14948130
16	-2.67000000	2.00000000	.80035957	.80035957	3.33600050	.53094099
17	-2.67000000	-2.00000000	.80035957	.80035957	3.33600050	.53094099
18	-7.3286527	0.00000000	1.00000000	1.00000000	7.32986527	1.16658429
19	-6.84946107	0.00000000	1.00000000	1.00000000	6.84946107	1.09012559
20	-6.88339026	0.00000000	1.00000000	1.00000000	6.88339026	1.09552559
21	-6.87284972	0.00000000	1.00000000	1.00000000	6.87284972	1.09388801
22	-6.87582177	0.00000000	1.00000000	1.00000000	6.87582177	1.09432102
23	-6.87848928	0.00000000	1.00000000	1.00000000	6.87848928	1.09474557
24	-2.00000000	0.00000000	1.00000000	1.00000000	2.00000000	.31430989
25	-2.00000000	0.00000000	1.00000000	1.00000000	2.00000000	.31430989
26	-2.00000000	0.00000000	1.00000000	1.00000000	2.00000000	.31430989
27	-1.92500000	2.32874795	.63712766	.63712766	3.02137254	.48086637
28	-1.92500000	-2.32874795	.63712766	.63712766	3.02137254	.48086637
29	-34.38000000	19.84982620	.86501969	.86501969	39.69886648	6.31927093
30	-34.38000000	-19.84982620	.86501969	.86501969	39.69886648	6.31927093
31	-10.57864440	0.00000000	1.00000000	1.00000000	10.57864440	1.68364355
32	-52.89335550	0.00000000	1.00000000	1.00000000	52.89335550	8.41823900
33	-34.34200000	0.00000000	1.00000000	1.00000000	34.38200000	5.47206525
34	-45.00000000	0.00000000	1.00000000	1.00000000	45.00000000	7.16197244
35	-50.00000000	0.00000000	1.00000000	1.00000000	50.00000000	7.95774715
36	-2.00000000	0.00000000	1.00000000	1.00000000	2.00000000	.31830989
37	-2.00000000	0.00000000	1.00000000	1.00000000	2.00000000	.31830989
38	-.85950000	0.00000000	1.00000000	1.00000000	.85950000	.13679367
39	-1.00000000	0.00000000	1.00000000	1.00000000	1.00000000	.15915494

puter routines used for the above calculations of the feedback gains are discussed.

Computer Routines Used for Multi-stage Design

The previous sections in this chapter mention the use of the routine RGEIG for the eigenanalysis, the routine MINVC for the inversion of complex matrices, the routine MCRM for post-multiplication of complex matrices by real ones, and the routine MRCM for the post-multiplication of real matrices by complex ones. This section presents other routines used for the multi-stage modal controller design.

The code for the program MODAL is given in Appendix A4 and was used for the multi-stage design. The program requires the availability of data for the non-zero elements of the \underline{A} , \underline{B} , \underline{C} , and \underline{H} matrices and proper logical DATA statements are provided by the user to iterate the design stage-by-stage. To save central memory storage, the program uses test routines for various inputs as each plant matrix is found. These routines are NOISE for covariance analysis, XFRFNCT for transfer function analysis, and BODE for frequency response analysis. The internal workings of these routines are outlined in Appendices A5, A6, and A7, and further discussion on the results of their use is provided in Chapter IV.

The basic flow of operations and calculations in the MODAL program are as follows. After the establishment of array names and other declarations, data for various parameters is established and the program is ready for execu-

tion. Next, the data for the \underline{A} , \underline{B} , \underline{C} , \underline{H} , and KOPT matrices is read using the routine REED; KOPT is the gain matrix for the AFFDL optimal controller. The plant matrix \underline{A} is also duplicated into the arrays AA and A2 for later use. (This step is particularly necessary when the EISPACK routine RGEIG is used since EISPACK routines destroy the matrix which is analyzed.) The routine ZERO is used to set all the elements of an array to zero. After the zeroing, the arrays EVALUE, EVECTOR, AND WIFE are used by RGEIG to calculate the eigenvalues and the eigenvectors. The routine EPRT prints out the eigenvalues of the matrix analysis by RGEIG, and EPACK converts the dual array storage mode of the eigenvalues and eigenvectors into complex arrays. An example of the output from EPRT for the open-loop system is given in Table II. The codings for REED, ZERO, EPRT, and EPACK are given in Appendix A3.

At this point, the modal analysis information for the open-loop system is calculated and that system is ready for testing. Following the testing of the open-loop system, the design loop is entered. This loop is cycled until the entire design, or the desired intermediate stage of the design, is complete. Intermediate design iterations are necessary because RGEIG does not always return the eigenvalues and eigenvectors in the same order from one stage to the next. Thus, the design must proceed through several iterations (resubmittal of the deck) in order to build up the data deck of eigenvalue-shift cards.

With each pass through the design loop, the P_i and $\text{mag}P_i$ matrices are printed. These tables are followed by a table showing the status of the design. In turn, the feedback vector is calculated, stored, and printed. With the gains determined, the interim, new plant matrix is formed in accordance with Eq (23), and a modal analysis of the new plant is made.

The design loop is repeated until completion or until user abort is caused by DATA control. When the design is completed, a summary table of the transpose of the feedback matrix is printed, and the closed-loop system is tested. This testing is followed by testing of the optimal controller system for comparative purposes. With testing of the optimal controller finished, histories (if any are generated) are plotted, and the program is finished. Additional details on MODAL, the subroutines, and their use are given in Appendix A.

This chapter has discussed the design of the modal controller developed during this thesis project. The results of this design are presented in the next chapter along with a comparison between the characteristics of the open-loop system, the modal controller system, and the AFFDL optimal controller system.

IV. Results and Comparisons

The purpose of this chapter is to present the results of the design given in Chapter III, and to compare those results with the AFFDL optimal controller results given in AFFDL-TM-74-138-FGB [Ref 7]. In addition, the results of the modal controller design are compared with the previous B-52 CCV work where possible. To achieve this purpose, the results are first presented. Next, the modal controller design is evaluated against the specification, and then a comparison is made with the open-loop system and the optimal controller system. Due to a difference in models and a lack of correlation of some of the modal controller performance data, a comprehensive comparison with other B-52 CCV work is not possible.

Results of the Multi-stage Modal Controller Design

The results of the multi-stage modal controller design can be viewed in terms of three results. The first result of the design is that the eigenvalues are shifted to the specified values. This is to be expected because the theory "guarantees" the shifts will occur for full-state feedback. The availability of all the states was an assumption throughout the project.

The second result of the design is the fact that only three of the five inputs were selected for use in the design. This occurs because the procedure selects the specific input for each eigenvalue shift on the basis of which

input has the largest effect on the mode. As a consequence, the flaperons were not selected to shift the eigenvalues associated with the fifth and seventh structural modes even though those surfaces are almost as effective as the elevator that was selected. This is brought out in rows 3, 4, 7, and 8 of Table V. Similarly, the flaperons were not selected for use in shifting the eigenvalues of the eighth structural mode. This is shown in rows 6 and 7 of Table VI where the horizontal canard is chosen as the appropriate force producer. The multi-stage design procedure selects the minimum number of inputs to shift the prescribed number of eigenvalues for the order of the inputs selected. However, as seen in the next section, the design using only three inputs as developed in Chapter III did not meet all the specifications. Further refinement of the design is needed by reordering the inputs and/or moving the eigenvalues to other locations or possibly shifting other eigenvalues.

The third result of the design is that a computer program has been written to initiate the design and to aid in further development of the design. This program was used to design the multi-stage modal controller presented herein, and provides routines for testing and comparing that system with the open-loop system and the AFFDL optimal control system. The comparisons made between the open-loop system, the optimal controller and the modal controller are discussed in the following sections.

The Modal Controller Design Versus the Specification

The multi-stage modal controller design developed during this thesis project was oriented toward meeting a design specification. This specification was the same as that used by the AFFDL CCV ADPO for their optimal controller design. The initial design for the modal controller does not meet that specification.

To be more specific, the specification as presented in Appendix B states 53 separate requirements to be met if all five control surfaces are used in the design. Since modal control could be achieved with only three surfaces, the list of 53 requirements is reduced to 41 because the requirements for stability, displacement, and rate limits on the inboard ailerons and flaperons are deleted. Furthermore, the data for the surface deflections and rates and for the stress at WS222 due to pilot-induced elevator oscillations can not be correlated with the similar data given in AFFDL-TM-74-138-FGB. This lack of correlation is discussed in another section, but at this point in the discussion these 13 items are considered as not being met. The remaining 28 requirements are given in paragraphs 1.1, 1.2, and 1.4 of the specifications; 23 of these are met and are summarized in Table X. In total, then the modal controller designed for this thesis is known to meet 23 of 41 specified requirements. Because not all of the requirements are met, the present system design is not considered to be satisfactory.

Comparison of Open-loop and Closed-loop Systems

Table X		
Summary of Specification Requirements Met By Multi-Stage Modal Controller		
<u>Specification Paragraph</u>	<u>Item Measured</u>	<u>Met By Modal Controller?</u>
1.1.1.1	Acceleration @ BS172	No
	Acceleration @ BS860	Yes
	Acceleration @ BS1655	No
1.1.1.2	Stress @ BS475	No
	Stress @ BS760	Yes
	Stress @ BS1412	No
	Stress @ WS222	Yes
	Stress @ WS975	Yes
1.1.3	Stress @ SBL56	No
	Pitch Rate @ BS815	Yes
1.2	Gain Margins in 3 Control Loops	3 of 3
	Phase Margins in 3 Control Loops	3 of 3
1.4	ω_n & ζ limits on Shifted Structural Modes	12 of 12

In this section, the closed-loop modal controller system performance is compared with that of the unaugmented open-loop system and the closed-loop AFFDL optimal controller system. The basis for the comparisons is taken from the data generated by the routines in MODAL. The data is predominantly numerical since the achievement of specification requirements is best determined from such data. However, one time-history plot is presented to depict aircraft rigid-body pitch-rate response to a step elevator disturbance.

Performance in Wind-induced Turbulence. Paragraph 1.1.1

of the specification states the requirements to be met for normal accelerations at three body-axis stations and for normal stresses at three body-axis stations, two wing stations, and one horizontal-stabilizer buttock line station in the presence of wind-induced turbulence. The wind-induced turbulence is given as zero-mean, Gaussian, white noise with a magnitude of 8 fps rms. The results of forcing the three systems with this input noise is found by covariance analysis using the test routine NOISE. The data calculated by NOISE is presented in Table XI.

Table XI shows the comparative open-loop, modal controller, and optimal controller data for wind-induced turbulence, and also shows the specification requirements. From the table, it is seen that the modal controller meets only four of the nine requirements. This compares with the optimal controller meeting eight of the nine. The data given in Table XI compares favorable (within two decimal places) with the similar data given in AFFDL-TM-74-138-FGB [Ref7:22], except that the data in Table XI is eight times greater than that in the AFFDL report. An initial reaction might be that the data in AFFDL-TM-74-138-FGB is only for a 1 fps rms gust level. However Mr. Poyneer, the author, explains this is not the case if the data from his report is compared with the Ride Control System design data [Ref 2:62]. The disparity of the factor of 8 is thus unknown and the finding of an actual reason is not possible in the time available to complete this project. It is necessary to lo-

Table XI
 Comparison of Measured RMS Values of Specified
 Accelerations and Stresses for Open-loop,
 Modal Controller and Optimal Controller Systems
 When Forced By Wind-induced Turbulence

<u>Item Measured</u>	<u>Open-loop System</u>	<u>Optimal Controller</u>	<u>Modal Controller</u>	<u>Spec Req'm't</u>
Accel. in g's @ BS172	1.98	1.28	2.22	<1.386
Accel. in g's @ BS860	1.75	1.31	1.55	<1.837
Accel. in g's @ BS1655	2.57	1.72	2.53	<1.799
Stress in psi @ BS475	4752	4056	9320	< 4279
Stress in psi @ BS760	8107	6771	5503	< 7296
Stress in psi @ BS1412	3407	4397	4792	< 3066
Stress in psi @ WS222	13115	10650	8995	<11804
Stress in psi @ WS974	9680	7732	7689	< 8712
Stress in psi @ SBL56	7111	4536	7985	< 6400

cate the source of this difference before a meaningful comparison of the results can be made. It is noted however, that exactly the same items are met by the optimal controller as were reported in AFFDL-TM-74-138-FGB. This includes the optimal controller showing essentially (within 2 significant figures) the same reductions as previously reported [Ref 7:22].

The reasons for the modal controller not meeting the specification are not known at this time. However the design presented herein represents only a first attempt at a design and does not reflect what might be accomplished if other control-input sequences or eigenvalue shifts were tried. The controller presented does not perform the task of ride control; this is evident in the increased accelera-

tions at the crew station (N_{z172}). Further, the empennage normal acceleration is not reduced as seen in the N_{z1655} data in Table XI. The stress reduction considerations of the specification relate to the CCV concept of Fatigue Reduction. The modal controller is seen to reduce only three of the six stresses. One of those not reduced is the same as that not reduced by the optimal controller: the normal stress at BS1412. It is noted however that for two of the three items of stress reduction caused by the modal controller, these two reductions are significantly greater than those achieved by the optimal controller. The percentage reductions for the closed-loop systems versus the open-loop system is summarized in Table XII.

Parameter	Specification	Modal Controller	Optimal Controller
N_z @ BS172	30%	-12.1%	35.4%
N_z @ BS860	-5%	11.4%	25.1%
N_z @ BS1655	30%	1.6%	33.1%
Stress @ BS475	10%	-96.1%	14.6%
Stress @ BS760	10%	32.1%	16.5%
Stress @ BS1412	10%	-40.7%	-29.1%
Stress @ WS222	10%	31.4%	18.8%
Stress @ WS974	10%	20.6%	20.1%
Stress @ SBL56	10%	-12.3%	36.2%

Performance with Pilot-induced Elevator Oscillations.
Paragraph 1.1.2 of the specification requires a 30% reduction in wing-root bending stress at WS222 when the aircraft

is subjected to a zero-mean, Gaussian, white noise input of a 0.1 rad rms level. This input represents random elevator deflections which the pilot might induce. The analysis of the three systems to determine their compliance with paragraph 1.1.2 was made using the routine NOISE. The data calculated is 164 psi for the open-loop system, 133 psi for the optimal controller system, and 112 psi for the modal controller. Based on these numbers, the specified maximum level of stress would be 114.8 psi for a 30% reduction. The optimal controller reduces the stress by 18.9%, and the modal controller reduces it by 31.7%. Based on these values, the modal controller as designed shows a satisfactory reduction of the stress at WS222.

On the other hand, the above data does not correlate with the results given in AFFDL-TM-74-138-FGB: 4865 psi for the open-loop system and 3417 psi for the optimal controller. This is a reduction of 29.7%. The lack of correlation is not understood and the reason was not pursued due to project time constraints. Because of the lack of correlation, the specification requirement of reducing the stress @ WS222 is considered not to be satisfied.

Performance for Step-elevator Input. Paragraph 1.1.3 of the specification requires that the pitch rate response of the aircraft to a step elevator input fall within the "bounds" of Fig. B1. This requirement is basically one oriented toward aircraft handling qualities. The measured quantity used for determination of this para-

meter is taken as sensed pitch rate at BS815. The responses of the open-loop and closed-loop systems to a unit step was calculated by the test routine XFRFNCT, and the resulting time history for a five-second period is shown in Fig. 9.

Fig. 9 gives an illustration of the open-loop system response and the effects of the modal and optimal controllers. The open-loop system is fairly responsive with a peak overshoot of 4.1% at 1.65 seconds and a settling time of 2.19 seconds to reach 2% of the steady-state value of .062102 units/sec.

The closed-loop optimal controller system shows a well-damped behavior with no overshoot and a settling time which is outside the five-second time length calculated. The almost sluggish response of the optimally-controlled system is primarily due to the increased damping and reduced natural frequency of the short period mode and the shift of one of the washout filter time constants from 0.5 seconds to 1.526 seconds. These details are listed in Table XIII. Table XIII shows the eigenvalues of the AFFDL optimal controller system.

For the modal controller, its behavior shows a slightly faster rise time than the open-loop system. The curve peaks at 1.60 seconds with a 0.7% overshoot and shows a much reduced settling time of 1.22 seconds. As was the case for the open-loop system and for the optimal controller system, the modal controller system steady-state value of $\dot{\theta}_{815}$ is 0.062102 units/sec.

The pitch rate response data given in Fig. 9 can not be correlated with similar data presented in Fig. 4 of AFFDL-

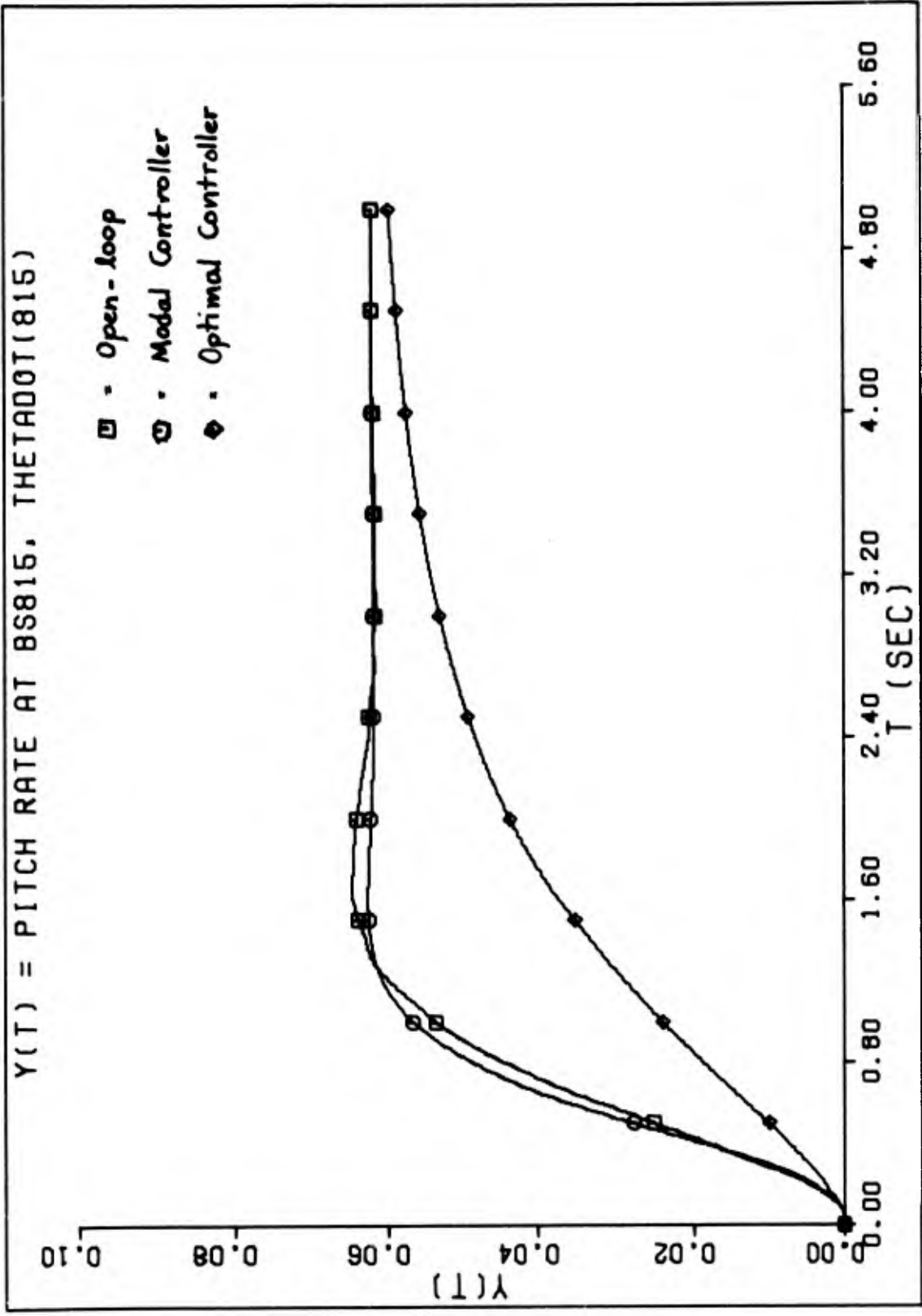


Fig. 9. B-52 CCV Pitch Rate Response Based on Sensor Output @ BS815

Table XIII - Eigenvalue Data for Closed-loop Plant with Optimal Controller

NR	REAL PART	IMAG PART	DAMPING RATIO	NAT FREQ(RPS)	NAT FREQ(HZ)
1	-65.34773780	49.78382491	.79563035	82.18263489	13.07977257
2	-65.34773780	-49.78382491	.79563035	82.18263489	13.07977257
3	-53.34705338	0.00000000	1.00000000	53.38795388	8.49695676
4	-48.01277283	0.00000000	1.00000000	48.31277283	7.64147012
5	-2.99997322	31.39151443	.09513294	31.53453690	5.01887742
6	-2.99997322	-31.39151443	.09513294	31.53453690	5.01887742
7	-.39511337	19.76563319	.01993592	19.76054193	3.14642669
8	-.39511337	-19.76563319	.01993592	19.76054193	3.14642669
9	-1.49134700	18.34941501	.08107779	18.40991930	2.93022974
10	-1.49134700	-18.34941501	.08107779	18.40991930	2.93022974
11	-.91332986	14.34772998	.06356973	14.37680842	2.29814013
12	-.91332986	-14.34772998	.06356973	14.37680842	2.29814013
13	-2.27119731	11.77419313	.18940463	11.99124519	1.90846594
14	-2.27119731	-11.77419313	.18940463	11.99124519	1.90846594
15	-1.00174850	6.00742746	.16449157	6.09037642	1.90346594
16	-1.00174850	-6.00742746	.16449157	6.09037642	1.90346594
17	-1.35103336	1.05031227	.78949137	1.71127058	.96931351
18	-1.35103336	-1.05031227	.78949137	1.71127058	.96931351
19	-.65505695	0.00000000	1.00000000	.65505695	.27235717
20	-.65505695	0.00000000	1.00000000	.65505695	.27235717
21	-2.09151911	0.00000000	1.00000000	2.09151911	.33297561
22	-2.09151911	0.00000000	1.00000000	2.09151911	.33297561
23	-8.01069497	0.00000000	1.00000000	8.01069497	3.1859207
24	-8.01069497	0.00000000	1.00000000	8.01069497	3.1859207
25	-6.33195548	0.00000000	1.00000000	6.33195548	1.27494234
26	-6.33195548	0.00000000	1.00000000	6.33195548	1.27494234
27	-7.10883739	0.00000000	.99999992	7.10883739	1.00776201
28	-7.10883739	0.00000000	.99999992	7.10883739	1.00776201
29	-6.87964855	0.00000000	1.00000000	6.87964855	1.13140661
30	-6.87964855	0.00000000	1.00000000	6.87964855	1.13140661
31	-6.87550434	0.00000000	1.00000000	6.87550434	1.09477102
32	-6.87550434	0.00000000	1.00000000	6.87550434	1.09477102
33	-6.87706556	0.00000000	1.00000000	6.87706556	1.09451915
34	-6.87706556	0.00000000	1.00000000	6.87706556	1.09451915
35	-1.92500000	2.32874795	.63712766	3.02137254	.48086637
36	-1.92500000	-2.32874795	.63712766	3.02137254	.48086637
37	-34.38000000	19.84982620	.86501969	39.69886648	6.31827083
38	-34.38000000	-19.84982620	.86501969	39.69886648	6.31827083
39	-52.89335556	0.00000000	1.00000000	52.89335556	8.41923900
40	-52.89335556	0.00000000	1.00000000	52.89335556	8.41923900
41	-10.57864440	0.00000000	1.00000000	10.57864440	1.68364355
42	-10.57864440	0.00000000	1.00000000	10.57864440	1.68364355
43	-34.38200000	0.00000000	1.00000000	34.38200000	5.47206525
44	-34.38200000	0.00000000	1.00000000	34.38200000	5.47206525
45	-50.00000000	0.00000000	1.00000000	50.00000000	7.95774715
46	-50.00000000	0.00000000	1.00000000	50.00000000	7.95774715
47	-2.00000000	0.00000000	1.00000000	2.00000000	.31830989
48	-2.00000000	0.00000000	1.00000000	2.00000000	.31830989
49	-.85950000	0.00000000	1.00000000	.85950000	.13679367
50	-.85950000	0.00000000	1.00000000	.85950000	.13679367
51	-1.00000000	0.00000000	1.00000000	1.00000000	.15915494
52	-1.00000000	0.00000000	1.00000000	1.00000000	.15915494

TM-74-138-FGB [Ref 7:23]. That figure is reproduced herein as Fig. B1, and is considered to be a bound. The text of the AFFDL technical memorandum may imply that the upper curve of Fig. B1 is the response of the open-loop airplane and that the lower curve is the response of the optimally-controlled airplane. However, the data presented in Fig. 9 is believed to be a correct representation of the $\dot{\theta}_{815}$ response. It does not show a 57% overshoot for the open-loop system, nor does the optimal controller curve display a lightly damped oscillation after the transients die out. Finally, Fig. 4 of AFFDL-TM-74-138-FGB does not reflect any time scale on its abscissa. Therefore, the curves shown there are considered to be bounds and not actual system responses. The lack of correlation in this information is not considered to be a problem; the curves shown in Fig. 9 and the accompanying data in the text is taken as correct.

Control Loop Stability. Control loop stability requirements are given in paragraph 1.2 of the specification. The requirements are 6 db gain margins and 60° phase margins. Compliance with these requirements is determined only for the modal controller system and the routine BODE is used. The data computed is tabulated below along with the similar data for the optimal controller [Ref 7:21].

Loop	<u>Gain Margin</u>		<u>Phase Margin</u>	
	Modal Controller	Optimal Controller	Modal Controller	Optimal Controller
Elevator	∞ db	15 db	167.5°	69.6
Flaperon	N/A	10 db	N/A	39.3
Outboard Aileron	∞ db	10 db	90°	180.0
Canard	∞ db	20 db	78.2°	31.9

From the above table, it is seen that the modal controller provides very satisfactory control loop stability for the three loops used. All have infinite gain margin and have phase margins greater than 60° . The data for the modal controller should not be compared with the data for the optimal controller however. The data from Reference 7 was derived by a completely different approach and is listed here only to show the stability of the optimal controller loops.

Control Surface Displacements and Rates. Paragraph 1.3 of the specification provides limits that must be met for control surface displacements and rates. As previously stated, the data for the modal controller designed during this project does not correlate with the limits given in the specification nor with the data for the optimal controller as given in AFFDL-TM-74-138-FGB [Ref 7:26]. The data as calculated by the routine NOISE is listed in Table XIV for both wind-induced turbulence and pilot-induced elevator oscillations.

The possible reasons for a lack of correlation is now discussed. The data presented in Table XIV was obtained from a covariance analysis which made calculations based on the input being white noise. That is, all frequencies were assumed to be included in the input signal. In addition, the outputs for the surface displacements and rates were computed using the state-response matrix and the control-response matrix given in AFFDL-TM-74-138-FGB. Therein, these matrices were used in accordance with Eq (42) to ob-

tain rms values of the responses. The use of these matrices by themselves for this project should cause no problem, but they may when used in an infinite-bandwidth covariance analysis. The method used to set up these matrices is unknown. Further, their use may be restricted to the Honeywell optimal control program and its internal and unknown method of performing a covariance analysis. Whatever the reasons may be however, the data in Table XIV shows the lack of correlation and is recorded for future attempts at making a correlation. It is pointed out that the same method was used to obtain the data given in Table XI and the data for elevator oscillation-induced stress at WS222. The finding of reasons for the lack of correlation for the surface data may also explain the reason for the lack of correlation of the WS222 data and the reason for the factor of eight in the other stress data.

Eigenvalue Location Restrictions. Paragraph 14 specifies limits on changes to structural-mode natural frequency and damping ratios. These restrictions are illustrated on Fig. 7. The modal controller meets the requirements of this paragraph in every way since closed-loop eigenvalue locations are guaranteed under the premise of full-state feedback.

Comparison of Modal Controller Performance With Other B-52 CCV Controllers

The previous section compared the performance of the modal controller design developed during this project with the open-loop system and the AFFDL optimal controller. In

Table XIV

Covariance Analysis Data From Routine NOISE
for Surface Displacements and Rates For
Wind-Induced Turbulence and For
Pilot-Induced Elevator Oscillations

	Parameter	Open Loop System	Optimal Controller System	Modal Control System	Spec Reqm't	Data from Ref 7
	Displacements in deg, rates in deg/sec					
Wind-induced Turbulence	δ_e	0	597	676	<19	1.54
	δ_f	0	513	0	<20	1.14
	δ_{ao}	0	459	906	<20	1.04
	δ_c	0	374	1217	<12	0.82
	$\dot{\delta}_e$	0	4.53	5.14	<80	22.2
	$\dot{\delta}_f$	0	4.49	0	<80	18.2
	$\dot{\delta}_{ao}$	0	3.92	2.70	<80	18.1
	$\dot{\delta}_c$	0	4.85	7.67	<83	8.93
Pilot-induced Elevator Oscillations	δ_e	0	7.46	8.45	<19	4.96
	δ_f	0	6.41	0	<20	3.56
	δ_{ao}	0	5.73	11.32	<20	0.97
	δ_c	0	4.67	15.20	<12	1.25
	$\dot{\delta}_e$	0	0.057	0.064	<80	42.9
	$\dot{\delta}_f$	0	0.056	0	<80	19.7
	$\dot{\delta}_{ao}$	0	0.049	0.034	<80	24.7
	$\dot{\delta}_c$	0	0.061	0.096	<83	25.4

this section, the modal controller performance is compared with the Ride Control System data presented in AFFDL-TR-73-84 [Ref 2]. Due to the lack of project time and lack of commonality of operating points, the modal controller design developed for this thesis can not readily be compared with the results of other previous B-52 CCV programs.

One area of comparison can be discussed when the modal controller system is evaluated against the RCS: aircraft

accelerations and stresses due to wind-induced turbulence. Other areas of comparison may be possible if the calculated modal controller surface displacements and rates were correlated. Table VII of the RCS report lists the rms accelerations at BS172, BS860, and BS1655. With the units of g/fps, the respective values are 0.0240, 0.0251, and 0.0451. That table also lists the open-loop rms accelerations as 0.0358, 0.0296, and 0.0443 g/fps for the same stations. If these numbers are multiplied by 8 fps, they compare very well with the data given in AFFDL-TM-74-138-FGB. If the factor of 8 is applied again, the open-loop values from the RCS report match very well with the corresponding numbers in this report. As previously mentioned, the reason for the additional factor of 8 is not understood; if it can be logically explained, the open-loop rms accelerations compare satisfactorily. The number for the RCS show reductions in the acceleration at BS172 by 33% and at BS860 by 15%. The change at BS1655 is a 2% increase, but a reduction there was not an RCS program goal. In comparison, the modal controller performance is not satisfactory for providing ride control in turbulence.

Summary of Results and Comparisons

This fourth chapter has presented the results of an initial modal controller design and has compared the results with the specification requirements as given in Appendix B, and with the results of the AFFDL optimal controller. The results show that the modal controller uses three control

surfaces to precisely shift the 14 eigenvalues of six structural modes and the short period mode when full-state feedback is utilized. The initial design is shown to meet 23 of 41 specification requirements; many of the remaining requirements may be met once the data for those parameters is successfully correlated with the requirements and the AFFDL optimal controller data. Although the design as presented is not satisfactory, the computer program which was developed as part of this project is available and can be used in any future effort to improve the modal controller design. The next chapter presents specific recommendations in this regard.

V. Conclusions and Recommendations

Based on the foregoing discussion of modal control theory, the determination of an initial design, and the presentation of an initial design, and the presentation of results and comparisons, this chapter draws three conclusions and lists several recommendations.

Conclusions

The first conclusion that might be made is that the initial design attempt did not meet the specifications. The design presented here is only an initial design and as such was not expected to meet the requirements in total. Because over 90% of the project time was spent building and testing the software for the computer program, little time was available to do the task of designing a modal controller for the B-52 CCV. Therefore, the first and most important conclusion to be reached is that this thesis has resulted in a computer program which can now be used for the design project originally intended.

The second conclusion of this thesis is that a modal controller can at least in part perform the role of an active system for the control of structural modes in a large, flexible aircraft. Of 41 requirements, 23 are met by the initial design presented. The only design variations that were accomplished were the initial three short-period mode eigenvalue locations. The modal control theory permits eigenvalue relocation with ease and the early study showed

the influence of the pair of short-period roots on the pitch rate response. Using the program now available, additional studies of the effects of shifting the six pairs of structural mode roots should permit several more of the specification requirements to be met without a major effort.

A third conclusion that is reached is that although modal control theory is well developed and there are numerous design techniques available, there is negligible work published in the area of selecting closed-loop eigenvalue locations. The paper by Pai, et.al., provided some insight, but intuition served as the primary guide for this project. Part of the problem may be that the specification used was written in standard aircraft control language where performance is based on sensor readings; i.e, system outputs. In contrast, the modal controller design for this project used state feedback rather than output feedback. This makes it difficult to relate system output responses to internal structural dynamics by any means other than intuition. However, if the relationships of eigenvalue locations and system responses were to be developed rigorously, then a modal controller can indeed be designed.

Recommendations

Several recommendations are now presented. The first and foremost recommendation is based on the second conclusion above. Throughout this project, a full-state feedback design was assumed feasible and with the initial design meeting over one-half of the specified requirements, the use

of the appended computer program should permit a satisfactory design to be found. However, this is not to say that a design can be formulated quickly; but with the ability to readily test the design, the task should be fairly straight forward. If the project is continued, the initial study should include an analysis of the effects of shifting each of the structural modes about the nominal values given in Table IV in order to more fully understand the influence of each mode on each of the outputs. (Here, outputs refer to the response matrix outputs of stresses, accelerations and surface parameters along with the 10 outputs given in Table I.) In addition to this study, initial efforts should also be made at correlating the results given in Chapter IV. Such a correlation is absolutely necessary if a modal controller design is to be compared with the AFFDL optimal controller, or is to be a viable candidate for future CCV programs. An extension of this project should include a study of using other sequences of the inputs. For example, choosing the horizontal canard as the first input to be used may show that the flaperons or inboard ailerons are needed to complete the design. For full-state feedback this would require more feedbacks than the 109 listed in Table VIII, but the values of some of the larger gains may be appreciably reduced and thus offset the complications associated with over 30 more paths. Finally, an extension should also include a study of using less than complete state feedback. This step is necessary to achieve a practical design which could be implemen-

ted. Several papers that may be useful in this effort are those by Davison, Davison and Chatterjee, Davison and Goldberg, and Fallside and Seraji [Ref 18-21]. Furthermore, the computer program is now available to make these suggested continuations a reasonable project. By comparison, it is recalled that when the AFFDL started their optimal controller design study they started with a program already written and with an initial guess at a suitable weighting matrix.

The second recommendation to come from this project is also one to extend this thesis. This recommendation proposes that output feedback be evaluated as an alternate modal control design. Papers such as that by Fallside and Seraji [Ref 22] are available in the literature and such a design would offer great practicality since the sensed outputs of accelerations and pitch rate are available. This effort could also include a study of the use of a state observer to reconstruct those states which are known to be observable but are not easily measured. The use of an observer might also present a practical and successful design.

The third recommendation to be made deals with the computer program written for this thesis. As it exists, it is special-purpose, being useful for the design of multi-stage modal controllers with 39 states. Another thesis project might include streamlining this program for efficiency, adding options for other types of modal controller designs, such as dyadic, and converting the program (perhaps in reduced size) to an interactive program for intercom and graph-

ics design purposes. The algorithms for the various designs can be coded fairly easily and a minimum of modern control theory knowledge would be necessary to pursue this effort.

A fourth and final recommendation to be included in this list is one offered by the faculty at the Air Force Institute of Technology. Their recommendation is that of determining the feasibility of using modal control theory to achieve a set of initial, stable starting gains for an optimal controller, and then using a routine such as the aforementioned Honeywell "Quadratic Methodology" program to home in on the final design. The use of modal control theory and optimal control theory together may help to overcome the difficulty in selecting the weighting matrix and in remedying some of the conclusions presented in AFFDL-TM-74-138-FGB.

In summary, this thesis has presented the theory and results of a study to design a modal controller for the B-52 CCV. Although the theory is straight forward, the implementation of the theory and associated testing techniques into a working computer program took up a large amount of time. As a consequence, only an initial design was completed. That design does not meet its specification, but sufficient results are presented to conclude that a modal controller may be a feasible system when compared with an optimal controller designed to the same specification. It is thus concluded that the modal controller technique is feasible and various recommendations for extending the work are made. The experience gained in this project in terms of altering the design has shown that a modal controller design can be

used to achieve satisfactory results.

Bibliography

1. Burris, P. M. and M. A. Bender. Aircraft Load Alleviation and Mode Stabilization (LAMS). Technical Report AFFDL-TR-68-158. Wright-Patterson Air Force Base, Ohio: Air Force Flight Dynamics Laboratory, April, 1969.
2. Stockdale, C. R. and R. D. Poyneer. Control Configured Vehicle Ride Control System (CCV RCS). Technical Report AFFDL-TR-73-83. Wright-Patterson Air Force Base, Ohio: Air Force Flight Dynamics Laboratory, July, 1973.
3. Stockdale, C. R., et al. Control Configured Vehicles Ride Control System Flight Test Results. Technical Report AFFDL-TR-74-66. Wright-Patterson Air Force Base, Ohio: Air Force Flight Dynamics Laboratory, June, 1975.
4. The Boeing Company, Wichita Division. B-52 CCV Program Summary. Technical Report AFFDL-TR-74-92, Vol I. Wright-Patterson Air Force Base, Ohio: Air Force Flight Dynamics Laboratory, 1975. (Summary volume of six volume report, all having the same TR number.)
5. Van Dierendonck, A. J. and G. L. Hartmann. Quadratic Methodology, Vol I. Honeywell Report No. F0161-FR, Vol I. Minneapolis: Honeywell, Inc., October, 1973. ADA006731
6. ----- Quadratic Methodology, Vol II. Honeywell Report No. F0161-FR, Vol II. Minneapolis: Honeywell, Inc., October, 1973. ADA006732
7. Poyneer, R. D. Control Configured Vehicles, Multi-Surface System Design. Technical Memorandum AFFDL-TM-74-138-FGB. Wright-Patterson Air Force Base, Ohio: Air Force Flight Dynamics Laboratory, July, 1974.
8. Simon, J. D. and S. K. Mitter. "A Theory of Modal Control." Information and Control, 13: 316-353 (1968).
9. Porter, B. and T. R. Crossley. Modal Control, Theory and Applications. New York: Barnes and Noble Books, 1972.
10. Chen, C. T. Introduction to Linear System Theory. New York: Holt, Rinehart, and Winston, Inc., 1970.
11. Mering, E. D. Linear Algebra and Matrix Theory (Second Edition). New York: John Wiley and Sons, Inc., 1970.
12. Kwakernaak, H. and R. Sivan. Linear Optimal Control Systems. New York: Wiley-Interscience, 1972.

13. Pai, M. A., S. S. Prabhu, and I. V. Ramana. "Modal Control of a Power System" International Journal of Systems Science;6: 87-100 (1975).
14. D'Azzo, J. J., and C. H. Houppis. Linear Control System Analysis and Design: Conventional and Modern. New York: McGraw-Hill Book Company, 1975.
15. Gould, L. A., A. T. Murphy, and E. F. Berkman. "On the Simon-Mitter Pole Allocation Algorithm-Explicit Gains for Repeated Eigenvalues." IEEE Transactions on Automatic Control, AC-15: 259-260 (April, 1970).
16. Smith, B. T., et al. Matrix Eigensystem Routines, EISPACK Guide (Lecture Notes in Computer Science, Vol 6) Berlin: Springer-Verlag, 1974.
17. Bisplinghoff, R. L., et al. Aeroelasticity. Cambridge, Massachusetts: Addison-Wesley Publishing Co., Inc., 1955.
18. Davison, E. J. "On Pole Assignment in Linear Systems with Incomplete Feedback" IEEE Transactions on Automatic Control, AC-15: 348-351 June 1970.
19. Davison, E. J., and R. Chatterjee. "A Note on Pole Assignment in Linear Systems with Incomplete Feedback" IEEE Transactions on Automatic Control, AC-16: ~~98~~-99 February 1971.
20. Davison, E. J., and R. W. Goldberg. "A Design Technique for the Incomplete State Feedback Problem in Multivariable Control Systems" Automatica, 5: 335-345, 1969.
21. Fallside, F., and H. Seraji. "Direct Design Procedure for Multivariable Feedback Systems" Proceedings of IEE, 118: 797-801, June 1971.
22. Fallside, F., and H. Seraji. "Pole-shifting Procedure for Multivariable System Using Output Feedback" Proceedings of the IEE, 118: 1648-1654, November 1971.

Appendix A

Computer Routines

This appendix is composed of seven sections which present routines or information on routines used for this thesis project.

	Page
A1: EISPACK and the Routine RGEIG	100
A2: Complex Matrix Inversion via MINVC	102
A3: General Matrix Manipulation and I/O Routines	103
A4: B-52 CCV Modal Controller and Comparison Program: MODAL	118
A5: Covariance Analysis via NOISE	134
A6: Transfer Function Analysis via XFRFNCT	145
A7: Frequency Response Analysis via BODE	156

Appendix A1: EISPACK and the Routine RGEIG

The EISPACK library of eigensystem routines is a read-only permanent file of binary records available on the Aeronautical Systems Division Computer Center CDC 6600. The complete package consists of 34 routines which can be used for the determination of eigenvalues and eigenvectors, of most matrices. A user's guide is available and is listed as Reference 16 in the bibliography. Of interest to this thesis however, is the fact that a set of four driver routines has been developed by Purdue University to perform eigenanalysis of four classes of matrices. These drivers are available in modified form on the ASD Computer Center CDC 6600 under the names RSEIG, RGEIG, CGEIG, AND CHEIG. In the order listed these routines compute the eigenvalues and optionally the eigenvectors of real symmetric matrices, real general matrices, complex general matrices, and complex Hermitian matrices. The driver RGEIG is used in the program MODAL and the subroutine BODE.

The driver routine RGEIG solves for the eigenvalues of a real general matrix, A , and optionally, the eigenvectors. The call is of the form

```
CALL RGEIG (M, N, A, IND, EIGVAL, EIGVEC, WORK)
```

The input arguments are as follows:

M = Row dimension of A.
N = Order of matrix A, where $N \leq M$.
A(M,K) = Two-dimensional real general matrix where
 $K \geq N$.

IND = Integer index which must be passed to RGEIG. Set IND = 0 for calculation of eigenvalues only. Set IND \neq 0 for calculation of eigenvalues and eigenvectors. IND must be set for each call to RGEIG.

WORK = $2 \times N$ working array.

The output arguments are

EIGVAL = Complex N-vector of eigenvalues. EIGVAL may be declared as DIMENSION EIGVAL(2,N) or COMPLEX EIGVAL(N) in the calling program. The dimension statement causes the eigenvalues to be returned by RGEIG in the dual-array storage mode. The complex statement causes the eigenvalues to be returned by RGEIG in the complex storage mode.

EIGVEC = Complex $N \times K$ array of N eigenvectors. EIGVEC may be declared as DIMENSION EIGVEC(2,N,K) or as COMPLEX EIGVEC(N,K) with the same results as for EIGVAL.

For this thesis, $N = M = K = 39$ in all calls to RGEIG. A very important comment is that RGEIG (like all EISPACK drivers) will destroy the matrix A.

Appendix A2: Complex Matrix Inversion via MINVC

The routine MINVC is used in the program MODAL and the subprogram BODE for the inversion of complex matrices. MINVC is a routine available in the AFITSUBPROGRAM library. The call is made as

```
CALL MINVC (A, B, N)
```

where the inverse of the $N \times N$ matrix \underline{A} is to be found and stored in the $N \times N$ matrix \underline{B} . The matrix \underline{A} is destroyed unless the call is made as

```
CALL MINVC (B, B, N)
```

where \underline{A} has been previously duplicated into \underline{B} (see routine CDUP, Appendix A3). For the use of MINVC, 311 cells of blank common should be allowed (see card 26 in MODAL as example).

Appendix A3: General Matrix Manipulation and I/O Routines

This section provides coding for the following subprograms useful in matrix multiplication, data read-in from cards, matrix print-outs, matrix duplication, matrix zeroing, and matrix transposition. The use of the routines is explained in the routines.

	Page
MRCM	104
MCCM	105
MCRM	106
MRRM	107
REED	108
RPRT	109
CPRT	110
EPRT	111
RDUP	112
CDUP	113
ZERO	114
EPACK	115
RXPOSE	116
CXPOSE	117

```

C
C
C
C
C
SUBROUTINE MPCM(A, B, C, K, L, M)
C THIS ROUTINE MULTIPLIES TOGETHER REAL MATRIX A AND COMPLEX MATRIX
R TO GET COMPLEX MATRIX C: C = A*B
C THIS ROUTINE USES 1209 WORDS OF CM.
C
DIMENSION A(K,L)
COMPLEX B(L,M), C(K,M)
DO 3 JJ = 1,M
DO 3 II = 1,K
C(II,JJ) = (0.0,0.0)
DO 2 KK = 1,L
2 C(II,JJ) = C(II,JJ) + A(II, KK) * B(KK, JJ)
IF (ABS(REAL(C(II,JJ))).LT..00000001) C(II,JJ) = CMPLX(0.0,AIMAG(C
+(II,JJ)))
IF (ABS(AIMAG(C(II,JJ))).LT..00000001) C(II,JJ) = CMPLX(REAL(C(II,
+JJ)),0.0)
3 CONTINUE
RETURN
END

```

```

SUBROUTINE MCCM (A, P, C, K, L, M)
C THIS ROUTINE MULTIPLIES TOGETHER TWO COMPLEX MATRICES A AND B
C TO GET ANOTHER COMPLEX MATRIX C: C = A*B.
C THIS ROUTINE USES 1229 WORDS OF CM.
C
  COMPLEX A(K,L), B(L,M), C(K,M)
  DO 5 JJ = 1,M
  DO 5 II = 1,K
    C(II,JJ) = (0.0,0.0)
  DO 4 KK = 1,L
    C(II,JJ) = C(II,JJ) + A(II,KK) * B(KK,JJ)
  IF (ABS(REAL(C(II,JJ))).LT..00000001) C(II,JJ) = CMPLX(0.0,AIMAG(C
+(II,JJ)))
  IF (ABS(AIMAG(C(II,JJ))).LT..00000001) C(II,JJ) = CMPLX(REAL(C(II,
+JJ)),0.0)
  5 CONTINUE
  RETURN
  END

```

```

C
C
C SURROUTINE MCR4 (A,R,C,K,L,M)
C THIS ROUTINE MULTIPLIES TOGETHER COMPLEX MATRIX A AND REAL
C MATRIX P TO GET COMPLEX MATRIX C: C = A*B.
C THIS ROUTINE USES 1179 WORDS OF CM.
C
  DIMENSION B(L,M)
  COMPLEX A(K,L), C(K,M)
  DO 9 JJ = 1,M
  DO 9 II = 1,K
    C(II,JJ) = (0.0,0.0)
  DO 8 KK = 1,L
    C(II,JJ) = C(II,JJ) + A(II,KK) * R(KK,JJ)
  IF (ABS(REAL(C(II,JJ))).LT..00000001) C(II,JJ) = CMPLX(0.0,AIMAG(C
    +(II,JJ)))
  IF (ABS(AIMAG(C(II,JJ))).LT..00000001) C(II,JJ) = CMPLX(REAL(C(II,
    +JJ)),0.0)
  9 CONTINUE
  RETURN
  END

```

```

SUBROUTINE NRRM (A,R,C,K,L,M)
C THIS ROUTINE MULTIPLIES TOGETHER TWO REAL MATRICES, A AND B, TO
C GET REAL MATRIX C: C = A*B
C THIS ROUTINE USES 1038 WORDS OF CM.
C
DIMENSION A(K,L), B(L,M), C(K,M)
DO 152 JJ = 1,M
  DO 151 KK = 1,L
    C(KK,JJ) = 0.0
  151 C(KK,JJ) = C(KK,JJ) + A(KK,II) * B(KK,JJ)
  IF (ABS(C(KK,JJ)) .LT. .0000000001) C(KK,JJ) = 0.0
152 CONTINUE
RETURN
END

```

```

C C C C C
C  SUPROUTINE REED (NN,A,M1,M2)
C  THIS ROUTINE FIRST INITIALIZES THE MATRIX A TO ZERO THROUGHOUT,
C  AND THEN READS INTO THE MATRIX THE NON-ZERO DATA FROM THE NN CARDS.
C  THIS ROUTINE USES 1428 WORDS OF CM.
C
C  DIMENSION A(M1,M2), IROW(5), JCOL(5),FIN(5)
C  DO 1  II = 1,M1
C  DO 1  JJ = 1,M2
C  1  A(II,JJ) = 0.0
C  DO 12  K=1,NN
C  READ 10,(IROW(J),JCOL(J),FIN(J),J=1,5)
C  10  FORMAT (5(2I2,E12.5))
C  DO 12  I = 1,5
C  IF (IROW(I)) 12,12,11
C  11  A(IROW(I),JCOL(I)) = FIN(I)
C  12  CONTINUE
C  RETURN
C  END

```

C SUBROUTINE RPRT (A,K,L,M)
 C THIS ROUTINE PRINTS THE REAL MATRIX A BY ROWS, WHERE A IS K*L,
 C AND M IS NON-ZERO FOR F-FIELD FORMAT OR ZERO FOR E-FIELD FORMAT.
 C THIS ROUTINE USES 3500 WORDS OF CM.

```

DIMENSION A(K,L)
IF (M) 35,43,35
35 IF (L-10) 36,38,40
36 PRINT 37, (II, (A(II,JJ),JJ=1,L),II=1,K)
37 FORMAT (//,5X,"ROW",/,39(6X,I2,5F15.5,/) )
RETURN
38 PRINT 39, (II, (A(II,JJ),JJ=1,L),II=1,K)
39 FORMAT (//,5X,"ROW",/,39(6X,I2,5F15.5,/,8X,5F15.5,/) )
RETURN
40 DO 41 II = 1,K
41 PRINT 42, II, (A(II,JJ),JJ=1,L)
42 FORMAT (//,5X,"ROW",I3,/,4(1X,8F12.5,/) ,1X,7F12.5)
RETURN
43 IF (L-10) 44,46,48
44 PRINT 45, (II, (A(II,JJ),JJ=1,L),II=1,K)
45 FORMAT (//,5X,"ROW",/,39(6X,I2,5E15.5,/) )
RETURN
46 PRINT 47, (II, (A(II,JJ),JJ=1,L),II=1,K)
47 FORMAT (//,5X,"ROW",/,39(6X,I2,5E15.5,/,8X,5E15.5,/) )
RETURN
48 DO 49 II = 1,K
49 PRINT 50, II, (A(II,JJ),JJ=1,L)
50 FORMAT (//,5X,"ROW",I3,/,4(1X,8E12.5,/) ,1X,7E12.5)
RETURN
END

```

```

C
C
C
C
C
SUBROUTINE CPRT (A,K,L,M)
C THIS ROUTINE PRINTS THE COMPLEX MATRIX A BY ROWS, WHERE A IS K*L,
C AND M IS NON-ZERO FOR F-FIELD FORMAT OR ZERO FOR E-FIELD FORMAT.
C THIS ROUTINE USES 3528 WORDS OF CM.
C
      COMPLEX A(K,L)
      IF (M) 51,59,51
      IF (L-10) 52,54,56
      51 PRINT 53, (II,(A(II,JJ),JJ=1,L),II=1,K)
      52 FORMAT (//,1X,"ROW",/,39(1X,I2,5(4X,2F11.7),/))
      RETURN
      54 PRINT 55, (II,(A(II,JJ),JJ=1,L),II=1,K)
      55 FORMAT (//,1X,"ROW",/,39(1X,I2,5(4X,2F11.7),/,4X,5(4X,2F11.7),/))
      RETURN
      56 CO 57 II = 1,K
      57 PRINT 58, II, (A(II,JJ),JJ=1,L)
      58 FORMAT (//,5X,"ROW",I3,/,7(5(4X,2F11.7),/),4(4X,2F11.7))
      RETURN
      59 IF (L-10) 60,62,64
      60 PRINT 61, (II,(A(II,JJ),JJ=1,L),II=1,K)
      61 FORMAT (//,1X,"ROW",/,39(1X,I2,5(4X,2E11.4),/))
      RETURN
      62 PRINT 63, (II,(A(II,JJ),JJ=1,L),II=1,K)
      63 FORMAT (//,1X,"ROW",/,39(1X,I2,5(4X,2E11.4),/,4X,5(4X,2E11.4),/))
      RETURN
      64 NO 65 II = 1,K
      65 PRINT 66, II, (A(II,JJ),JJ=1,L)
      66 FORMAT (//,5X,"ROW",I3,/,7(5(4X,2E11.4),/),4(4X,2E11.4))
      RETURN
      END

```



```

C
C SUPPLEMENTARY EPRINT (LL,EVALUE,ZETA,FREQR,FREQHZ)
C
C THIS ROUTINE PRINTS OUT THE LL EIGENVALUES OF A LL*LL MATRIX,
C GIVEN THE 2*LL COMPLEX EIGENVALUE ARRAY "EVALUE" FROM THE EISPACK
C DRIVER CALLED "RGEIG". THE REAL AND IMAGINARY PARTS OF THE
C EIGENVALUES ARE PRINTED, ALONG WITH THE DAMPING RATIO, NATURAL
C FREQUENCY IN RAD/SEC (RPS), AND NATURAL FREQUENCY IN HERTZ (HZ).
C THIS ROUTINE USES 1578 WORDS OF CM.
C
DIMENSION EVALUE(2,LL), ZETA(LL), FREQR(LL), FREQHZ(LL)
PRINT 70
70 FORMAT (//, " THE EIGENVALUES FOR THE PLANT MATRIX ARE:", //, 10X, "NO
\ ", 6X, "REAL PART", 5X, "IMAG PART", 4X, "DAMPING RATIO", 2X, "NAT FREQ(RP
\ S)", 3X, "NAT FREQ(HZ)", //)
DO 74 M = 1, LL
IF (EVALUE(1,M)) 72, 71, 72
71 ZETA(M) = 0.0
GO TO 73
72 ZETA(M) = ABS(COS(ATAN2(EVALUE(2,M), EVALUE(1,M))))
73 FREQR(M) = SORT(EVALUE(1,M)**2 + EVALUE(2,M)**2)
74 FREQHZ(M) = FREQR(M)/6.28318531
\ PRINT 75, (K, EVALUE(1,K), EVALUE(2,K), ZETA(K), FREQR(K), FREQHZ(K),
\ K=1, LL)
75 FORMAT (10X, I2, 2X, F14.8, F14.8, 4X, F12.8, 3X, F12.8, 3X, F12.8)
RETURN
END

```

```

C
C SUPROUTINE RDUP (A,9,K,L)
C THIS ROUTINE DUPLICATES REAL MATRIX A INTO REAL MATRIX B: A = 9.
C THIS ROUTINE USES 519 WORDS OF CM.
C
C DIMENSION A(K,L), B(K,L)
C DO 6 I = 1,K
C DO 6 J = 1,L
C 6 B(I,J) = A(I,J)
C RETURN
C END

```

```

SUBROUTINE CDUP (A,B,K,L)
C THIS ROUTINE DUPLICATES COMPLEX MATRIX A INTO COMPLEX MATRIX B: A = B.
C THIS ROUTINE USES 548 WORDS OF CM.
C
      COMPLEX A(K,L), B(K,L)
      DO 7 I = 1,K
      DO 7 J = 1,L
      7 R(I,J) = A(I,J)
      RETURN
      END

```

```

C      SURPOITINE ZERO (A,N)
C      THIS ROUTINE ZEROES OUT THE FIRST N LOCATIONS IN THE SUBSCRIPTED VARIABLE A.
C      N IS THE TOTAL NUMBER OF WORDS TO BE SET TO ZERO; E.G., IF A IS
C      A DOUBLY-SUBSCRIPTED ARRAY OF DIMENSION 3-8Y-7 AND THE ENTIRE
C      ARPAY IS TO BE SET TO ZERO, THEN N = 3*7*2 = 42.
C      THIS ROUTINE USES 15R WORDS OF CM.
C
C      DIMENSION A(N)
C      DO 67 II = 1,N
C      67 A(II) = 0.0
C      RETURN
C      END

```

```

C
C SURROUTINE EPACK (IJ, IK, EVALUE, EVECTOR, E, EV)
C THIS ROUTINE PACKS THE REAL AND IMAGINARY PARTS OF THE EIGENSYSTEM
C OUTPUTS FROM EISPACK, NAMELY EVALUE AND EVECTOR, INTO COMPLEX ARRAYS,
C E AND EV. THE ARGUMENTS IJ AND IK ARE THE DIMENSIONS OF THE EIGEN-
C SPACE.
C THIS ROUTINE USES 63R WORDS OF CM.
C
C DIMENSION EVALUE(2,IJ), EVECTOR(2,IJ,IK)
C COMPLEX E(IJ), EV(IJ,IK)
C NO 76 II = 1, IJ
C F(II) = CMPLX(EVALUE(1,II), EVALUE(2,II))
C NO 76 JJ = 1, IK
C 76 EV(II, JJ) = CMPLX(EVECTOR(1,II, JJ), EVECTOR(2,II, JJ))
C RETURN
C END

```

```

C
C SUBROUTINE RXPPOSE (A, I, K, L)
C THIS ROUTINE FINDS R AS THE TRANSPOSE OF THE REAL MATRIX A,
C WHERE A IS K*L AND B IS L*K.
C THIS ROUTINE USES 53R WORDS OF CM.
C
C DIMENSION A(K,L), R(L,K)
C DO 13 II = 1, K
C DO 13 JJ = 1, L
C 13 R(JJ, II) = A(II, JJ)
C RETURN
C END

```

```

C      SURROUTINE CYPOSE (A,B,K,L)
C      THIS ROUTINE FINDS R AS THE TRANSPOSE OF THE COMPLEX MATRIX A,
C      WHERE A IS K*L AND R IS L*K.
C      THIS ROUTINE USES 558 WORDS OF CM.
C
C      COMPLEX A(K,L), B(L,K)
C      DO 14 II = 1,K
C      DO 14 JJ = 1,L
C      14 B(JJ,II) = A(II,JJ)
C      RETURN
C      END

```

Appendix A4: B-52 CCV Modal Controller and Comparison Program: MODAL

This section provides the coding for the program MODAL. The user can control program options through changes in the DATA declarations, and must comply with the data requirements of the subprograms used. The program MODAL also uses the subprograms GAIN and TIMPLOT listed in this section.


```

PROGRAM MODAL (INPUT=1028,OUTPUT=4028,TAPE2)

LOGICAL PRINT, PRINT3, TPLOTS, PLOTTER
LOGICAL PRINT1, GUSTS, PIO, PASS
LOGICAL OLTFST, CLTEST, OPTTEST, DESIGN, OLDATA
LOGICAL RMSTEST, STEPRSP, FREQRSP
REAL INITIM
COMMON /PLOT1/ ALPHA(501), NLINE, LLINE, INITIM, DUPATN, DEL,FLET,
+ IX, IPTS
COMMON /PLOT2/ TYME(503), OUTPOOT(503), COMP(1505)
COMMON /SYSTEM/ A(39,39), a(39,5), C(10,39), H(39,2), G(5,39)
COMMON /DUPSYS/ AA(39,39), A2(39,39), KOPT(5,10)
COMMON /PARTFR/ SAVE1(234)
COMMON /PARTL1/ SAVE2(243)
COMMON /MAIN1/ NDIM, NDIM1, XRAY(39,39)
COMMON /MAIN2/ DUM1(39,39)
COMMON /MAIN3/ SAVE3(4563)
COMMON /MAIN4/ SAVE4(3071)
COMMON /MAIN5/ ZETA(39), FREOR(39), FREORZ(39), EVALUE(2,39),
+ EVECTOR(2,39,39), WIFE(78), DESRHO(39), RHO(39), P3(39), BVAL(39),
+ TOP, BOTTOM, PRON, RH, RES(10,1,39), PMAG(39,5), GPRIME(39),
+ LTITL(8), JTITL(5), KTIT1(8), KTIT2(5), CNTLDAT(15)
COMMON /MAIN6/ FVAL(39), U(39,39), UINV(39,39), V(39,39),
+ P1(39,5), P2(39,2), R(10,39)
COMMON /POLARC/ AC, BD, FACT, FACTR
COMMON DUMMY(311)
INTEGER CNTLDAT, CNTLNR(5)
COMPLEX EVAL, U, UINV, V, P1, P2, R
COMPLEX DESRHO, RHO, P3, BVAL, TOP, BOTTOM, PROD, RH, RES

C THE FOLLOWING DATA IS FIXED AND SHOULD NOT BE CHANGED.
C
C
DATA K1/1/,K2/2/,K3/3/
DATA L1,L2,L3,L4/4*1/
DATA M1,M2/2*39/,M3/5/,M4/10/,M5/12/,M7/2/,M8/6/,M9/311/
DATA N1/58/,N2/2/,N3/41/,N4/1/,N5/4/,N6/8/,N7/3/

```

C

Pages 119, 120 and 121 are blank.

C
C
C

C THE FOLLOWING DATA MAY VARY WITH EACH RUN AND CAN BE CHANGED TO
 C REFLECT VARIOUS TEST OPTIONS.
 C

```

DATA DESIGN, OLDATA/2*.TRUE./
DATA MLOOP/4/
DATA M6/ 4/
DATA PRINTR, PRINTF, PRINT1/3*.TRUE./
DATA OLTEST, CLTEST, OPTTEST/3*.TRUE./
DATA RMSTEST, STEPRSP/2*.FALSE./, FREQRSP/.TRUE./
DATA INITIM/0.1/, DUPATN/5.0/, DEL/0.1/, IPTS/51/, NSYM/10/
DATA GUSTS/.TRUE./, PIN, PASS/2*.FALSE./

```

C

```

REWIND 2
LLINE = 0
NLINE = 0
IF (FREQRSP) GO TO 145
IF (OLTEST .AND. (STEPRSP .OR. RMSTEST)) NLINE = NLINE + 1
IF (CLTEST) NLINE = NLINE + 1
IF (OPTTEST .AND. .NOT. FREQRSP) NLINE = NLINE + 1

```

```

145 PRINT 147
PRINT 150, NLINE
PRINT 147
NDIM = M1
NDIM1 = NDIM + 1
CALL REED (N1, A, M1, M2)
CALL RQUP (A, A1, M1, M2)
CALL RQUP (A, A2, M1, M2)
CALL REED (N2, B, M1, M3)
CALL REED (N3, C, M4, M2)
CALL REED (N4, H, M2, M7)
CALL REED (N5, KOPT, M3, M4)
CALL ZERO (G, 135)
IF (.NOT. OLDATA .AND. .NOT. DESIGN) GO TO 260
CALL ZERO (EVALUE, 78)
CALL ZERO (EVECTR, 3042)

```

```

CALL ZERO (WIFE,78)
CALL RGEIG (M1,M2,A,L1,EVALUE,EVECTR,WIFE)
CALL FPRT (M1,EVALUF,ZETA,FREQR,FREQHZ)
CALL EPACK (M1,M2,EVALUE,EVECTR,EVAL,U)
CALL GQUP (U,UINV,M1,M2)
CALL MINVC (UINV,UINV,M1)
CALL XPOSE (UINV,V,M2,M1)
CALL MCR4 (UINV,R,P1,M1,M2,M3)
CALL MCR4 (UINV,H,P2,M1,M2,M7)
CALL MPC4 (C,U,R,M4,M2,M2)
PRINT 148

```

```

147 FORMAT (//)
148 FORMAT (/)
150 FORMAT (*1 THE NUMBER OF CURVES PER PLOT TO BE GENERATED BY THIS
+ RUN IS:*,I2)
IF (FREQSP) OLTEST = .FALSE.
IF (.NOT. OLTEST) GO TO 175

```

```

C OPEN-LOOP TESTING IS RESTRICTED TO COVARIANCE ANALYSIS OF ACCEL-
C ERATIONS AND STRESSES DUE TO TURBULANCE OR P.I.O. OF ELEVATOR,
C OR TO TRANSFER FUNCTION ANALYSIS. FREQUENCY RESPONSE ANALYSIS
C IS NOT DONE, NOR IS COVARIANCE ANALYSIS OF SURFACE DISPLACEMENTS
C AND RATES.

```

```

LLINE = LLINE + 1
STEPSP = .NOT. RMSTEST
IF (RMSTEST) CALL NOISE (M1,M4,M7,K1,GUSTS,PIO,MR,K1,K2,N6,N7,
+ PRINT1,PASS)
IF (STEPSP) CALL XFFNCT (M2,K1,M4,NX,M7,K2,P2,R,EVAL,RES,P3,
+ PRINT2,PASS,PRINTF,RVAL)

```

```

C LOOP 240 IS THE DESIGN LOOP FOR A MULTI-STAGE MODAL CONTROLLER.
C IF DESIGN = .FALSE., THE PROGRAM ADVANCES TO STATEMENT 241.

```

```

175 IF (.NOT. DESIGN) GO TO 241
179 FORMAT (/ ,1X,8A10)

```

```

180 READ 180, LTIIL
    FORMAT (3A10)
181 READ 181, JTIIL
    FORMAT (5A10)
    DO 240 IJ = 1, M6
      PRINT 147
      IF (IJ .EQ. M6 .AND. M6 .EQ. MLOOP) GO TO 184
      PRINT 179, LTIIL
      PRINT 182, JTIIL
      FORMAT (/ , 3X, 5(11X, A10, 5X))
      CALL CPRT (P1, M1, M3, N)
      DO 183 I = 1, M1
        DO 183 J = 1, M3
          183 PMAG(I, J) = CARB(P1(I, J))
      PRINT 147
      PRINT *, "THE MAGNITUDES OF THE TERMS OF THE ROWS OF THE P-MATRIX
+ARE: .."
      CALL PRPT (PMAG, M1, M3, 0)
      DO 185 I = 1, M1
        185 RHO(I) = EVAL(I)
      READ 156, (CNTLDAT(I), I=1, 15)
      186 FORMAT (15I3)
      TF (CNTLDAT(1) .EQ. 0) GO TO 240
      CNTLNR(IJ) = NGAIN = CNTLDAT(1)
      N = CNTLDAT(2)
      M = CNTLDAT(3)
      READ 180, KTIIT1
      READ 181, KTIIT2
      PRINT 187, KTIIT1, KTIIT2
      187 FORMAT (//, 1X, 13A10)
      CALL ZERO (DESRHO, 78)
      DO 189 I = 1, M
        READ 190, K, RH
        189 DESRHO(K) = RH
      190 FORMAT (I2, 2E12.5)
      DO 192 I = 1, N

```

```

192 PHO(CNTLDAT(I+3)) = DESRHO(CNTLDAT(I+3))
   DO 193 I = 1,M1
   TF (DESRHO(I) .NE. (0.,0,0)) EVAL(I) = DESRHO(I)
193 CONTINUE
   PRINT 194, (I, RVAL(I), RHO(I), EVAL(I), I=1,M1)
194 FORMAT (//,* THE LISTS OF ACTUAL AND DESIRED EIGENVALUES ARE:*,//,
+4X,*NR*, 8X,*CURRENT ACTUAL VALUES*,8X,*CURRENT DESIRED VALUES*,
+6X,*CLOSED-LOOP DESIRED VALUES*,//,39(4X,I2,3(4X,2F13.6),//))
   DO 195 I = 1,M1
198 P3(I) = P1(I,CNTLDAT(1))
   CALL GAIN (RHO,BVAL,V,P3,GPRIME,M1,M2)
   DO 199 I = 1,M1
   DO 199 J = 1,M2
199 NUM1(I,J) = R(I,CNTLDAT(1)) * GPRIME(J)
   PRINT 147
   PRINT*, "THE ELEMENTS OF THE G' ROW VECTOR ARE: "
   PRINT 149
   PRINT 203, (I, GPRIME(I), I=1, M1)
200 FORMAT (39(I3,4X,F20.8,//))
   DO 225 I = 1,M1
225 G(NGAIN,I) = GPRIME(I)
   IF (IJ .NE. (M1-1)) GO TO 230
   PRINT 242
   PRINT 243, ((G(I,J), I=1,M3), J=1,M1)
230 DO 235 I = 1,M1
   DO 235 J = 1,M2
235 A(I,J) = AA(I,J) + NUM1(I,J)
   CALL PDUP (A,AA,M1,M2)
   CALL ZERO (FVALUE,78)
   CALL ZERO (FVECTR,3042)
   CALL ZERO (WIFE,78)
L2 = 1
   CALL RGEIG (M1,M2,A,L2,EVALUE,EVECTR,WIFE)
   CALL EPRT (M1,FVALUE,ZFTA,FREQR,FREQHZ)
   CALL EPACK (M1,M2,EVALUE,EVECTR,EVAL,U)
   CALL COUP (U,UINV,M1,M2)

```

```

CALL MINVC (UINV, UINV, M1)
CALL CXPOSE (UINV, V, M2, M1)
CALL MCRM (UINV, R, P1, M1, M2, M3)
240 CONTINUE
241 CONTINUE
242 FORMAT (//, *1*, 9X, *THE MODAL CONTROLLER FEEDBACK MATRIX IS: //,
+ 4X, *ELEVATOR*, 4X, *FLAPERON*, 2X, *INBD. AIL.* , 3X, *OBD. AIL.* , 6X,
+ *CANARD*)
243 FORMAT (/, 39(5(1X, G11.5), /))
IF ((.NOT. DESIGN) .OR. (.NOT. CLTEST)) GO TO 260
C
C CLOSED-LOOP TESTING MAY BE ACCOMPLISHED BY COVARIANCE ANALYSIS,
C TRANSFER FUNCTION ANALYSIS, OR FREQUENCY RESPONSE ANALYSIS. THESE
C TESTS ARE MUTUALLY EXCLUSIVE.
C
IF ((RMSTEST .AND. STEPRSP) .OR. (STEPRSP .AND. FREQRSP) .OR.
+ (FREQRSP .AND. RMSTEST)) STOP
CALL MCRM (UINV, H, P2, M1, M2, M7)
CALL MPCM (C, U, R, M4, M2, M2)
LLINE = LLINE + 1
IF (RMSTEST) CALL NOISE (M1, M4, M7, K1, GUSTS, PIO, M8, K1, K2, N6, N7,
+ PRINT1, PASS)
IF (STEPRSP) CALL XFRFNCT (M2, K1, M4, NX, M7, K2, P2, R, EVAL, RES, P3,
+ PRINTR, PASS, PRINTF, PVAL)
IF (FREQRSP) CALL RODE (CNTLNR, M1, M3, M6, L4, M9, DUMMY, NX, PASS)
260 CONTINUE
C
C THIS SECTION CALCULATES THE REQUIRED PARAMETERS FOR THE AFFDL
C OPTIMAL CONTROLLER AND TESTS THAT SYSTEM FOR COMPARISONS. THESE
C CALCULATIONS ARE NOT MADE IF OPTTEST = .FALSE. OR IF FREQRSP =
C .TRUE.. COVARIANCE ANALYSIS OR TRANSFER FUNCTION ANALYSIS MAY
C BE PERFORMED.
C
IF (.NOT. OPTTEST .OR. FREQRSP) GO TO 280
CALL MRRM (KOPT, C, G, M3, M4, M2)
CALL MRRM (F, G, NUM1, M1, M3, M2)

```

```

PRINT 264
PRINT 243, ((G(I,J), I=1,M3), J=1,M1)
264 FORMAT (//, +1*, 9X, *THE OPTIMAL CONTROLLER FEEDBACK MATRIX IS: *, //,
+ 4X, *ELEVATOR*, 4X, *FLAPERON*, 2X, *INBD. AIL.* , 3X, *OBD. AIL.* , 6X,
+ *CANARD*)
NO 265 I = 1, M1
NO 265 J = 1, M2
265 A(I,J) = A2(I,J) + DU41(I,J)
LLINE = LLINE + 1
CALL ROUNP (A, AA, M1, M2)
CALL ZERO (EVALUE, 78)
CALL ZERO (EVECTR, 7042)
CALL ZERO (WIFF, 78)
CALL RGEIG (M1, M2, A, L3, EVALUE, EVECTR, WIFE)
CALL FPRT (M1, EVALUE, ZETA, FREQR, FREQHZ)
CALL EPACK (M1, M2, EVALUE, EVECTR, EVAL, U)
CALL CDUP (U, UINV, M1, M2)
CALL MINVC (UINV, UINV, M1)
CALL CXPOSE (UINV, V, M2, M1)
CALL MCR4 (UINV, B, P1, M1, M2, M3)
CALL MCR4 (UINV, H, P2, M1, M2, M7)
CALL MRC4 (C, U, R, M4, M2, M2)
C BEGIN TESTING OF OPTIMAL CONTROLLER
C
C IF (RMSTEST) CALL NOISE (M1, M4, M7, K1, GUSTS, PIO, M8, K1, K2, N6, N7,
+ PRINT1, PASS)
C IF (STEPTEST) CALL XFRFNCT (M2, K1, M4, NX, M7, K2, P2, R, EVAL, RES, P3,
+ PRINTR, PASS, PRINTF, RVAL)
280 CONTINUE
C
C THE LAST SECTION OF THE PROGRAM USES THE ROUTINE TIMPLOT TO GENERATE
C TIME HISTORY PLOTS OF THE SELECTED OUTPUTS. PLOTTER AND PRINT3
C CONTROL INTERNAL LOGIC IN TIMPLOT. IF PLOTTER = .TRUE., CALCOMP
C PLOTS ARE GENERATED. IF PRINT3 = .TRUE.,
C TIMPLOT WILL ALSO PRINT THE DATA OF THE HISTORIES FOR EVERY NPTS-TH

```

```

C POINT SPECIFIED IN THE DATA DECK. THIS SECTION IS IGNORED IF TPLOTS
C = .FALSE. OR IF FREQRSP = .TRUE.
  IF (FREQRSP .OR. .NOT. TPLOTS) GO TO 300
  IF (STEPRSP) IX = 10
  NPLOTS = IX
  NCURVES = NLINE
  NPOINTS = IPTS
  NTIME = IPTS + 2
  NCOMP = (3*IPTS) + 2
  CALL TEMPLT (PLOTTER,PRINT3,NPLOTS,NCURVES,NPOINTS,NTIME,NCOMP,
+   NSYM,TYME,RMSTEST,STEPRSP,OUTPOOT,COMP,A)
  IF (PLOTTER) CALL PLOTE
300 CONTINUE
  PRINT 147
  PRINT 147
  STOP
  END

```



```

C
C SURROUTINE GAIN (RHO, RVAL, V, P, GPRIME, K, L)
C
C THIS ROUTINE CALCULATES THE GAIN VECTOR "GPRIME" BASED ON EQ
C (6.58) OF PORTER AND CROSSLEY. "RHO" IS THE VECTOR OF DESIRED
C EIGENVALUES AT EACH STAGE. "RVAL" IS THE VECTOR OF ACTUAL EIGEN-
C VALUES AT EACH STAGE. "V" IS THE NORMALIZED MODAL MATRIX
C ASSOCIATED WITH THE TRANSPOSE OF THE PLANT MATRIX; I.E., V =
C TRANSPOSE OF "UINV". "P" IS THE APPROPRIATE VECTOR OF THE MODE-
C CONTROLLABILITY MATRIX. "K" AND "L" ARE THE DIMENSIONS OF THE
C PLANT MATRIX, WHERE K = L.
C THIS ROUTINE USES 2168 WORDS OF CM.
C
C DIMENSION GPRIME(K)
C COMPLEX TOP, BOTTOM, RHO(K), RVAL(K), PROD, V(K,L), P(K)
C CALL ZERO (GPRIME, K)
DO 149 J = 1, L
IF (P(J) .EQ. (0.0, 0.0)) GO TO 149
TOP = (1.0, 0.0)
DO 146 I = 1, K
146 TOP = TOP * (RHO(I) - RVAL(J))
IF (TOP .EQ. (0.0, 0.0)) GO TO 149
BOTTOM = (1.0, 0.0)
DO 147 I = 1, K
IF (RVAL(I) .EQ. RVAL(J)) GO TO 147
BOTTOM = BOTTOM * (RVAL(I) - RVAL(J))
147 CONTINUE
PROD = TOP / (P(J) * BOTTOM)
DO 148 I = 1, K
148 GPRIME(I) = GPRIME(I) + REAL(PROD * V(I, J))
149 CONTINUE
DO 150 J = 1, L
150 IF (ABS(GPRIME(J)) .LT. .000001) GPRIME(J) = 0.0
RETURN
END

```

```

SUBROUTINE TIMPLOT (PLOTTER, PRINT3, M, N, NDOT, NT, NS, NR, TYME, RMSTEST,
+ STEPRSP, OUTPOOT, COMP, YOUT)
C
C THIS ROUTINE GENERATES TIME HISTORIES IN GRAPHIC AND TABULAR
FORM IF PLOTTER = TRUE, AND PRINT3 = TRUE. THE ROUTINE REQUIRES
C TWO SETS OF TITLES AND OUTPUT FORMAT CONTROL CARDS IAW WITH
STATEMENTS 117-120. THE DATA FOR THIS ROUTINE IS READ IN FROM
C TAPE2. NDOT POINTS PER CURVE AND N CURVES PER PLOT ARE GENERATED
C FOR EACH OF THE M PLOTS.
C THIS ROUTINE USES 7008 WORDS OF CM.
C
C LOGICAL PLOTTER, PRINT3, RMSTEST, STEPRSP
REAL INITIM
COMMON /PLOT1/ ALPHA(501), NLINE, LLINE, INITIM, DURATN, DEL, FLET,
+ IX, IPTS
C DIMENSION FORM(8), TITL(8), TITLE(7)
DIMENSION TYME(NT), OUTPOOT(NT), COMP(NS), YOUT(NDOT, M, N)
C
C RETURN 2
IF (.NOT. PLOTTER .AND. .NOT. PRINT3) RETURN
DO 106 IT = 1, IPTS
TYME(IT) = INITIM
106 INITIM = INITIM + DEL
IF (RMSTEST) GO TO 109
IF (STEPRSP) CONTINUE
DO 107 K = 1, NLINE
DO 107 J = 1, M
PEAN (2) (YOUT(I, J, K), I=1, IPTS)
107 CONTINUE
GO TO 110
108 DO 109 K = 1, NLINE
DO 109 I = 1, IPTS
READ (2) (YOUT(I, J, K), J=1, M)
109 CONTINUE
110 CONTINUE
IF (.NOT. PLOTTER) GO TO 115

```

```

CALL SCALE (TYME,7.,IPTS,1)
DO 114 II = 1,M
CALL PLOT(7,-3.,-3)
CALL PLOT(0,3.,-3)
ICNT = 0
DO 111 JJ = 1,NLINE
DO 111 KK = 1,IPTS
ICNT = ICNT+1
111 COMP(ICNT) = YOUT(KK,II,JJ)
CALL SCALE (COMP,5.,ICNT,1)
OUTPUT(IPTS+1) = COMP(ICNT+1)
OUTPUT(IPTS+2) = COMP(ICNT+2)
CALL AXIS (0,0,74T (SEC),-7,7,0,TYME(IPTS+1),TYME(IPTS+2))
CALL AXIS (0,0,4HY(T),4,5,90.,OUTPUT(IPTS+1),OUTPUT(IPTS+2))
DO 113 JJ = 1,NLINE
DO 112 KK = 1,IPTS
112 OUTPUT(KK) = YOUT(KK,II,JJ)
IJ = JJ-1
IF (JJ.EQ. NLINE) IJ = 5
113 CALL LINE (TYME,OUTPUT,IPTS,1,NR,IJ)
PEAD 120, TITLF, FLET
LETTERS = FLET
CALL SYM90L ((7.-LETTERS*.10)*.5),5.20,.10,TITLE,0,LETTERS)
CALL PLOT(-.5,-.5,3)
CALL PLOT(7.5,-.5,2)
CALL PLOT(7.5,5.4,2)
CALL PLOT(-.5,5.4,2)
CALL PLOT(-.5,-.5,2)
CALL PLOT(10.,0,-3)
CALL NSP (7)
114 CONTINUE
IF (.NOT.PRINT3) RETURN
115 CONTINUE
PEAD 118, FORM
READ 119, TITL
PEAD 119, NPTS

```

```
DO 116 II = 1, M
  READ 121, TITLE, FLET
  PRINT 117, TITLE
  PRINT TITL
  DO 115 KK = 1, IPTS, NPTS
    116 PRINT FORM, TYME(KK), (YOUT(KK,II,JJ), JJ=1, NLINE)
    RETURN
    117 FORMAT (//, 1X, 7A10, /)
    118 FORMAT (9A10)
    119 FORMAT (I3)
    120 FORMAT (7A10, F3.0)
  END
```

Appendix A5: Covariance Analysis via NOISE

The coding for the covariance analysis subroutines are used in this program. The listing are for the test routine NOISE and the associated subprograms INTEG, XNORM, and MEXP.

```

C SURROUTINE NOISE (K,MX,L,LX,WIND,SURF,JX,M,N,N6,N7,PRINT,SKIP3)
C THIS ROUTINE PERFORMS A COVARIANCE ANALYSIS OF THE SYSTEM IN ORDER
C TO OBTAIN RMS VALUES OF RESPONSES OF INTEREST. THE STATE-RESPONSE
C MATRIX, RESP, AND THE CONTROL-RESPONSE MATRIX, D, ARE USED. LOGIC IS
C PROVIDED FOR OPEN-LOOP OR CLOSED LOOP SYSTEM CALCULATIONS. ZERO-
C MEAN GAUSSIAN WHITE NOISE IS ASSUMED. LOGICALS WIND AND SURF(ACE)
C CONTROL THE STRENGTH FOR 9 FPS OR 0.1 RAD LEVELS OF INPUTS, RESPECT-
C IVELY. THE OUTPUT IS STOPPED ON TAPE2.
C THIS ROUTINE USES 5039 WORDS OF CM.

```

```

C LOGICAL SKIP1, SKIP2, SKIP3, WIND, SURF, PRINT
C LOGICAL SKIP5
C REAL INITIM
C COMMON /PLOT1/ ALPHA(501), NLINE, LLINE, INITIM, DURATN, DEL,FLET,
+ IX, IPTS
C COMMON /SYSTEM/ A(39,39), B(39,5), C(10,39), H(39,2), G(5,39)
C COMMON /DUPSYS/ AA(39,39), A2(39,39), KOPT(5,10)
C COMMON /MAIN1/ NDIM,NDIM1,PX(39,39)
C COMMON /MAIN2/ PHIPPHI(39,39)
C COMMON /MAIN3/ ZED(39,39), PHI(39,39), PHIXPSE(39,39)
C COMMON /MAIN4/ RESP(37,39), RESPXPS(39,37), D(37,5)
C COMMON /MAIN5/ O(1,1), E(39,1), EXPSE(1,39), GQ(39,1),GQGT(39,39),
+ DK(37,39), RESPONS(37,37)

```

```

C IM = IPTS - 1
C SKIP1 = .FALSE.
C SKIP2 = .TRUE.
C SKIP5 = .FALSE.
C DO 192 IJ = 1,IM
C IF (SKIP1) GO TO 162
C IF (WIND) Q(1,1) = 64.0
C IF (SURF) Q(1,1) = 0.01
C IF (WIND) IX = 21
C IF (SURF) IX = 11
C CALL ZERO (ALPHA,IX)

```

```

WRITE (2) (ALPHA(I), T=1, IX)
DO 161 II = 1, K
161 EXPSF(M, II) = E(II, M) = H(II, LX)
CALL MRR4 (E, Q, G, K, M, M)
CALL MPR4 (G, EXPSE, GGGT, K, M, K)
CALL INTEG (K, AA, GGGT, ZED, DEL)
CALL MEXD (K, AA, DEL, PHI)
CALL RXPOS (PHI, PHIXPSE, K, K)
CALL PDUP (ZFD, PX, K, K)
SKIP1 = .TRUE.
162 CONTINUE
IF (SKIP2) GO TO 164
CALL MRR4 (PHI, PX, GGGT, K, K, K)
CALL MPR4 (GGGT, PHIXPSE, PHIPPHI, K, K, K)
DO 163 II = 1, K
DO 163 JJ = 1, K
163 PX(II, JJ) = PHIPPHI(II, JJ) + ZED(II, JJ)
164 SKIP2 = .FALSE.
IF (SKIP5) GO TO 170
IF (SKIP5) GO TO 165
CALL PEE7 (151, RESP, 37, 39)
CALL PEE7 (10, 0, 37, 5)
CALL RXPOSE (RESP, RESXPSE, 37, 39)
SKIP3 = .TRUE.
SKIP5 = .TRUE.
165 IF (SKIP3) GO TO 170
CALL MRRM (0, 6, 0K, 37, 5, 39)
DO 168 I = 1, 37
DO 168 J = 1, 39
168 RESP(I, J) = RESP(I, J) + DK(I, J)
CALL RXPOSE (RESP, RESXPSE, 37, 39)
SKIP5 = .TRUE.
170 CALL MRR4 (RESP, PX, DK, 37, 39, 39)
CALL MPR4 (DK, RESXPSE, RESP, 37, 39, 37)
ICNT = 0
IF (WIND) GO TO 172

```

```
IF (SURF) ICNT = ICNT + 1
ALPHA(ICNT) = SORT(RESPONS(5,5))
GO TO 176
172 DO 174 I = 1,11
    ICNT = ICNT + 1
174 ALPHA(ICNT) = SORT(RESPONS(I,I))
176 DO 178 I = 20,24
    ICNT = ICNT + 1
178 ALPHA(ICNT) = SORT(RESPONS(I,I))
    DO 180 I = 33,37
        ICNT = ICNT + 1
180 ALPHA(ICNT) = SORT(RESPONS(I,I))
    WRITE (2) (ALPHA(I), I=1,IX)
192 CONTINUE
    RETURN
    END
```


INTG 1

```

SUBROUTINE INTEG(N,A,C,S,T)
C THIS ROUTINE IS ADAPTED FROM A ROUTINE OF THE SAME NAME GIVEN BY
C D. L. KLEINMAN IN "COMPUTER PROGRAMS USEFUL IN LINEAR SYSTEM
C STUDIES" AND REVISED FOR AFIT USE BY HEATH AND DILLOW, MARCH 1975.
C THIS ROUTINE USES 411R WORDS OF CM.

```

INTG 2
INTG 3

```

C S=INTEGRAL FA*C*EA FROM 0 TO T
C A IS DESTROYED
C DIMENSION A(1),C(1),S(1)
C COMMON/MAIN1/ NDIM,NDIM1, X(39,39)
C COMMON/MAIN2/COEF(39,39)

```

INTG 4
INTG 5

```

C NN=N*NDIM
C NM1=N-1
C IND=0
C ANORM=XNORM(N,A)
C DT=T
C IF (AMOR4*ABS(DT).LE.0.5) GO TO 10
C DT=DT/2.
C IND=IND+1
C GO TO 5

```

INTG 7
INTG 8
INTG 9

```

C DO 15 I=1,NN,NDIM
C J=I+NM1
C DO 15 JJ=I,J
C S(JJ)=DT*C(JJ)
C T1=DT**2/2.
C DO 25 IT=3,15
C CALL MOP4 (A,C,X,N,N,N)
C DO 20 I=1,N
C II=(I-1)*NDIM
C DO 20 JJ=I,NN,NDIM
C II=II+1
C (JJ)=(X(JJ)+X(II))*T1
C (JJ)=S(JJ)+C(JJ)

```

INTG 10
INTG 11
INTG 12
INTG 13
INTG 14
INTG 15
INTG 16
INTG 17
INTG 18
INTG 19
INTG 20
INTG 21
INTG 22
INTG 23
INTG 24
INTG 25
INTG 26
INTG 27
INTG 28

```

10  
15  
20

```

INTG 29
 INTG 30
 INTG 31
 INTG 32
 INTG 33
 INTG 34
 INTG 35
 INTG 36
 INTG 37
 INTG 38
 INTG 39
 INTG 40
 INTG 41
 INTG 42
 INTG 43
 INTG 44
 INTG 45
 INTG 46
 INTG 47
 INTG 48
 INTG 49
 INTG 50
 INTG 51
 INTG 52
 INTG 53
 INTG 54
 INTG 55
 INTG 56
 INTG 57
 INTG 58
 INTG 59
 INTG 60
 INTG 61
 INTG 62
 INTG 63
 INTG 64

```

25  T1=DT/FLOAT(IT)
    JF(INO,EO,0) GO TO 100
    COEF(11)=1.0
    DO 30 I=1,10
      TI=11-I
    COEF(II)=DT*COEF(II+1)/FLOAT(I)
    II=1
    DO 40 I=1,NN,NDIM
      J=I+NM1
    DO 35 JJ=I,J
      X(JJ)=A(JJ)*COEF(1)
      X(II)=X(II)+COEF(2)
      II=II+NDIM1
    DO 50 L=3,11
      CALL MPPY (A,X,C,N,H,N)
      II=1
      T1=COEF(L)
    DO 55 J=1,NN,NDIM
      J=I+NM1
    DO 50 JJ=I,J
      X(JJ)=C(JJ)
      X(II)=X(II)+T1
      TI=II+NDIM1
      X=EXP(A*DT)
      L=0
    L=L+1
    CALL MPPY (X,S,C,N,N,N)
    II=1
    DO 90 I=1,H
      J=II
      IF (I,EO,1) GO TO 75
    DO 70 JJ=I,II,NDIM
      S(JJ)=S(J)
      J=J+1
    DO 85 JJ=I,N
      KK=JJ
  
```

INTG 65
INTG 66
INTG 67
INTG 68
INTG 69
INTG 70
INTG 71
INTG 72
INTG 73
INTG 74
INTG 75
INTG 76
INTG 77

```
80 80 K=I,NN,NDIM  
S(J)=S(J)+C(K)*X(KK)  
KK=KK+NDIM  
J=J+NDIM  
85 87 JJ=I,NN,NDIM  
C(JJ)=X(JJ)  
II=II+NDIM  
90 90 IF(L.EQ.IND) GO TO 100  
CALL MPRM (C,C,X,N,N,N)  
GO TO 60  
CONTINUE  
RETURN  
100 END
```

```

FUNCTION XNORM(N,A)
C THIS ROUTINE IS ADAPTED FROM A ROUTINE OF THE SAME NAME GIVEN BY
C D. L. KLEINMAN IN "COMPUTER PROGRAMS USEFUL IN LINEAR SYSTEM
C STUDIES" AND REVISED FOR AFIT USE BY HEATH AND DILLOW, MARCH 1975.
C THIS ROUTINE USES 1078 WORDS OF CM.
C
C COMPUTES AN APPROXIMATION TO NORM OF A-- NOT A BOUND
C DIMENSION A(1)
C COMMON/MAIN1/ NDIM,NDIM1
C
NN=N*NDIM
C1=0.
TR=A(1)
IF(N.EQ.1) GO TO 20
I=2
DO 10 II=NDIM1,NN,NDIM
J=II
DO 5 JJ=I,II,NDIM
C1=C1+ABS(A(J)*A(JJ))
J=J+1
TR=TR+A(J)
I=I+1
TR=TR/FLOAT(N)
DO 15 II=1,NN,NDIM1
C1=C1+(A(II)-TR)**2
XNORM=ABS(TR)+SQRT(C1)
RETURN
END

```

NORM 1

NORM 2
NORM 3
NORM 4
NORM 5
NORM 6
NORM 7
NORM 8
NORM 9
NORM 10
NORM 11
NORM 12
NORM 13
NORM 14
NORM 15
NORM 16
NORM 17
NORM 18
NORM 19
NORM 20
NORM 21
NORM 22

MEXP001

SUBROUTINE MEXP(N,A,T,EA)

C THIS ROUTINE IS ADAPTED FROM A ROUTINE OF THE SAME NAME GIVEN BY
 C N. L. KLEINMAN IN "COMPUTER PROGRAMS USEFUL IN LINEAR SYSTEM
 C STUDIES" AND REVISED FOR AFIT USE BY HEATH AND DILLOW, MARCH 1975.
 C THIS ROUTINE USES 5608 WORDS OF CM.

C DIMENSION A(1),EA(1),C(39),D(40),E(39)
 C COMMON/MAIN1/NDIM,NDIY1,X(1)

NN=NDIM*N

NM1=N-1

IF(N.GT.1) GO TO 5

EA(1)=EXP(T*A(1))

RETURN

5 W=1.0

DO 10 I=1,NN,NDIM

TL=I+NM1

DO 10 J=I,IL

10 EA(J)=A(J)

C1=XNOPM(N,A)

IND=C

L=1

T1=T

15 IF(ABS(T1*C1).LE.3.0) GO TO 20

T1=T1/2.

IND=IND+1

GO TO 15

20 C2=0.

DO 25 I=1,NN,NDIM1

25 C2=C2-EA(I)

C2=C2/FLOAT(L)

C(L)=C2

N(L+1)=0.

II=N+1-L

E(II)=W

MEXP002
MEXP003

MEXP004
 MEXP005
 MEXP006
 MEXP007
 MEXP008
 MEXP009
 MEXP010
 MEXP011
 MEXP012
 MEXP013
 MEXP014
 MEXP015
 MEXP016
 MEXP017
 MEXP018
 MEXP019
 MEXP020
 MEXP021
 MEXP022
 MEXP023
 MEXP024
 MEXP025
 MEXP026
 MEXP027
 MEXP028
 MEXP029

MEXP030
 MEXP031
 MEXP032
 MEXP033
 MEXP034
 MEXP035
 MEXP036
 MEXP037
 MEXP038
 MEXP039
 MEXP040
 MEXP041
 MEXP042
 MEXP043
 MEXP044
 MEXP045
 MEXP046
 MEXP047
 MEXP048
 MEXP049
 MEXP050
 MEXP051
 MEXP052
 MEXP053
 MEXP054
 MEXP055
 MEXP056
 MEXP057
 MEXP058
 MEXP059
 MEXP060
 MEXP061
 MEXP062
 MEXP063
 MEXP064
 MEXP065

```

II=1
DO 35 I=1,NN,NDIM
  IL=I+NM1
  DO 30 J=I,IL
    30 Y(J)=EA(J)
    X(II)=X(II)+C2
    35 II=II+NDIM1
    IF(L.EQ.N) GO TO 40
    CALL MPRM (X,A,EA,N,N,N)
    W=W*Y1/FLOAT(L)
    L=L+1
    GO TO 20
  40 CONTINUE
  C***** CAN CHECK X 0 FOR ACCURACY
  J=N+25
  DO 50 L=N,J
    DO 45 K=1,N
      45 E(K)=E(K+1)-W*C(K))*Y1/FLOAT(L)
    50 W=D(1)
  II=1
  DO 60 I=1,NN,NDIM
    IL=I+NM1
    DO 55 J=I,IL
      55 EA(J)=E(1)*A(J)
      FA(II)=EA(II)+E(2)
    60 II=II+NDIM1
    IF (N.EQ.2) GO TO 85
    DO 80 L=3,N
      CALL MPRM (EA,A,X,N,N,N)
      II=1
      C2=E(L)
    DO 75 I=1,NN,NDIM
      IL=I+NM1
      DO 70 J=I,IL
        70 FA(J)=X(J)
  
```

MEXP066
MEXP067
MEXP068
MEXP069
MEXP070
MEXP071
MEXP072
MEXP073
MEXP074
MEXP075
MEXP076
MEXP077 .

```
EA(II)=EA(II)+C2  
75 II=II+NDIM1  
80 CONTINUE  
85 IF (IND.EQ.C) RETURN  
90 100 L=1,IND  
90 90 I=1,MN,NDIM  
IL=I+NM1  
90 90 J=I,IL  
90 X(J)=EA(J)  
100 CALL MRRM (X,X,EA,N,N,N)  
RETURN  
END
```

Appendix A6: Transfer Function Analysis via XFRFNCT

This section gives the coding for the test subroutine XFRFNCT and the associated routines RESIDUE, PARTEL, POLAR, and FT. PARTEL is a special version of the AFITPROGRAM routine PARTL used for partial-fraction expansions.


```

FESI(KK) = AIMAG(RES(TI, JJ, KK))
FVR(KK) = -REAL(FV(KK))
FVI(KK) = -AIMAG(FV(KK))
95 EVI(KK) = EVI(KK) * 1.0
   IOUTPUT = IOUTPUT + 1
   CALL PARTEL (NX, PRINT?, IOUTPUT)
   T = INITIM
   DO 96 KK = 1, IPTS
   ALPHA(KK) = FT(T)
96 T = T + DEL
   WRITE (2) (ALPHA(I), I=1, IPTS)
97 CONTINUE
   RETURN
   END

```

```

C SURROUTINE RESIDUE (P,P,RES,PASS,PRINT1,EVLL,EV,K,L,M,NX)
C GIVN THE MODE-CONTROLLABILITY VECTOR, P, OF INTEREST, AND THE
C MODE-OBSERVABILITY MATRIX, R, THIS ROUTINE CALCULATES THE COEF-
C FICIENTS OF THE PARTIAL-FRACTION EXPANSIONS OF THE M TRANSFER
C FUNCTIONS OF INTEREST. THE COEFFICIENTS (ALSO CALLED THE RESIDUES
C OF THE POLES OF THE M TRANSFER FUNCTIONS) ARE STORED IN COMPLEX
C FORM IN THE MATRIX RES AND ARE PRINTED IF PRINT1 = .TRUE..
C K IS THE ORDER OF THE SYSTEM, L IS THE NUMBER OF INPUTS (SPECIFIC-
C LY, L = 1), AND NX IS THE NUMBER OF NON-ZERO RESIDUES IN THE
C FIRST TRANSFER FUNCTION. NX IS ASSUMED TO BE THE SAME FOR ALL
C M TRANSFER FUNCTIONS.
C THIS ROUTINE USES 5163 WORDS OF CM.

```

```

C LOGICAL PASS, PRINT1
C COMPLEX P(K,L), R(M,K), EVLL(K), RES(M,L,K), EV(K)

```

```

DO 77 II = 1,M
DO 77 JJ = 1,L
DO 77 KK = 1,K
RES(II,JJ,KK) = R(II,KK) * P(KK,JJ)
IF (ABS(REAL(RES(II,JJ,KK))).LT..000000001) RES(II,JJ,KK) = CMPLX(0.0,0,A
+IMAG(RES(II,JJ,KK)))
77 IF (ABS(AIMAG(RES(II,JJ,KK))).LT..000000001) RES(II,JJ,KK) = CMPLX(REAL
+(RES(II,JJ,KK)),0.0)
PASS = .FALSE.
IF (.NOT.PRINT1) GO TO 81
MJ = K
PRINT 90
78 DO 79 JJ = 1,L
PRINT 91, JJ, (I,I=1,5)
DO 79 KK = 1,MJ
79 PRINT 92, KK, (RES(J,JJ,KK),J=1,5)
DO 80 JJ = 1,L
PRINT 91, JJ, (I,I=6,10)
DO 80 KK = 1,MJ

```

```

80 PRINT 92, KK, (RES(J,JJ,KK),J=6,10)
   IF (PASS) 89,81
81 CONTINUE
   DO 82 KK = 1,K
82 EV(KK) = EVLL(KK)
   KN = K-1
   DO 83 KK = 1,KN
   IF (RES(1,1,KK) .EQ. (0.0,0.0)) GO TO 85
   NM = KK+1
   DO 84 KL = NM,K
   IF ((ABS(REAL(EV(KK))-PEAL(EV(KL))).GT..0000000001) .OR. (ABS(AIMA
+G(EV(KK))).GT..0000000001)) GO TO 84
   DO 85 LK = 1,M
   PES(LK,1,KK) = RES(LK,1,KK) + RES(LK,1,KL)
83 PES(LK,1,KL) = (0.0,0.0)
84 CONTINUE
85 CONTINUE
   NX = NM = 0
   DO 86 KK = 1,KN
   IF (NM .GT. K) GO TO 88
   NX = NX+1
   IF (RES(1,1,NX) .NE. (0.0,0.0)) GO TO 88
   NM = NX
86 NM = NM+1
   IF (NM .GT. K) GO TO 88
   IF (RES(1,1,NM) .EQ. (0.0,0.0)) GO TO 86
   EV(NX) = EV(NM)
   EV(NM) = (0.0,0.0)
   DO 87 LK = 1,M
   PES(LK,1,NX) = RES(LK,1,NM)
87 PES(LK,1,NM) = (0.0,0.0)
88 CONTINUE
   NX = NX-1
   PASS = .TRUE.
   IF (.NOT. PRINT1) GO TO 89
   MJ = NX

```

```

PRINT 93
GO TO 79
89 CONTINUE
RETURN
90 FORMAT(///,* THE UNMODIFIED LISTS OF RESIDUES FOR EACH TRANSFER F
+FUNCTION ARE:*)
91 FORMAT (/,* FOR INPUT #*,I2,/,* NR*,5(4X,*TRANSFER FUNCTION *,I2,
+1X))
92 FORMAT (1X,I2,5(2X,2F12.5))
93 FORMAT(///,* THE MODIFIED LISTS OF RESIDUES FOR EACH NON-ZERO DEN
+OMINATOR TERM OF EACH TRANSFER FUNCTION ARE:*)
END

```



```

F1(JJ) = E1(JJ)/FACTP
F1(JJ) = F1(JJ) - FACT
122 CONTINUE
DO 123 JJ = 1,L
TEMP = AMON(F1(JJ),PI2)
IF (ABS(TEMP) .GT. PI) TEMP = TEMP - SIGN(PI2,TEMP)
123 F1(JJ) = TEMP
DO 124 JJ = 1,L
C1(JJ) = E1(JJ) * COS(F1(JJ))
D1(JJ) = F1(JJ) * SIN(F1(JJ))
124 IF (ABS(D1(JJ)) .LE. .0001) D1(JJ) = 0.0
AS = AS + C1(1)
BS = BS + D1(1)
A(II) = C1(2)
R(II) = D1(2)
F1(2) = F1(2) * DEGRF
F(II) = SQRT(A(II)**2 + B(II)**2)
F(II) = F1(2)
125 CONTINUE
IF (ABS(AS) .LT. .0001) BS = 0.0
NPOLES = N+1
A(NPOLES) = AS
R(NPOLES) = BS
C(NPOLES) = 0.0
D(NPOLES) = 0.0
F(NPOLES) = SQRT(AS**2 + BS**2)
F(NPOLES) = ATAN2(RS,AS) * DEGRE
IF (.NOT. PRINT) GO TO 131
PRINT 125, NRXPDEFN
126 FORMAT (//,1X,*FOR OUTPUT #*,I2,* , THE FOLLOWING PARTIAL FRACTION
+ EXPANSION DATA*,/,1X,*AND TIME FUNCTION WAS CALCULATED BY SUBROUT
+INE ,PARTEL*,/,1X,*FACTOR",9X,"POWER",17X,"COEFFICIENT",/,5X,"
+REAL",8X,"IMAG",13X,"REAL",8X,"IMAG",5X,"MAGNITUDE",5X,"ANGLE")
DO 127 II = 1,NPOLES
127 PRINT 129, C(II), D(II), A(II), B(II), E(II), F(II)
128 FORMAT (2G12.5,2X,"1",2X,3G12.5,F11.3)

```

```

PRINT 130
130 FOPMAT (//,1X,*THE TIME FUNCTION IS:*,/,1X,*F(T)=*)
131 DO 135 NR = 1,NPOLES
    IF (D(NR)) 132,133,135
132 CR(NR) = 2.0 * F(NR)
    EC(NR) = 1.0 * (-C(NR))
    OM(NR) = 1.0 * (-D(NR))
    FE(NR) = F(NR) + 90.
    IF (.NOT.PRINTT) GO TO 135
    PRINT 136 ,CR(NR), EC(NR), OM(NR), FE(NR)
    GO TO 135
133 Y(NR) = E(NR)
    IF (ABS(F(NR)) .GE. 170.) Y(NR) = -E(NR)
    W(NR) = 1.0 * (-C(NR))
    IF (.NOT.PRINTT) GO TO 134
    PRINT 137, Y(NR), W(NR)
134 IF (C(NR) .EQ. 0.0) FIN = FIN + Y(NR)
135 CONTINUE
136 FOPMAT (G19.5,1X,"EXP(",G11.5,"T) SIN(",G11.5,"*T+",F8.3,"")")
137 FOPMAT (G19.5,1X,"EXP(",G11.5,"*T")")
    RETURN
    END

```


SUBROUTINE POLAR

C THIS ROUTINE CALCULATES THE POLAR COORDINATES OF A POINT (AC,BD)
C GIVEN IN RECTANGULAR COORDINATES. ALL DATA IS PASSED IN LABELLED
C COMMON /POLARC/. THE MAGNITUDE IS FACT AND THE ANGLE IS FACTR.
C FACTR IS IN THE RANGE -PI TO +PI RADIANS.
C THIS ROUTINE USES 378 WORDS OF CM.

COMMON /POLARC/ AC, RD, FACT, FACTR
DATA PI/3.1415926535/, HALFPI/1.5707963286/

FACTR = SQRT(AC**2 + RD**2)
IF (AC) 106,101,105
101 IF (RD) 102,103,104
102 FACT = -HALFPI
RETURN
103 FACT = 0
RETURN
104 FACT = HALFPI
RETURN
105 FACT = ATAN(BD/AC)
RETURN
106 IF (BD) 107,103,109
107 FACT = ATAN(RD/AC) - PI
RETURN
108 FACT = -PI
RETURN
109 FACT = ATAN(RD/AC) + PI
RETURN
END

```

FUNCTION FT(T)
C THIS FUNCTION IS USED TO FIND OUTPUT VALUES BASED ON THE TIME, T.
C THIS ROUTINE USES 1100 WORDS OF CM.
C
COMMON /PART1/ Z(20),XR,NXX,WASTE(10),Y(35),W(35),CR(35),EC(35),
+ OM(35),FE(35),L
C
PAD = 3.1415926535/180.
IF (NXX .EQ. 0) GO TO 142
EX = EXP(XR*T)
F1 = 0.
DO 141 I = 1,20
F1 = F1 + Z(I)*EX
141 EX = EX*T
GO TO 143
142 F1 = 0.
143 F2 = 0.
F3 = 0.
DO 144 I = 1,L
F2 = F2 + Y(I) * EXP(W(I)*T)
F3 = F3 + CR(I) * EXP(EC(I)*T) * SIN(OM(I)*T) + FE(I)*RAD
144 FT = F1 + F2 + F3
RETURN
END

```

Appendix A7: Frequency Response Analysis via BODE

The coding for the subroutine BODE is given in this section. The associated routine MARGIN is also included. BODE is used to find control loop phase and gain margins. The routine RESIDUE listed in Appendix A6 is also used.

```

C SUPROUTINE PODE (CNTLNR,M1,M3,M6,L4,M9,DUMMY,NX,PASS)
C THIS ROUTINE EVALUATES THE SYSTEM DEFINED BY THE PLANT "AA" FOR ITS
C FREQUENCY RESPONSE. THE EVALUATION IS MADE FROM THE RESIDUES OF THE
C POLES OF THE PARTIAL-FRACTION EXPANSION. THE FREQUENCIES USED ARE
C FROM 0.1 TO 100, PLUS 1000 AND 10000 RPS. THE DATA IS PRINTED IN
C TABULAR FORM FOR FREQUENCY (OMEGA), MAGNITUDE (AMAG), LOG-MAGNITUDE
C (ALCMAG), PHASE ANGLE (PHASE), REAL PART (SIGMA), AND IMAG PART
C (ZIMAG).
C THIS ROUTINE USES 6209 WORDS OF CM.
C
C LOGICAL D21NTR, PASS
C REAL KXPSE
C INTEGER CNTLNR(M3)
C COMMON /SYSTEM/ A(39,39), R(39,5), C(10,39), H(39,2), G(5,39)
C COMMON /DUPSYS/ AA(39,39), A2(39,39), KOPT(5,10)
C COMMON /PARTFRC/ REFR(39), RESI(39), EVR(39), EVI(39), EMAG(39),
C + FANG(39)
C COMMON /MAIN2/ DUM1(39,39)
C COMMON /MAIN5/ SAVE(21), KXPSE(1,39), BI(39,1), WIFE(78), R(1,39),
C \ P(39,1), PES(1,1,39), EV(39)
C COMMON /MAIN6/ EVAL(39), U(39,39), UINV(39,39)
C COMPLEX EVAL, U, UINV, R, P, RES, EV
C DIMENSION DUMMY(M9)
C
C PRINT = .FALSE.
C MX = 46 - 1
C DO 200 I = 1, MX
C JR = CNTLNR(IJ)
C DO 202 I = 1, M1
C RI(I,1) = R(I,JR)
C KXPSE(1,I) = G(JR,I)
C
C 202 CONTINUE
C CALL MRRM (BI,KXPSE,DUM1,M1,L4,M1)
C DO 203 I = 1, M1
C DO 203 J = 1, M1

```

```

203 A(I,J) = AA(I,J) - DUM1(I,J)
    LR = LR
    CALL RGEIG (M1,M1,A,L3,FVAL,U,WIFE)
    CALL CDUP (U,UINV,M1,M1)
    CALL MINVS (UINV,UINV,M1)
    CALL MOP4 (KXPSF,U,P,L4,M1,M1)
    CALL MOP4 (UINV,P1,P,M1,M1,L4)
    CALL RESIDUE (P,R,RES,PASS,PRINTR,EVAL,EV,M1,L4,L4,NX)
    DO 205 I = 1,NX
    RESP(I) = REAL(RES(1,1,I))
    PCSI(I) = AIMAG(RFS(1,1,I))
    FVP(I) = -REAL(EV(I))
    205 EVI(I) = (-AIMAG(EV(I))) * 1.0
    PRINT 212

    DO 206 I = 1,NX
    206 PRINT 213, RESP(I), PCSI(I), EVR(I), EVI(I)
    PASS = .FALSE.
    OMEGA = 1.0
    CALL MARGIN (NX,OMEGA,AMAG,PHASE,ALGMAG,PASS,SIGMA,ZIMAG)
    PRINT 214, AMAG,ALGMAG, PHASE
    PRINT 217, JP
    OMEGA = 0.95
    DO 207 I = 1,781
    OMEGA = OMEGA + 0.05
    CALL MARGIN (NX,OMEGA,AMAG,PHASE,ALGMAG,PASS,SIGMA,ZIMAG)
    PRINT 211, OMEGA,AMAG,ALGMAG,PHASE,SIGMA,ZIMAG
    207 CONTINUE
    OMEGA = 40.0
    DO 208 I = 1,11
    OMEGA = OMEGA + 5.0
    CALL MARGIN (NX,OMEGA,AMAG,PHASE,ALGMAG,PASS,SIGMA,ZIMAG)
    PRINT 211, OMEGA,AMAG,ALGMAG,PHASE,SIGMA,ZIMAG
    208 CONTINUE
    209 CONTINUE
    RETURN
    210 FORMAT (//,* FOR CONTROLLER NO.*,I2,*,THE FOLLOWING FREQUENCY RESP

```

```

+OISE DATA WAS COMPUTED BY SUBROUTINES RODE AND MARGIN*,//,5X,*FREQ
+ (PSP)*,5X,*MAGNITUDE*,8X,*LM (DR)*,4X,*PHASE (DEG)*,6X,*REAL PART
+*,5X,*IMAG PART*)
211 FOPMAT (5X,F5.2,2X,5G15.4)
212 FOPMAT (*1*,//,* ROUTINES RODE AND RESIDUE HAVE CALCULATED THE*,
/ * FOLLOWING*,//,* PARTIAL-FRACTION EXPANSION DATA:*,//10X,
/ *RESIDUE*,24X,*POLE*,//,2X,*REAL PART*,4X,*IMAG PART*,8X,
/ *REAL PART*,4X,*IMAG PART*,/)
213 FOPMAT (2(Y,G12.5),3X,2(1X,G12.5))
214 FOPMAT (//,* FOR ZERO FREQUENCY, THE ROUTINE MARGIN FINDS THE *,
/ * FOLLOWING:*,//,5X,*MAGNITUDE =*,1X,F7.4,/,5X,*LOGMAG =*,1X,
/ F7.4,/,5X,*PHASE ANGLE =*,1X,F7.2,//,* IF THE PHASE ANGLE IS *,
/ *-180 DEGREES, A MINUS SIGN SHOULD BE ASSUMED AND *,/,
/ * ALL SUBSEQUENT PHASE DATA SHOULD BE SHIFTED BY 180 DEGREES.*)
END

```

C SURROUTINE MARGIN (K,W,MAGTUDE,PHANGLE,LOGMAG,PASS,REEL,XIMAG)
 C THIS ROUTINE FINDS THE BODE PLOT DATA FOR A TRANSFER FUNCTION IN
 C PARTIAL-FRACTION EXPANSION FORM FOR EACH VALUE OF FREQUENCY, W.
 C THIS ROUTINE USES 1478 WORDS OF CM.

LOGICAL PASS
 REAL LOGMAG, MAGTUDE, MAG
 COMMON /POLARC/ AC, B0, FACT, FACTR
 COMMON /PARTFC/ A(39), B(39), C(39), D(39), E(39), F(39)
 DATA PI2,PI,2.23143577, PI/3.14159265357, DEGRT/57.29578

C IF (PASS) GO TO 156

DO 155 II = 1,K

AC = A(II)

RD = B(II)

CALL POLAR

E(II) = FACTR

F(II) = FACT

155 CONTINUE

156 PASS = .TRUE.

PEEL = 0.0

XIMAG = 0.0

DO 157 I = 1,K

AC = C(I)

RD = D(I) + W

CALL POLAR

MAG = E(I)/FACTR

ANGL = F(I) - FACT

TEMP = AMOD(ANGL,PI2)

IF (ABS(TEMP) .GT. PI) TEMP = TEMP - SIGN(PI2,TEMP)

ANGL = TEMP

X = MAG * COS(ANGL)

Y = MAG * SIN(ANGL)

IF (ABS(Y) .LE. .0001) Y = 0.0

REEL = REEL + X

```
XIMAG = XIMAG + Y
157 CONTINUE
AC = REEL
RO = XIMAG
CALL POLAR
MAGTUDE = FACTR
PHANGLE = FACT * DEGRE
LOGMAG = 20.* ALOG10(MAGTUDE)
RETURN
END
```


Appendix B

System Specification for a B-52 CCV

Longitudinal-axis Controller

The following system specification was adapted from AFFDL-TM-74-138-FGB [ref 7] and was used for the design of a multi-stage modal controller. This specification is the same as that used for the Multi-Surface System optimal controller reported in the AFFDL technical memorandum. The design requirements are based on achieving percentage improvements of specific parameters of the unaugmented open-loop aircraft longitudinal axis. If all five available control surfaces are used for the control task, the specification consists of 43 criteria to be met. The paragraph numbering used will permit the addition of lateral-direction axis requirements if so desired for extension of this thesis work. The word "system" in the specification refers to the closed-loop system. For the purposes of meeting the specification, wind-induced turbulences are defined as zero-mean, Gaussian, white noise at a level of 8 fps rms. Similarly, pilot-induced elevator oscillations are defined as zero-mean, Gaussian, white noise at a level of 0.1 rad rms.

1. Longitudinal Axis
 - 1.1 Performance
 - 1.1.1 Wind-induced Turbulence

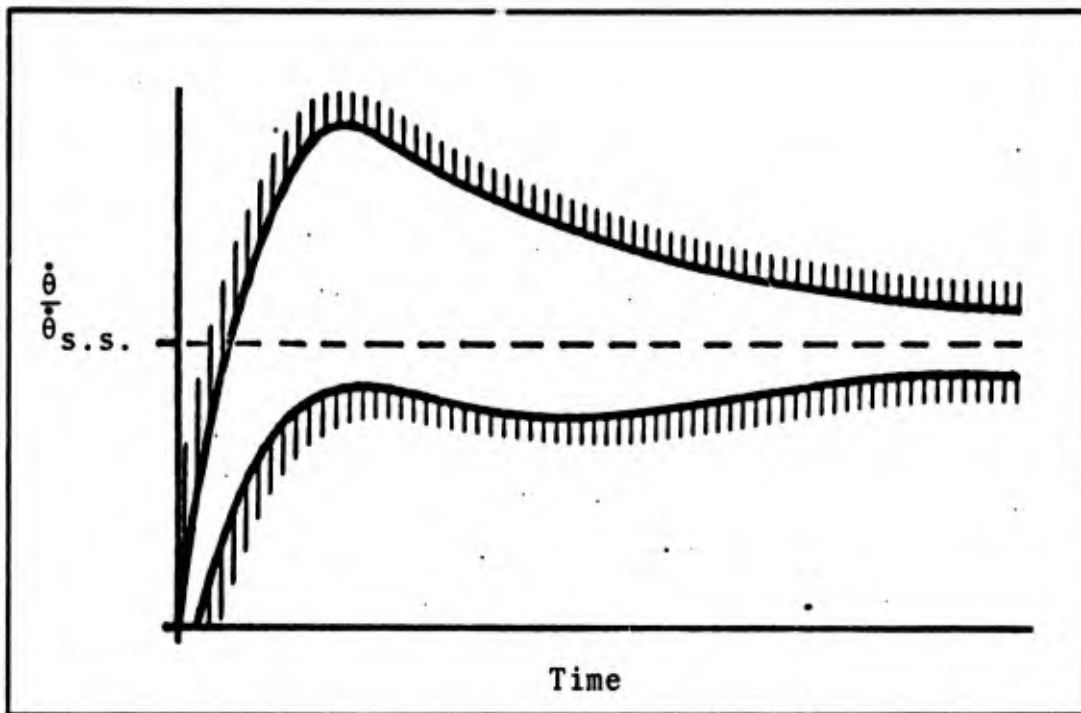


Fig. B1. Normalized Pitch Rate Response to a Step Elevator Input [from Ref 7:23]*

1.1.1.1 Acceleration

In the presence of wind-induced turbulence, the system shall reduce the normal acceleration at the crew station (BS 172) and the empennage (BS1655) by at least 30%. The system shall not increase the normal acceleration at the center-of-gravity (BS860) by more than 5%.

1.1.1.2 Stress

In the presence of wind-induced turbulence, the system shall reduce the normal stresses at the following locations by at least 10%: BS475, BS760, BS1412, WS222, WS974, SBL56.

1.1.2 Pilot-induced Elevator Oscillations

In the presence of pilot-induced elevator oscillations, the system shall reduce the normal stress at WS222 by 30%.

1.1.3 Step Elevator Input

For a step elevator input, the system shall provide a pitch rate response within the bounds of the curve given in Fig. B1.*

* Fig. B1 is taken directly from AFFDL-TM-74-138-FGB. There are no further details on the "bounds" except that the upper curve has a peak value of 1.57.

1.2 Control-loop Stability

The system shall have gain margins of 6 db and phase margins of 60° for each control loop used. These loops may include the elevator, flaperon, inboard aileron, outboard aileron, and horizontal canard control surfaces.

1.3 Surface Displacements and Rates

In the presence of wind-induced turbulence or pilot-induced elevator oscillations, the system shall not exceed the surface displacement or rate limits given below.

<u>Surface</u>	<u>Displacement limit in degrees</u>	<u>Rate limit in deg/sec</u>
Elevator	19	80
Flaperon	20	80
Inboard Aileron	17	120
Outboard Aileron	20	80
Horizontal Canard	12	83

1.4 Structural Mode Frequency and Damping

The system shall not change the natural frequency of structural modes by more than 10% and shall not reduce the damping of the structural modes by more than 10% for modes 1, 2, 5, 7, 8, and 12. The baseline natural frequencies and damping ratios for the unaugmented aircraft structural mode are as follows:

<u>Mode</u>	<u>Natural Frequency (rad/sec)</u>	<u>Damping Ratio</u>
1st	6.167	0.143
2nd	12.654	0.118
5th	15.055	0.031
7th	19.261	0.048
8th	19.571	0.013
12th	38.037	0.030

Vita

Ronald Martin Adams was born [REDACTED]. He graduated from Ann Arbor Pioneer High School in 1965, and began undergraduate studies in Aerospace Engineering at the University of Michigan that fall. He received his degree of Bachelor of Science in Engineering (Aerospace) in May 1970 and was commissioned in the USAF through the ROTC program. He entered active duty later that month and was assigned to the Aeronautical Systems Division (AFSC) at Wright-Patterson AFB, Ohio. From May 1970 to May 1974, he performed duties as a Flight Control Development Engineer within ASD's Deputy for Engineering and the Drone/Remotely Piloted Vehicle Systems Program Office. He was assigned as a student to the School of Engineering, Air Force Institute of Technology in June 1974.

Permanent address: [REDACTED]